The Institute of Paper Chemistry

Appleton, Wisconsin

Doctor's Dissertation

The Configuration and Hydrodynamic Properties of Fully Acetylated Guaran

Joseph Victor Koleske

June, 1963

THE CONFIGURATION AND HYDRODYNAMIC PROPERTIES OF FULLY ACETYLATED GUARAN

A thesis submitted by

Joseph Victor Koleske

B.S. 1958, University of Wisconsin
M.S. 1960, Lawrence College

in partial fulfillment of the requirements
of The Institute of Paper Chemistry
for the degree of Doctor of Philosophy
from Lawrence College,
Appleton, Wisconsin

June, 1963

TABLE OF CONTENTS

SUMMARY

Although there are numerous naturally occurring polysaccharides, very little work has been done on the physical solution properties of the majority of them. Several investigations have been made on the derivatives of cellulose and amylose which indicate that these materials are characterized by a large molecular extension and a relatively high intrinsic viscosity as compared to the more flexible synthetic polymers.

The plant gums provide a rich field of endeavor for further work to extend knowledge of the naturally occurring polysaccharides. Guaran is a naturally occurring polysaccharide obtained from the endosperm of the guar seed. The main chain of guaran is similar to cellulose in that it is composed of β-1,4-linked anhydromannose units while cellulose is composed of β-1,4-linked anhydroglucose units. However, guaran also differs from cellulose in that it has single unit branches of galactose linked α-1,6 to every other unit of the main mannan chain. The presence of these side spurs was expected to affect the physical properties of this gum. The degrees of polymerization of the two polysaccharides are similar. Fractions of cellulose with a degree of polymerization of about 9000 have been reported, and the fractions of guaran studied in this work had a degree of polymerization that ranged to over 12,000. The fiber repeat distance of guaran is the same as for cellulose and, from a model study, the conformation of the main chain of guaran was ascertained to be C1 which is identical to that of cellulose. These factors allow use of the same statistical model for guaran as is used for cellulose.

In this investigation, guaran was prepared from guar gum, fully acetylated, and carefully fractionated. The configuration and hydrodynamic properties of guaran triacetate (GTAc) were studied in acetonitrile as a function of molecular weight.

Sedimentation velocity runs were made on two of the higher molecular weight fractions to obtain an estimate of the polymolecularity of all fractions. Sizable corrections were required for polymolecularity to compare the experimental results with theoretical results.

Light scattering was used to obtain the weight-average molecular weight, $\underline{M}_w$, z-average radius of gyration, $(\overline{s}^2_z)^{1/2}$, and second virial coefficient, A_2. Values of $\underline{M}_w$ ranged from 5.34×10^6 to 7.4×10^4, of $(\overline{s}^2_z)^{1/2}$ from 1300 A. to 250 A., and of A_2 from 0.38×10^{-4} to 4.70×10^{-4} moles cc. $g.^{-2}$. Examination of the scattering envelopes indicated that GTAc approximated a random coil-like model at the high molecular weights and a rodlike model at the low molecular weights.

Viscosity was the principal hydrodynamic property studied. The polymer solutions were shear dependent above molecular weights of 1×10^6, and all intrinsic viscosities, $[\eta]$, were corrected to zero shear stress. Over the molecular weight range investigated, the $[\eta]$ was 9.45 to 0.44 deciliters per gram and the polymer molecules showed a transition from a nondraining to a partially free draining state. A plot of log $[\eta]$ versus log $\underline{M}_w$ could be represented by two straight lines. At molecular weights greater than 8.5×10^5 the relationship was $[\eta] = (3.11 \times 10^{-3})\underline{M}_w^{0.52}$, and for molecular weights less than this value the relationship was $[\eta] = (2.62 \times 10^{-5})\underline{M}_w^{0.87}$.

The molecular expansion factor for GTAc was small, 1.04 to 1.20, indicating the molecules are highly expanded, and in this respect are similar to cellulose derivatives. The polymer chain was sterically hindered to a high degree with respect to rotation about the carbon-oxygen linkages. The large steric hindrance resulted in a high limiting persistence length of 67 A. when evaluated from the Porod-Kratky theory. Deviations from this theory were attributed to a shift in

bond population that favored one rotational conformation as the molecular weight decreased. A comparison of $(\overline{s^2}_z)^{1/2}$ for GTAc as a function of extended polymer chain length with that of cellulose trinitrate, cellulose tricaproate, and hydroxyethyl cellulose indicates that these molecules are all sterically hindered to about the same degree at a given chain length.

Results from $[\eta]$, M_w and $(\overline{s^2}_z)^{1/2}$ indicated that the excluded volume effects were negligible. The effective bond length of 23.5 A. evaluated from the $[\eta]$ was in good agreement with the value of 27 A. obtained from light-scattering data. Theoretical values for the root-mean-square end-to-end distance calculated from all hydrodynamic theories investigated except the Debye-Bueche theory were in fair agreement with the experimental results for the two highest molecular weights. However, as the molecular weight decreased, the theoretical results greatly deviated from the experimental results.

The Flory constant, Φ, was evaluated for all fractions, and corrections were made for polymolecularity. The corrected value of Φ approached the theoretical value of 2.86×10^{21} for the highest molecular weights and decreased rapidly with decreasing molecular weight. The decrease in Φ was attributed to an increase in the free-draining characteristics and to a shift in the bond population.

During a trial fractionation, crystalline guar gum triacetate was obtained. The crystallinity was ascertained from melting points, x-ray data, and electron photomicrographs.

INTRODUCTION

GENERAL PROBLEMS IN THE INVESTIGATION OF POLYSACCHARIDE MOLECULES

The general problems that arise in the investigation of polysaccharides include determination of their size and structure. Isolation of these polymeric substances is a necessary preliminary to all investigations, and the possibilities of chemical modification during isolation or preparation of a derivative must be considered. Organic and biochemical studies allow determination of the nature of the chemical structure units and are a necessary prelude to physicochemical studies which provide information on the size, shape, and hydrodynamic properties of the polysaccharides.

Thus, to obtain a thorough understanding of the nature of a particular polysaccharide, it is necessary to combine information obtained from organic, biochemical, and physicochemical studies. Presently there is a considerable wealth of chemical information available on the polysaccharides, but there is a definite need for physicochemical studies on these materials as discussed in the review articles by Greenwood (1) and Aspinall (2). This particular thesis is devoted to the physicochemical aspect of the general polysaccharide problem.

PHYSICOCHEMICAL PROBLEMS

Many problems are present that might be treated under the subject of physicochemical problems when considering the study of polysaccharide solutions. These include problems concerned with molecular weight determination, molecular weight averages and distributions, physical shape of molecules, polymer-solvent interactions, and hydrodynamic properties. The present work is concerned with contributing to the knowledge of the size, shape, and hydrodynamic properties of naturally occurring polysaccharides in dilute solution.

A large number of experimental and theoretical tools are available for the purpose of a physical study. From an experimental standpoint, osmometry, ultracentrifugation, diffusion, viscometry, and light-scattering techniques may be used to study the properties of polymer solutions. These solution properties are closely related at the theoretical level, and in general much can be learned by a combination of data from any two of these methods. This study will use a combination of light scattering, viscometry, and ultracentrifugation since these yield intimate information regarding the size, shape, and hydrodynamic properties of the polysaccharide molecule. Extensive theoretical literature is available concerning the relations between these properties, and it will be presented in a later section.

Ideally, to make effective use of the available theories, a number of requirements should be met by the particular polysaccharide to be studied. First, it must be possible to fractionate the polymer so as to determine the size, shape, and hydrodynamic properties as a function of molecular weight. If the polysaccharide contains different anhydrosugar units (a heteroglycan), the ratio of sugars must be a constant for all fractions, and the units must be linked in the same fashion for all fractions. If the polysaccharide contains only one kind of polymerized sugar unit (a homoglycan) but if the units are linked in different ways, the fractions should not differ from one another as to the manner in which the anhydrosugar units are linked. The sequence of units in the polymeric chain should be known and invariant between the fractions. Chain architecture should be known. That is, is the polymer linear, branched, or a three-dimensional network. If the polysaccharide is branched, it is important to know the degree of branching and the length of the branches.

Once a material has been fractionated, it is desirable to know the molecular weight distributions of the fractions. Theories on the hydrodynamic properties of polymers assume in general that all of the molecules in a given fraction have the same molecular weight. In practice, such homogeneity of molecular size never is achieved. Unless the molecular weight distribution is known, which is seldom the case, an assumed molecular weight distribution must be used in comparing experimental results with theory.

Although a number of polysaccharides are water soluble in their natural condition, the solutions often are unstable. In such instances it often is desirable to prepare an organic derivative of the polysaccharide and to carry out the subsequent investigation in organic solvents. The mildest method available should be used in derivative preparation so as to keep degradation to a minimum. For light-scattering studies it usually is desirable to carry out investigations on derivatives in organic solvents since such solutions are easier to work with than aqueous solutions. Aqueous solutions tend to acquire dust particles which are difficult to remove to the degree necessary for reliable work.

If the polysaccharide is to be investigated by means of light scattering and ultracentrifugation, considerable care must be exercised in the choice of a suitable solvent. The refractive index gradient is an important factor in light scattering and in ultracentrifugation. In light-scattering work this factor should be as small as possible, yet it must not be so small that the error in determining it precludes its use or that the scattering intensity is too weak and subject to large errors. In ultracentrifugation, on the other hand, a large refractive index is desirable since the optical systems are based on detection of refractive index gradients. An additional problem is encountered in ultracentrifugation. This problem has to do with the partial specific volume of the polysaccharide and the density of the solution. These two quantities must be such

that the polymer will sediment in the gravitational field of the ultracentrifuge. Thus, it is obvious that a judicious choice of solvent must be made. To further complicate solvent choice, in certain instances only a few solvents are available.

GENERAL OUTLINE OF THESIS

This thesis is divided into five main sections. First, an introduction is used to present the problems involved in investigating polysaccharide molecules by physicochemical methods. Then the structure and conformation of the guaran molecule are examined to present a chemical and physical view of the naturally occurring polysaccharide chosen for this investigation. In the theoretical section the various hydrodynamic theories that are pertinent to the dilute solution properties of polymer molecules are outlined. The experimental portion of the thesis deals with the methods used to examine the polymer molecules and contains the results of the experimental investigation. This section is followed by a discussion of the experimental results obtained with guaran triacetate. The various molecular and configurational parameters and the hydrodynamic behavior of these molecules are calculated and examined.

THE GUARAN MOLECULE

CHOICE OF THE POLYSACCHARIDE

Guaran, a particular fraction of guar gum, has been sufficiently well characterized chemically to make it attractive as a suitable polysaccharide for investigation. Its structure has been well established from a chemical standpoint. Guaran can be acetylated and fractionated into chemically homogeneous fractions. The main chain is known to be a linear β-1,4 linked mannan with single unit side spurs of anhydrogalactose linked α-1,6 to every other unit of the main chain. The gum contains no ionizable side groups which eliminates undesirable, complicating electrical effects.

STRUCTURE OF THE MOLECULE

Guar gum is a neutral polysaccharide obtained from the endosperm of the guar seed (Cyamposis tetragonalaba). The polysaccharide which precipitates from a water dispersion of the gum upon addition of between 25 and 40% ethanol by volume is termed guaran (3). Guaran represents approximately 86% of the original polysaccharide. It has been fractionated by Heyne and Whistler (3), and the fractions were considered chemically homogeneous since they had the same mannose anhydride content and the same galactose anhydride content. The chemical composition of guaran was found to be 34.5% D-galactose anhydride, 63.4% D-mannose anhydride, and 0.1% nitrogen. In addition, the fractions of guaran had the same specific rotation of 53° in normal sodium hydroxide. Further evidence of chemical homogeneity was given by the triacetate of guaran*. Each of seven fractions of guaran triacetate

*Strictly speaking, the repeating unit of fully acetylated guaran is 2,3,6-tri-O-acetyl-O-β-D-mannopyranosyl-(1→4)-O-[2,3,4,6-tetra-O-acetyl-α-D-galactopyranosyl-(1→6)]-2,3-di-O-acetyl-β-D-mannopyranosyl. Since there is an average of 3 acetyl groups per anhydrosugar unit in the chain molecule, it will be referred to as guaran triacetate.

had a constant specific rotation of 34° in chloroform and a melting point range of 224-228°C.

The structure of guaran based on periodate oxidation data (4, 5) and on methylation data (6, 7) indicates that the polysaccharide molecule is a straight-chain mannan with single-membered galactose branches. The ratio of mannose units to galactose units is two to one with the mannose units linked in a β-1,4-glycosidic linkage. One-half of these mannose units have a single D-galactopyranosyl unit substituted on the hydroxyl group of carbon atom six in an α-1,6 linkage as shown in Fig. 1. On the basis of x-ray patterns (8), obtained from stretched guar gum films it has been concluded that a straight mannan chain with side chains of one galactose unit on every second mannose unit is the structure in best accord with the data. Stress-strain measurements on guaran triacetate films (9) indicated that the molecule seemed to be linear with short side chains possible but that the molecule did not have a dendritic structure.

GUARAN

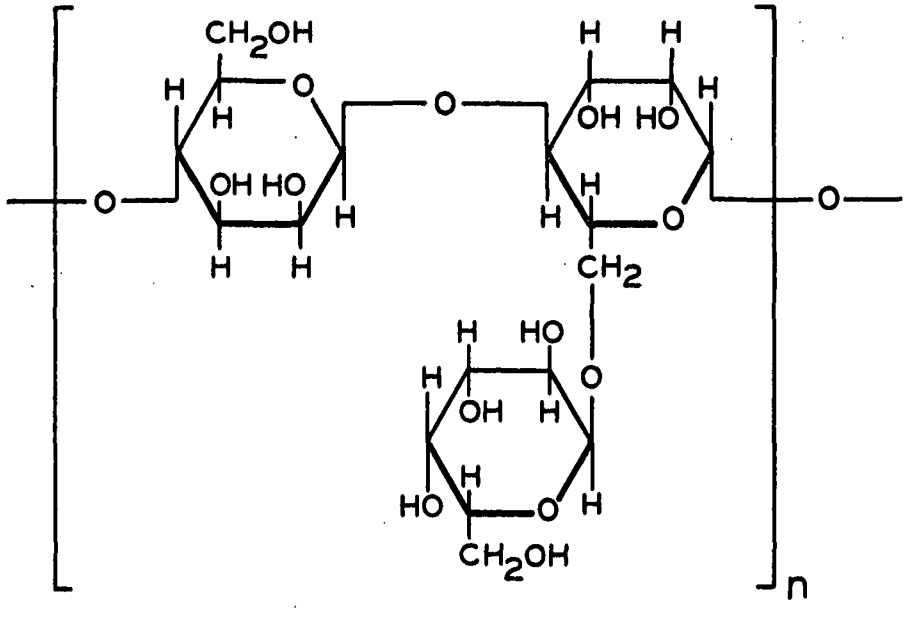

Figure 1. Most Probable Structure for the Repeating Unit in Guar Gum and in Guaran. The Heavy Lines Represent the Side of the Ring Nearer to the Observer

Moe, Miller, and Iwen (4) showed that the periodate oxidation of guar gum indicated the presence of 1,4 linkages, since one mole of oxidant was consumed for each hexose unit present. The possibility of branching was not eliminated. Whistler, Li, and Dvonch (5) showed that guaran was branched by means of periodate oxidation. The polysaccharide consumes one molecule of sodium periodate for each anhydrosugar unit, and one mole of formic acid is produced for approximately every 2.7 anhydroglycosidic units. This indicates a large number of pyranosidic non-reducing end units, i.e., about one for two units of the main structure which implies that the structure contains a large number of short branches.

Swanson (6) methylated purified guar gum and showed that 39.1% of the methylated product was 2,3,4,6-tetramethyl-D-galactose which was evidence that the galactose occurred as side chains linked to the main chain through its number one carbon atom. Ahmed and Whistler (7) methylated guaran and identified 2,3,4,6-tetramethyl-D-galactose, 2,3,6-trimethyl-D-mannose, and 2,3-dimethyl-D-mannose in about equal parts. These data indicate a structure which has a main chain of 1,4-linked anhydromannopyranose units with single side units of galactopyranose linked 1,6 to one-half of the mannose units.

Further evidence that the above-described structure is the true structure of guaran was given by Whistler and Durso (10) when they isolated and characterized 4-(β-D-mannopyranosyl)-β-D-mannopyranose and 6-(α-D-galactopyranosyl)-β-D-mannopyranose by subjecting guaran to a partial acid hydrolysis. Later these same investigators (11) succeeded in isolating the crystalline trisaccharide α-D-galactopyranosyl-(1,6)-β-D-mannopyranosyl-(1,4)-β-D-mannopyranose from another partial acid hydrolysis of guaran. Whistler and Smith (12) used an enzymatic hydrolysis on guaran and obtained the crystalline trisaccharide β-D-mannopyranosyl-(1,4)-β-D-mannopyranosyl-(1,4)-β-D-mannopyranose and also the previously determined 6-α-D-galactopyranosyl-β-D-mannopyranose.

Palmer and Ballantyne (8) working with stretched films of guar gum obtained x-ray evidence that the galactose side chains consist of one unit on every second mannose unit and that the main chain units are beta linked. A fiber repeat period of 10.3 A., which is identical with that of cellulose (13), was found. The unit cell is orthorhombic. At a moisture content of 16.5%, the unit cell has a volume of 1368 $A.^3$, and from the observed density of 1.44 g./cc., six hexopyranoside residues were calculated to be in the unit cell. At this moisture content the unit cell is described by a = 15.49 A., b = 10.32 A., and c = 8.65 A. At zero moisture content the unit cell size is described by a = 13.5 A., b = 10.3 A., and c = 8.66 A. The fiber repeat period is in best accord with the anhydromannan units having a Sachse-type pyranose ring in which the glycosidic oxygens are trans to one another.

Smart and Whistler (9) showed that guaran is a linear molecule with perhaps short side chains by preparing guaran triacetate and running load-elongation curves on films of the polymer which had been cast from a chloroform solution. Films of the unplasticized polymer obey Hooke's law over most of the range covered. The tensile strength in kg./sq. mm. is 7.5, 8.6, and 8.0 and the per cent elongation at break is 4.0, 4.0, and 17.0 for guaran triacetate, cellulose triacetate, and potato amylose triacetate, respectively. In addition, the elongated films shattered in a direction parallel to the direction of elongation. These properties were considered to be characteristic of linear molecules or of linear molecules with very short side chains. However, this would not completely eliminate the possibility of one or of a few long branches. Zimm and Stockmayer's (14) work infers that branching would have to be very extensive before such properties as tensile strength of the material would be significantly affected.

Boggs (15) investigated guaran triacetate which had been prepared by heating freshly precipitated guaran with pyridine and acetic anhydride at 105°C. for five hours. The number average molecular weight determined from osmotic pressure measurements was found to be 390,000 and its intrinsic viscosity was 6.0 dl./g.

Summarizing, guaran is a straight-chain mannan with single-membered galactose branches on every other mannose unit. The mannose units are joined by β-1,4-glycosidic linkages, and the galactose branches are joined to the main chain through α-1,6-glycosidic linkages.

CONFORMATION OF THE MOLECULE

The pyranose rings of a polysaccharide can exist in eight possible strainless ring conformations (16), Fig. 2. There are two chair configurations, C1 and 1C, and six boat configurations, B1, 1B, B2, 2B, B3, and 3B. In Fig. 2, the dark circles represent the ring oxygen atoms, and the numbered circles represent carbon atoms 1 to 5. The heavy lines represent the side of the ring nearer the observer.

If the stereochemical convention of Greenwood and Rossotti (17) is employed, a rather complete description of the position of substituents on the pyranose ring in the various conformations may be given in tabular form. In the discussion that follows, we will be interested in substituents other than hydrogen. The equatorial substituents, those which approximately project into the plane of the ring, will be indicated by dashes. Arrows will be used to indicate axial substituents which project above (↗) or below (↙) the plane of the ring. The positions of substituents on the pyranose rings of guaran are given in Table I.

There are several rules which make it possible to reduce the number of probable conformations. Conformations which contain two or more substituents in cis-axial positions are expected to be unstable (18). On this basis, the 1C, 1B, B2, 2B,

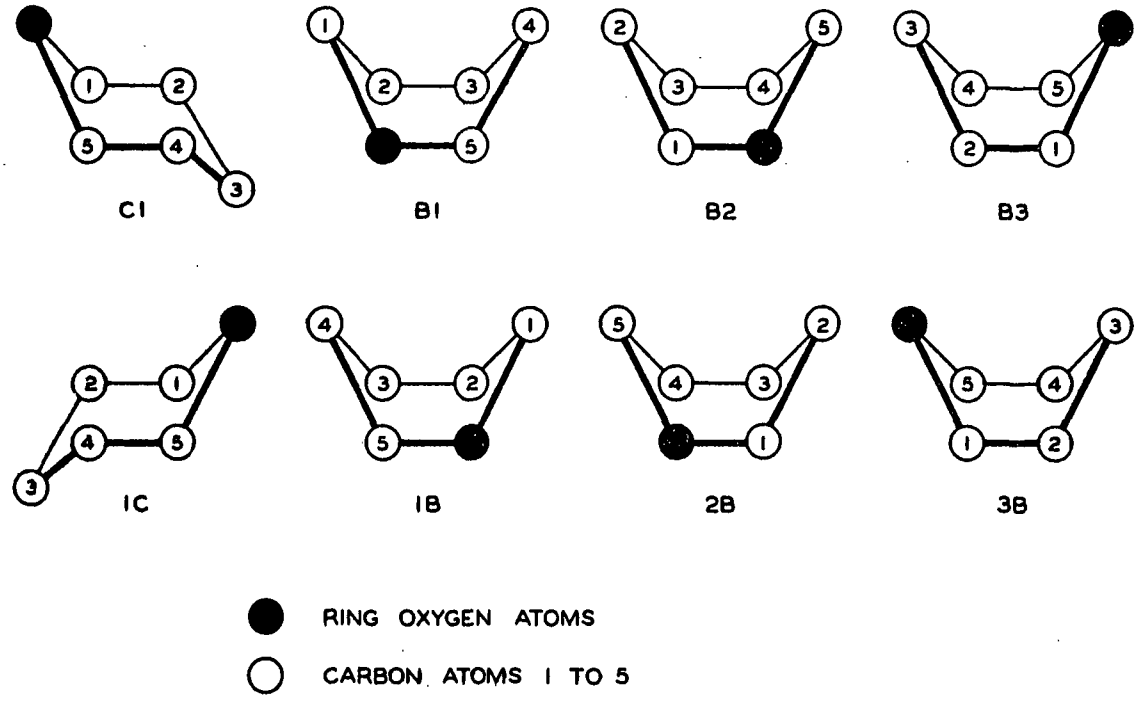

Figure 2. The Eight Strainless Conformations of the Pyranose Rings

and 3B conformations of the pyranose rings of the mannan chain are eliminated. According to Bently (19) the β-1,4 linkage is most easily formed from two groups in the equatorial position. The B1 and B3 conformations are eliminated for this reason. This leaves the C1 conformation as the preferred conformation for the pyranose rings of the mannan chain. The chair conformation is to be expected in solution. Reeves (18) examined the ring shape of fifty-two glycopyranosides in solution and observed that "pyranose rings assume a chair form in preference to any boat form whenever both are structurally possible."

TABLE I

POSITIONS OF SUBSTITUENTS ON THE PYRANOSE RINGS OF GUARAN

The β-Linked Anhydromannose Units

Conformation	Stereochemical Position of Large Substituents[a]				
	C_1-O-	C_2-OH	C_3-OH	C_4-O-	C_5-CH_2O-
C1	-	↗	-	-	-
1C	↙	-	↙	↗	↙
B1	↗	-	-	-	-
1B	-	↙	↙	↗	↙
B2	-	↗	-	↙	↗
2B	↙	-	↙	-	-
B3	-	-	↗	↙	-
3B	↙	↙	-	-	↙

The α-Linked Anhydrogalactose Units

C1	↙	-	-	↗	-
1C	-	↗	↙	-	↙
B1	-	↙	-	↗	-
1B	↗	-	↙	-	↙
B2	↙	-	-	-	↗
2B	-	↗	↙	↙	-
B3	↙	↙	↗	-	-
3B	-	-	-	↙	↙

[a]The equatorial substituents (those which approximately project into the plane of the ring) are indicated by dashes. Arrows indicate axial substituents which project above (↗) or below (↙) the plane of the ring (17).

It is interesting to note that the x-ray data of Palmer and Ballantyne (8) indicate that the mannan chain of guar gum exists in the Type 1 conformation. The Type 1 conformation has the substituent on carbon atoms 1 and 4 in the equatorial position (20) and is identical with the C1 conformation. In addition, guar gum has a fiber repeat distance of 10.3 A., which is the same as that of cellulose (13) which exists in the C1 conformation.

The 1C, 1B, 2B, B3, and 3B conformations of the pyranose rings of the α-linked anhydrogalactose units would be expected to be unstable, since they each contain two substituents in the cis-axial positions. The remaining conformations, C1, B1, and B2 each contain two axial substituents; however, in this instance the substituents are trans-axial and should be more stable. In the B2 conformation, one of the axial groups is the bulky $-CH_2OH$ group, and it might be expected to be less stable than the C1 or B1 conformations which have the smaller hydroxyl groups in the axial positions. It should be noted that the B1 conformation has an axial hydroxyl group on the two position carbon atom which is an especially important axial position that leads to instability (18). The C1 conformation has the substituent on the number one carbon atom in the axial position, but this steric hindrance should not be too great since the group is joined to the number six carbon atom of the main chain which is free to rotate and come into proper proximity for the α-1,4 linkage. Thus, the C1 conformation probably best describes the α-linked anhydrogalactose units, particularly since the chair form is preferred over the boat form as noted above. It should be kept in mind that regardless of the conformation of these side units, they will not affect the conformation of the units in the main mannan chain which are of the greatest importance.

Figure 3 shows the repeating unit of the guaran molecule in its most probable steric form, C1, which is identical with that of cellulose (21-23) except for the

side branches. The values of a/2 = 2.67 A. and b = 1.43 A. are those calculated by Burchard (23) for the cellulose molecule.

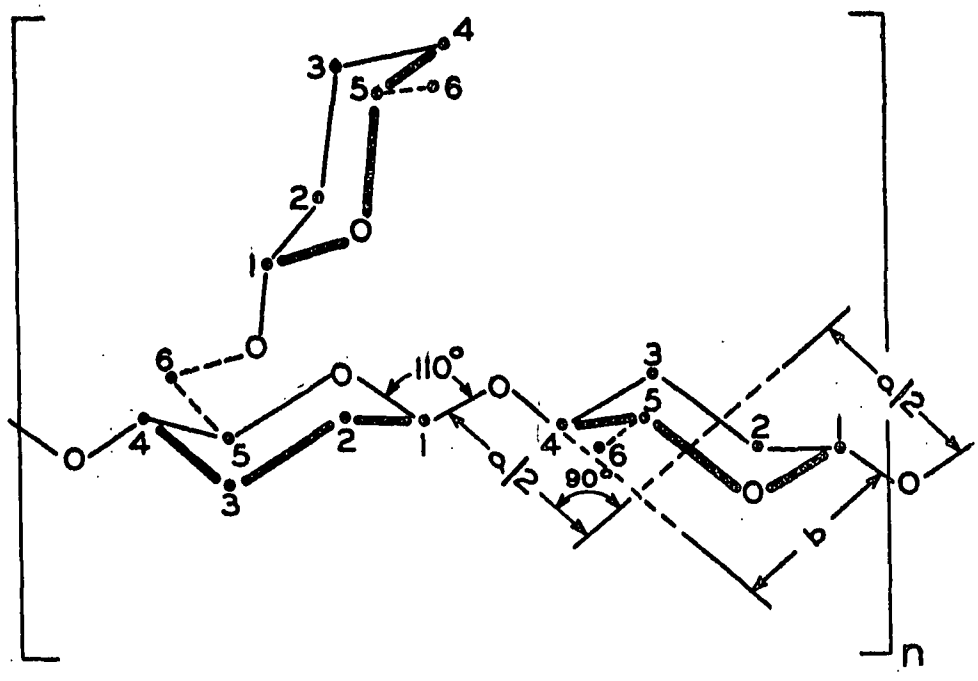

Figure 3. The Repeating Unit of Guaran in the C1 Conformation. The Anhydrogalactose Unit is Placed in an Arbitrary Position with Respect to the Mannan Main Chain. The Numbers Indicate the Particular Carbon Atoms.

THEORETICAL

FREE-DRAINING MOLECULE (24)

The "pearl string" model for a polymer molecule is useful as a starting point for discussing the hydrodynamic properties of the polymer chain. The polymer molecule is represented by beads on a string connected to one another in sequence, Fig. 4. Each bead offers a hydrodynamic resistance to flow of the surrounding medium, and the connecting string offers no resistance to flow. The pearl string molecule is subject to Brownian motion so that over long periods of time the molecule will have a large number of configurations available to it. As is commonly assumed, the distribution of beads about the center of gravity, i.e., the configuration, will be taken to be Gaussian. A frictional coefficient, ζ, may be assigned to each bead, and it is defined as the ratio of force on the bead to the relative velocity between a bead and the solvent. If the bead is spherical and the validity of Stokes law is assumed, the frictional coefficient is given by $\zeta = 6\pi\eta_o \underline{r}_b$ where $\underline{r}_b$ is the radius of the bead and η_o is the solvent viscosity.

Figure 4. The Pearl Necklace Model for a Polymeric Chain

The frictional coefficient of the bead is assumed to be small enough so that the motion of the polymer molecule causes only a slight disturbance in the surrounding medium. The velocity of the surrounding fluid is approximately the same as if no polymer molecule were present. For a molecule sedimenting in a gravitational field, each bead will sediment with the same velocity. If $\vec{V}_r$ is the relative velocity of the liquid with respect to some particular bead, i, then the force on the bead will be $\vec{f}_i = \zeta\vec{V}_r$. For the free-draining molecule, the relative velocity of each bead will be the same as that of the molecule, $\vec{V}$. Then, the total force on a molecule consisting of N beads is $\vec{F} = \Sigma\vec{f}_i = \Sigma\zeta\vec{V}_r = \Sigma\zeta\vec{V} = N\zeta\vec{V}$. The frictional coefficient for the entire molecule, Ξ, is therefore

$$\Xi = \vec{F}/\vec{V} = N\zeta. \tag{1}$$

This quantity is important, since it determines the sedimentation coefficient and the diffusion coefficient of the molecule. The sedimentation coefficient, S, is expressed as

$$S = M(1 - \bar{v}\rho)/N_A\Xi \tag{2}$$

where N_A is Avogadro's number, M is the molecular weight of the polymer, $\bar{v}$ is the partial specific volume of the polymer, and ρ is the density of the solution. The diffusion coefficient, D, is related to the frictional coefficient by means of the well-known Einstein relation

$$D = kT/\Xi \tag{3}$$

where k is the Boltzman constant, and T is the absolute temperature. Since the frictional coefficient is directly proportional to the length of the molecule or the number of beads in the chain, N, the sedimentation coefficient is predicted to be independent of molecular weight and the diffusion coefficient inversely

proportional to the molecular weight. As long as the molecule is free draining, the shape of the molecule will not be important in determining Ξ, $\underline{S}$, or $\underline{D}$.

If the free-draining molecule is placed in a shear gradient, beads located in different parts of the molecule will encounter different fluid velocities. In Fig. 5 the free-draining molecule is shown in a solvent under viscous flow. The flow of solvent is indicated relative to the center of gravity of the molecule. The liquid exerts a net torque on the molecule causing it to rotate with an angular velocity, ω, in radians per second, given by $\omega = \dot{\epsilon}/2$ where $\dot{\epsilon}$ is the rate of shear. The relative velocity between any bead and the solvent is proportional to the product of shear gradient and the distance of the bead from the center of gravity. The force on a bead is easily determined from the frictional coefficient of the bead, and since the product of force and velocity is the energy dissipated per unit time, one can determine the energy dissipated per bead. The energy dissipated per molecule is simply the sum of the contribution from each bead in the molecule. Since the viscosity is equal to the rate of energy dissipation divided by the square of the rate of shear, it is a simple matter to calculate the viscosity once the rate of energy dissipation is known. The result is that the intrinsic viscosity, $[\eta]$, of the free-draining pearl necklace molecule is given by

$$[\eta] = (1/36)(\zeta/\eta_o m')(\overline{r^2}) \qquad (4)$$

where $\underline{m}'$ is the mass of one bead and $(\overline{r^2})$ is the mean-square distance between the ends of the polymer molecule (25). For a linear random coil polymer, $(\overline{r^2})$ is proportional to molecular weight so that the intrinsic viscosity would be predicted to be proportional to molecular weight. In general, this proportionality between intrinsic viscosity and molecular weight is not found in practice since the pearl

necklace model fails to take into account excluded volume effects and hydrodynamic interaction between beads along the polymer chain.

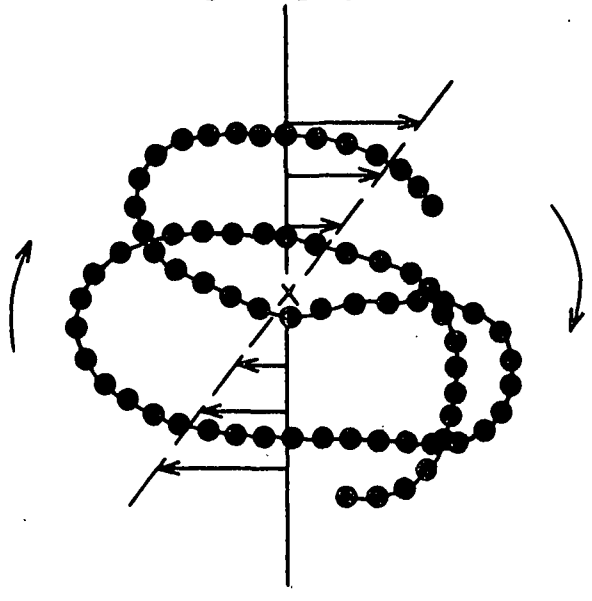

Figure 5. The Free-Draining Pearl Necklace Molecule in a Solvent in a Shear Gradient. The Center of Gravity is Denoted by x, and Rotation of the Molecule is as Indicated.

DEBYE-BUECHE THEORY

In the theory of Debye and Bueche (26) a generalization of Einstein's theory (27) for impermeable spheres is used to calculate the intrinsic viscosity, diffusion, and sedimentation of polymer molecules in solution. For the pearl string model of the polymer chain, the bead density is a function of the distance from the center of gravity and rapidly decreases with increasing distance from the center of gravity. In this theory, the average space occupied by the polymer molecule is considered to be a sphere with radius R_s. Within the sphere the bead density, ν, is a constant and outside the sphere the bead density is zero. If N is the number of beads in the molecule, then the bead density within the sphere is

$$\nu = 3N/4\pi R_s^3. \qquad (5)$$

The appropriate hydrodynamic equations therefore must be modified to include the frictional resistance of the beads within the sphere. Two terms enter into the solution of the hydrodynamic equations. These are the radius of the equivalent sphere, $\underline{R}_s$, and the shielding length, $\underline{L}$, which is defined as

$$1/L^2 = \nu(\zeta/\eta_o), \tag{6}$$

where ζ is the friction coefficient of a single bead and η_o is the viscosity of the solvent. The shielding length is a measure of the decrease in fluid velocity within the equivalent sphere and depends on the bead density and the ratio of a bead's friction coefficient to the solvent viscosity. Appropriate solution of the hydrodynamic equations leads to the following expression for intrinsic viscosity,

$$[\eta] = (\Omega_s/m)\phi(\sigma), \tag{7}$$

with σ, the shielding ratio, being given by $\sigma = \underline{R}_s/\underline{L}$. In this expression, Ω_s is the volume of the equivalent sphere of the polymer molecule and is expressed as $\Omega_s = (4\pi\underline{R}_s^3/3)$, $\underline{m}$ is the mass of the polymer molecule, and the hydrodynamic parameter $\phi(\sigma)$ is a function of the shielding ratio, σ. According to Equation (7) the features which determine the intrinsic viscosity are not primarily concerned with molecular weight. Rather, they are the volume occupied by the molecule divided by its mass multiplied by a hydrodynamic parameter.

The function $\phi(\sigma)$ is complicated, but for large values of σ it becomes 5/2 yielding Einstein's result for the intrinsic viscosity of rigid impermeable spheres,

$$[\eta] = (5/2)(\Omega_s/mN_A). \tag{8}$$

For small values of σ it reduces to

$$\phi(\sigma) = (\sigma^2/10)\,[1 - (2/35)\sigma^2]. \tag{9}$$

In the limit of $\sigma = 0$, the molecule becomes free draining and hence Equation (7) becomes

$$[\eta] = (1/10)(\zeta/\eta_o m')R_s^2, \tag{10}$$

where the mass of one bead is $\underline{m}' = \underline{m}/\underline{N}$. On comparing Equation (10) with the results for the free-draining pearl string model given by Equation (4) one finds,

$$(\overline{r^2})^{1/2} = (36/10)^{1/2} R_s. \tag{11}$$

On substituting Equation (11) into Equation (7) and making use of the definition of $\Omega_{\underline{s}}$ and the fact that $\underline{m} = \underline{M}/\underline{N}_{\underline{A}}$ one finds*

$$(\overline{r^2})^{1/2} = (36/10)^{1/2} \left\{ 300M\,[\eta]/4\pi N_A \phi(\sigma) \right\}^{1/3} \tag{12}$$

from which the dimensions of the polymer molecule can be obtained. Experimentally one finds that the dependence of intrinsic viscosity on molecular weight can be represented by

$$[\eta] = K' N^{\underline{a}} \tag{13}$$

where $\underline{N}$ is the degree of polymerization (i.e., the number of "beads") and $\underline{K}'$ is a constant. Values of $\phi(\sigma)$ and σ are tabulated as a function of the exponent $\underline{a}$ in Equation (13) so that the dependence of intrinsic viscosity on degree of polymerization can be used to determine the root-mean-square end-to-end distance of the polymer molecule from Equation (12).

Returning to Equation (7), it is interesting to note the manner in which the intrinsic viscosity depends on molecular weight. For a linear molecule, $(\overline{r^2})^{1/2}$

*Equation (12) is written for the intrinsic viscosity in the conventional units of dl./g. whereas all other equations in this theory consider the intrinsic viscosity to be in ml./g.

or $\underline{R}_s$ is proportional to $\underline{M}^{1/2}$ so that $[\eta]$ can vary from being proportional to $\underline{M}$ to being proportional to $\underline{M}^{1/2}$ depending on the shielding ratio, σ.

According to the Debye-Bueche theory, the friction coefficient of the polymer molecule is given by

$$\Xi = 6\pi\eta R_s \psi(\sigma), \tag{14}$$

where

$$\psi(\sigma) = [1 - (1/\sigma)\tanh(\sigma)]/\left\{1 + (3/2\ \sigma^2)[1 - (1/\sigma)\ \tanh(\sigma)]\right\} . \tag{15}$$

For small values of σ this reduces to

$$\psi(\sigma) = (2\sigma^2/9)(1 - 4\sigma^2/15 + \ldots). \tag{16}$$

In the limit of $\sigma = 0$, Equation (14) yields

$$\Xi = N\zeta, \tag{17}$$

the result for the free-draining molecule, Equation (1). For large values of σ,

$$\psi(\sigma) = [1 - (1/\sigma) - \ldots], \tag{18}$$

and this leads to

$$\Xi = 6\pi\eta R_s, \tag{19}$$

which is Stokes' formula for sedimenting spheres. As in the case of intrinsic viscosity, the experimentally determined friction coefficient can be written as

$$\Xi = K''N^a \tag{20}$$

Values of $\psi(\sigma)$ are tabulated as a function of σ and $\underline{a}$.

KIRKWOOD-RISEMAN THEORY

The theory of Kirkwood and Riseman (28) is based on the random coil model of the polymer chain and takes into account the hydrodynamic interaction of the monomer units of the chain molecule and the effect of inhibited flow through the chain. The theory is believed to be quantitatively more reliable than the Debye-Bueche theory since it is based on a more realistic model of the polymer chain.

The linear polymer molecule, $(CHX)_{2n+1}$, is composed of $2n + 1$ skeletal carbon atoms numbered from $-n$ to $+n$. These are connected by $2n$ bond vectors $\vec{b}_j$ of length b_o directed from skeletal atom $(j - 1)$ to j. Internal configurations of the chain are specified by the co-ordinates ϕ_j which are the angles between planes of successive bond pairs $(\vec{b}_{j-1}, \vec{b}_j)$ and $(\vec{b}_j, \vec{b}_{j+1})$. The internal rotation around each bond b_j is subject to a hindering torque that has $\phi_j = 0$ as a plane of symmetry. For large values of n, the mean square radius of gyration, $(\bar{s}^2_{0j})$, of chain element j is given by,

$$(\bar{s}^2_{0j}) = (3j^2 + n^2)b_e^2/6n \qquad (21)$$

where b_e is the effective bond length given by

$$b_e = b_o \left\{ \frac{[1 + (\cos\theta)][1 + (\cos\phi)_{av.}]}{[1 - (\cos\theta)][1 - (\cos\phi)_{av.}]} \right\} . \qquad (22)$$

In this expression, θ is the supplement of the fixed skeletal bond angle and $(\cos\phi)_{av.}$ is the mean value of the cosine of the angle between successive bond planes.

If a polymer molecule is placed in a low molecular weight fluid in which there is a velocity field, the field will be perturbed by the resistance offered by each monomer unit. If $\vec{V}_j$ is the fluid velocity at the point of location of monomer unit

$\underline{j}$ and $\vec{\underline{U}}_j$ is the velocity of the unit, then the unit will exert a force $\vec{\underline{F}}_j$ on the fluid and the force is given by,

$$\vec{F}_j = - \zeta(\vec{V}_j - \vec{U}_j) \tag{23}$$

where ζ is a friction coefficient characteristic of the fluid and the structure of the monomer. The fluid velocity, $\vec{\underline{V}}_j$, is calculated as the sum of the unperturbed velocity of the solvent in the absence of the polymer molecule and the sum of perturbations caused by all the elements of the chain. The perturbations are calculated by means of a formula advanced by Oseen (28). Once $\vec{\underline{U}}_j$ is specified and $\vec{\underline{V}}_j$ is known, the force $\vec{\underline{F}}_j$ that a given unit exerts on the fluid is known. Oseen's formula is used again with the known $\vec{\underline{F}}_j$ to determine $\vec{\underline{V}}'$, the perturbation in flow produced by the units in the molecule as a whole at a point $\vec{\underline{s}}$ from its center of mass.

In order to determine the intrinsic viscosity, the solvent is considered to be sheared between two parallel plates in a state of stationary viscous flow. Polymer molecules are then introduced resulting in a perturbation at the plane boundaries which is calculated as the sum of the perturbation $\vec{\underline{V}}'$ for each molecule. The intrinsic viscosity is then determined from the reduction in velocity gradient observed at a constant shear stress. The result is that the intrinsic viscosity is given by

$$[\eta] = (6\pi^3)^{1/2} N_A b_e N^{1/2} X F_o(X)/3600 M_o, \tag{24}$$

with

$$X = N^{1/2}[\zeta/(6\pi^3)^{1/2}\eta_o b_e], \tag{25}$$

where,

N_A = Avogadro's number

b_e = effective bond length

N = degree of polymerization

M_o = molecular weight of the monomeric unit

ζ = friction coefficient of the monomer unit

η_o = viscosity of the solvent, and

X = the draining parameter.

The functions X, $F_o(X)$, and $XF_o(X)$ are tabulated incorrectly in several places in the literature. The revised values reported by Kurata and Yamakawa (29) are currently felt to be free from error. The values of these functions in the original Kirkwood and Riseman article (28) are incorrect due to the use of an incomplete solution used in evaluating their integral equation. This was pointed out by Kirkwood and Riseman (30) and values of the functions were re-calculated by Kirkwood, Zwanzig, and Plock (31). According to Ptitsyn and Eizner (32) these values are in error. Auer and Gardner (33, 34) obtained the correct limiting value for $XF_o(X)$, but their methods of integration are incorrect (32).

The Kirkwood-Riseman theory leads to the following expression for the friction coefficient of the molecule,

$$\Xi = N\zeta/[1 + (8\lambda_o/3)N^{1/2}], \tag{26}$$

where

$$\lambda_o = \zeta/(6\pi^3)^{1/2}\eta_o b_e \tag{27}$$

KURATA-YAMAKAWA THEORY

Kurata, et al. (35) use a pearl necklace model with a continuous medium approximation. They take into consideration the intermolecular interaction and the intramolecular interaction of the segments. The "excluded volume" effect is taken into account by following the Ursell-Mayer theory of imperfect gases. The intrinsic viscosity and frictional coefficient are developed following the Kirkwood and Riseman scheme.

The molecule is considered to be composed of $N + 1$ spherical elements of diameter r_b connected by N segments of length b_o. The potential energy of interaction of any pair of elements is given by the pair potential

$$u(r_{ij}) = \begin{cases} \infty & \text{if } 0 \leq r \leq r_b \\ -u_o \exp(-3r^2/2d^2) & \text{if } r > r_b \end{cases} \tag{28}$$

where u_o is an energy parameter, r_{ij} is the distance between chain elements i and j, and d is a constant. The energy parameter is positive in a poor solvent (endothermic solution) and negative in a good solvent (exothermic solution).

Application of the Ursell-Mayer theory (35) leads to

$$(\bar{r}^2) = (\bar{r}^2)_o [1 + 4z/3 - \ldots] \tag{29}$$

for the mean-square end-to-end distance and to

$$(\bar{s}^2) = (\bar{s}^2)_o [1 + (134/105)z - \ldots] \tag{30}$$

for the mean square radius of gyration with

$$(\bar{r}^2)_o = Mb_o^2 \tag{31}$$

and

$$(\bar{s}^2)_o = (1/6)Mb_o^2. \tag{32}$$

In these expressions, $\underline{b}_o = \underline{b}/\underline{M}_o^{1/2}$.

When $\underline{u}_o \ll \underline{kT}$ and $\underline{d} = \underline{b}$, the excluded volume parameter $\underline{z}$ is given by,

$$z = (6/\pi)^{1/2}(r_{bo}/b_o)^3 \; [1 = (\theta/T)] \; M^{1/2} \tag{33}$$

and θ, the Flory temperature, is given by

$$\theta = [(\pi/6)^{1/2}(b/r_b)^3 - 1](u_o/k), \tag{34}$$

with $\underline{r}_{\underline{bo}} = \underline{r}_{\underline{b}}/\underline{M}_o^{3/2}$. The intrinsic viscosity is given by

$$[\eta] = [\eta]_\theta \; [1 + p(X)z - \ldots], \tag{35}$$

with the intrinsic viscosity at the Flory temperature, $[\eta]_\theta$, given by

$$[\eta]_\theta = [\pi^{3/2}N_A/6^{3/2}(100)] \; XF_o(X) \; b_o^3 M^{1/2}. \tag{36}$$

For the Kurata-Yamakawa model, the draining parameter, $\underline{X}$, is given by

$$X = (3/2\pi)^{1/2}(r_{bo}/b_o M_o^{1/2})M^{1/2}. \tag{37}$$

Values of $\underline{XF}_o(\underline{X})$ and $\underline{p}(\underline{X})$ are tabulated as a function of $\underline{X}$. The values of $\underline{XF}_o(\underline{X})$ are of course the revised Kirkwood-Riseman factors. The friction coefficient is also given and is

$$\Xi = 3\pi^{3/2}\eta_o[XG_o(X)] \; (\bar{s}^2)_o^{1/2} \; [1 + q(X)z - \ldots], \tag{38}$$

with η_o the viscosity of the solvent, and $\underline{XG}_o(\underline{X})$ and $\underline{q}(\underline{X})$ are tabulated functions of $\underline{X}$.

PETERLIN THEORY

Peterlin (36) considered the polymer molecule to be a loose coil in solution with the chain elements distributed in a random fashion. The solvent flow through the molecule was considered to be hindered due to the presence of the molecular elements, and a description of the transition from a free-draining coil to an impenetrable coil was devised for the intrinsic viscosity and sedimentation coefficient of the molecule. The expression for the intrinsic viscosity, in ml./g., is given without mathematical details as

$$[\eta] = (\pi R_h b^2 N) / \left\{ 4M_o [1 + 1.2(6/\pi)^{1/2}(R_h/b)N^{1/2}] \right\} , \qquad (39)$$

where $\underline{R_h}$ is the hydrodynamic radius of the molecule and the other symbols have been previously defined. Peterlin shows that his expression for intrinsic viscosity is similar to the expressions obtained by Debye and Bueche (26) and Kirkwood and Riseman (28), differing only in the numerical factors. This expression may be rewritten as $\underline{M}/[\eta] = \tan \gamma \, (\underline{M}^{1/2}) + \beta$, where $\tan \gamma$ and β are constants. When the definition of $\underline{b} = (\overline{r}^2)^{1/2}/\underline{N}^{1/2}$ and of $\underline{M} = \underline{M_o N}$ are applied to the slope, it is possible to evaluate the RMS end-to-end separation from

$$(\overline{r}^2)^{1/2} = 1.52 \times 10^{-6} (\tan \gamma)^{-1/3} M^{1/2} \qquad (40)$$

where $\tan \gamma$ is obtained from a plot of $\underline{M}/[\eta]$ against $\underline{M}^{1/2}$ and $[\eta]$ is in dl./g. It should be kept in mind that Equation (40) is for a molecule that has considerable coiling and hydrodynamic interaction.

FLORY-FOX THEORY

Flory and Fox (37) considered the polymer molecule in solution to have its chain elements distributed in a random fashion about the molecule's center of gravity. The intrinsic viscosity of the molecule was attributed primarily to the

effective volume and secondarily to the draining characteristics. Equation (24) which was obtained from the Kirkwood-Riseman theory may be rewritten as

$$[\eta] = (\pi/6)^{3/2}(N_A/100)\ XF(X)(\bar{r}^2)^{3/2}/M. \qquad (41)$$

For sufficiently large values of X, the function $XF(X)$ approaches its asymptotic limit, which should occur for polymers having a molecular weight in excess of 10,000 (24). Then Equation (41) may be written as

$$[\eta] = \Phi(\bar{r}^2)^{3/2}/M \qquad (42)$$

where Φ is a constant independent of the solvent. The only requirement is that the polymer molecule have the configuration of a random coil. After examining data obtained on several synthetic polymers, Flory (24) found Φ to have an experimental value of 2.1×10^{21} when $[\eta]$ is measured in dl./g., M in terms of molecular weight, and $(\bar{r}^2)^{1/2}$ in cm. Ptitsyn and Eizner (32) evaluated the correct asymptotic value of $XF(X)$ and found that the theoretical value of Φ was 2.86×10^{21} in an ideal solvent and that Φ decreased as the solvent power increased.

Newman, Krigbaum, Laugier, and Flory (38) indicate that the number average values of M and $(\bar{r}^2)^{1/2}$ should be used in Equation (42), which should then be written as

$$[\eta] = (2.86 \times 10^{21})(\bar{r}_n^2)^{3/2}/M_n \qquad (43)$$

for a polymer chain that has a random coil configuration. It is possible to rewrite this expression in terms of the averages obtained from light-scattering data as

$$[\eta] = (\Phi/q_o)(\bar{r}_z^2)^{3/2}/M_w \qquad (44)$$

in terms of the RMS end-to-end distance, or as

$$[\eta] = (\Phi'/q_o)(\bar{s}_z^2)^{3/2}/M_w \tag{45}$$

in terms of the RMS radius of gyration[1]. The term q_o is a factor that corrects the measured averages to the number averages. To evaluate q_o, a knowledge of the molecular weight distribution is required. If a Zimm-Schulz (39) type distribution is assumed, q_o is defined as

$$q_o = \frac{\Gamma(y+1)\left\{\Gamma(y+3)/\Gamma(y+2)\right\}^{3/2}}{(y+1)\left\{\Gamma(y+1.5)\right\}}, \tag{46}$$

where $\Gamma(\ )$ indicates a gamma function and y is a distribution width parameter and is related to the molecular weight by (40)

$$y = [(M_w/M_n) - 1]^{-1}. \tag{47}$$

Flory (24) introduces the molecular expansion factor, α, to account for interaction of the chain segments with the solvent and for the influence of the volume of the segments within the effective hydrodynamic volume, i.e., the excluded volume. The RMS end-to-end distance and the RMS radius of gyration are related to α by

$$(\bar{r}^2)^{1/2} = \alpha(\bar{r}^2)_o^{1/2} \tag{48}$$

$$(\bar{s}^2)^{1/2} = \alpha(\bar{s}^2)_o^{1/2} \tag{49}$$

where the subscript 'o' refers to the corresponding dimensions of the molecule in the absence of intermolecular interactions. The unperturbed molecule[2] can be

---

[1] The RMS end-to-end distance is related to the RMS radius of gyration of a random coil by $(\bar{r}^2)^{1/2} = (6)^{1/2}(\bar{s}^2)^{1/2}$ (24). Thus, $\Phi' = (6)^{3/2}\Phi$.

[2] When the interaction energy and the excluded volume just offset each other, the polymer will take on a random flight configuration that is determined by only bond angles and bond distances. This configuration is referred to as being in an unperturbed state. When a molecule in solution takes on this configuration, the solvent is termed an ideal or theta solvent.

considered to be a swarm of segments with a Gaussian distribution about the center of gravity. For the actual molecule in a good solvent, the spatial distribution of segments is assumed to be expanded uniformly by the factor α.

The molecular expansion factor may be evaluated by measuring the intrinsic viscosity in an ideal or theta solvent. Since $\alpha = 1$, Equation (42) can be written as

$$[\eta]_\theta = \Phi(\bar{r}^2)_o^{3/2}/M. \tag{50}$$

Upon substituting Equation (48) into (42), the intrinsic viscosity in a good solvent is given by

$$[\eta] = \Phi\alpha^3(\bar{r}^2)_o^{3/2}/M. \tag{51}$$

If Equations (50) and (51) are equated, the following expression for α results.

$$\alpha = \left\{[\eta]/[\eta]_\theta\right\}^{1/3}. \tag{52}$$

Thus, the expansion factor can be determined from the intrinsic viscosity. Often it is difficult to find a theta solvent and experimental difficulties are encountered when trying to work at the theta temperature, since the polymer will tend to precipitate at temperatures just below it. However, the intrinsic viscosity in a theta solvent may be evaluated from the knowledge of the intrinsic viscosity in a good solvent by an expression derived by Krigbaum (41).

$$[\eta]_\theta = [\eta] - 1.43 \times 10^{-25} A_2 M_w \Phi'. \tag{53}$$

Orofino and Flory (42) also derive an expression for the second virial coefficient which is related to the molecular expansion factor

$$A_2 = [(2)^{5/2}\pi N_A/27\Phi]\,([\eta]/M_w)\left\{\ln\left[1 + (\pi^{1/2}/2)(\alpha^2 - 1)\right]\right\}. \tag{54}$$

Equation (54) should be generally applicable with only the restrictions that the polymer molecule have a random coil configuration and that it be suitably represented by a Gaussian distribution of segments.

Stockmayer (43) recently modified the Orofino-Flory expression given by Equation (54) to include excluded volume effects for polymer chains with a non-Gaussian character. This relationship,

$$A_2 M_w / [\eta] = (1.65) \log_{10} [1 + 4.50(\alpha^2 - 1)], \qquad (55)$$

yields a much better fit of experimental data than the original expression.

EXPERIMENTAL

ISOLATION OF CRYSTALLINE GUAR TRIACETATE

Prior to the preparation of guaran and its triacetate, guar gum was acetylated to ascertain which of two methods provided the highest degree of substitution. For a trial fractionation, guar triacetate from one of these acetylations was fractionated by precipitation fractionation with nonsolvent. In the course of this fractionation, crystalline guar triacetate was obtained. The details of this work with guar gum are given below.

PREPARATION OF GUAR TRIACETATE

The guar gum used as a starting material had been prepared previously and characterized by Haug (44) who found the chemical composition to be 37.1% galactose anhydride, 60.9% mannose anhydride, 0.08% ash, and 0.10% nitrogen. Qualitative chromatography was used to assure that the material used was a galactomannan. A sample of the gum was hydrolyzed according to the method of Saeman, et al. (45). The hydrolyzate was concentrated in a vacuum evaporator, and then spotted on No. 1 Whatman paper. The chromatograms were developed in an 8:2:1 ethyl acetate–pyridine–water (46) tank for 18 and for 26 hours, dried, and sprayed with para-anisidine hydrochloride (47). The results indicated that xylose and glucose were absent, that mannose and galactose were present in large quantities, and that arabinose was present in a trace quantity. There were no uronic acids present in agreement with the findings of Heyne and Whistler (3).

By drying one-gram samples of the gum for 24 hours at 105°C. the moisture content was found to be 11.09%. Ignition of one-gram samples of the gum in a muffle furnace at 940°C. for 22 hours showed the ash content to be 0.15%. Appropriate corrections were made for moisture and ash when necessary.

The guar gum was acetylated by the method of Heyne and Whistler (3) which is described in detail by Boggs (15), Method I, and by the method of Carson and Maclay (48) as described by McKee (49), Method II.

Method I consists of treating forty grams of guar gum by soaking it in two liters of concentrated acetic acid for fifteen minutes. The acetic acid is then filtered off and two liters of pyridine are added. After fifteen minutes the pyridine is removed and the swollen guar gum is placed in a three-liter flask to which is added one liter of pyridine and one liter of acetic anhydride. The gum and acetylating mixture is then heated with continuous stirring, at 105°C. for five hours.

Method II consists of adding 40 grams of guar gum to 700 milliliters of formamide and shaking the mixture for three hours. Then 1300 milliliters of pyridine are added to the swollen gum and the shaking is continued for two hours. The mixture is then cooled in an ice-water bath and one liter of acetic anhydride is added in three equal portions over a three-hour period. The mixture is shaken during this period and is cooled in an ice-water bath before each addition of acetic anhydride. The mixture is shaken for one hour after the final addition of acetic anhydride and then allowed to stand at room temperature for fourteen hours.

With both Method I and Method II, the acetylated gum is precipitated by slowly pouring the acetylation mixture into a 5% aqueous methanol solution* at about 0°C. (cooled with ice) which is agitated in a Waring Blendor. The polymer is then filtered on a coarse sintered glass filter, washed with four liters of 2% hydrochloric acid to remove pyridine as pyridine hydrochloride, washed further

*The precipitation could have been carried out in water alone. However, it was found that use of a dilute methanol solution kept foaming to a minimum and yielded a brighter end product.

with distilled water until the filtrate is neutral to methyl orange, and then washed with an additional eight liters of distilled water to insure complete removal of the acid. The washed, acetylated gum is dried by solvent exchange with 95% ethanol, absolute ethanol, and low boiling petroleum ether (30 to 60°C.). The final product is then air dried for 12 hours and vacuum dried at room temperature for 12 hours to insure complete removal of the petroleum ether.

The results of acetylation by these methods are shown in Table II. The acetyl content was determined by the Eberstadt method which involves swelling the sample with warm aqueous alcohol followed by the addition of aqueous alkali and a long saponification at room temperature. Genung and Mallatt (50) describe the method in detail and note that it is the best available method for determining acetyl content.

TABLE II

RESULTS OF ACETYLATION OF GUAR GUM

Acetylation Number	Acetylation Method	Total Time of Acetylation, hours	Acetyl Content, % (Theoretical for Triacetate=44.78%)	Melting Point Range, °C.
2-9	II	19	--	237-239
3-10	II	19	43.59	225-228
4-16	I	5	42.61	230-245
5-17	II	29	43.91	225-228
6-23	II	21	44.01	227-229

The two methods of acetylating the polymer were tried to see if significant differences could be ascertained in the acetyl content of the derivative. Since Method II yielded higher acetyl contents and was considered to be the milder of the two methods, it is the acetylation procedure which was used for the acetylation of guaran.

FRACTIONATION OF GUAR TRIACETATE

A 0.2% chloroform solution of the guar triacetate prepared in Acetylation 3-10 was fractionated by means of precipitation fractionation with a nonsolvent. Ethanol (95%) was slowly added to the agitated solution until a cloudy haze appeared. Then, the solution was warmed until the turbidity just disappeared, and the solution was allowed to stand at room temperature for 24 hours. The precipitate was recovered by centrifuging for 10-15 minutes in an International Centrifuge, Size 2, Model V, at 2400 r.p.m., about 1000 g. The procedure was repeated until a total of six fractions was obtained.

The results of this fractionation are shown in Table III. These results indicate that slightly more than one-half of the guar triacetate is contained in Fraction 1 and that about 87% of the material is in the first two fractions.

TABLE III

RESULTS OF PRECIPITATION FRACTIONATION OF A 0.2% SOLUTION OF GUAR TRIACETATE IN CHLOROFORM
(Initial volume of solution, 175 ml.)

Fraction Number	Total Ethanol Added, ml.	Weight Precipitate, %	Per Cent of Total Gum
1	100	0.2657	51.5
2	550	0.1826	35.6
3	606	0.0139	2.7
4	691	0.0404	7.9
5	891	0.0051	1.0
6	1691	0.0059	1.1

CRYSTALLINE GUAR TRIACETATE

After Fraction 1 was removed from the centrifuge bottles by washing with 95% ethanol, the slurry of precipitate was partially concentrated by evaporation on a steam bath. The remainder of the liquid was allowed to evaporate at room temperature in a hood. After ten hours, the precipitate was examined. It contained a number of agglomerates that had the superficial appearance of large irregular "crystals." These agglomerates were 12 in number and had a size of approximately 6 mm. by 3 mm. by 5 mm. A typical crystal is shown in the top view in Fig. 6 and in the side view in Fig. 7.

The agglomerate shown in Fig. 6 and 7 was dried in air and observed under a 100-power microscope. Both translucent and transparent particles were visible; however, it could not be ascertained whether the material was crystalline. In a few instances, needlelike spikes of the material protruding from the sides of the large agglomerate were visible.

The same agglomerate which had been air dried and microscopically examined was easily disintegrated, washed with 95% ethanol, absolute ethanol, and petroleum ether (30 to 60°C.). After air drying and vacuum drying the material, a melting point determination was made. The material slightly contracted at 228.2°C. and melted between 228.6 and 229.2°C. These values were duplicated in several determinations. The melting point range for this fractionated material was unusually sharp for a polymer and much sharper than that of the whole polymer, which melted between 225 and 228°C. This suggested that the material could be crystalline.

A small amount of the dried polymer from the above-described agglomerate was exposed to x-rays in a Norelco Debye-Scherer powder pattern camera of 57.3 mm. radius, Type 52056B, of a Norelco x-ray diffraction unit, Type 12045B. Figure 8

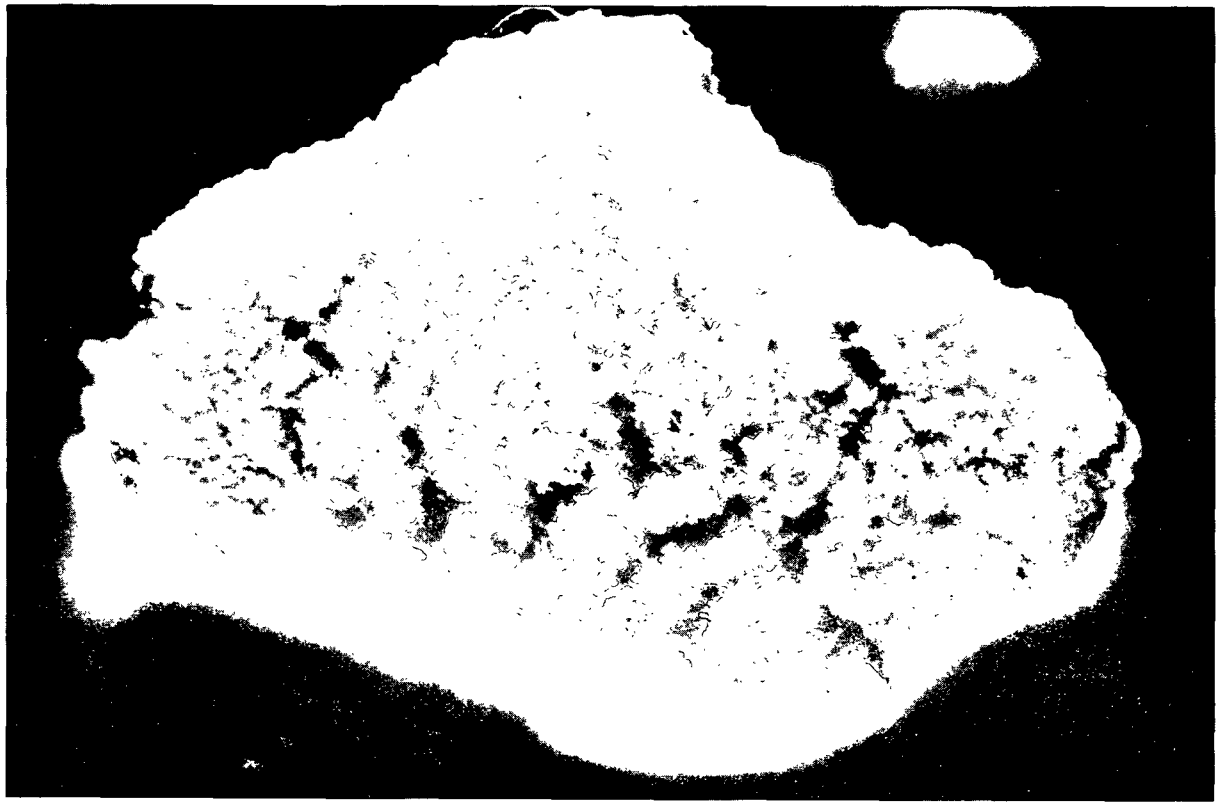

Figure 6. Top View of a Large Agglomerate of Guar Triacetate Which is Made up of Crystalline and Amorphous Material (20X)

Figure 7. Side View of a Large Agglomerate of Guar Triacetate Which is Made up of Crystalline and Amorphous Material (20X)

shows the powder pattern resulting from a six-hour x-ray exposure using a copper target and a nickel filter and operating at 50 kilovolts and 20 milliamperes. Definite indications of crystallinity are shown by the short sharp arcs in the powder pattern. In addition, indications of amorphous material are given by the broad halos in the powder pattern. Table IV lists the d-spacings which were found on the powder pattern of the crystalline material, some of which agree with or are very close to those obtained by Palmer and Ballantyne (8) who did x-ray work on stretched films of guar gum (unacetylated).

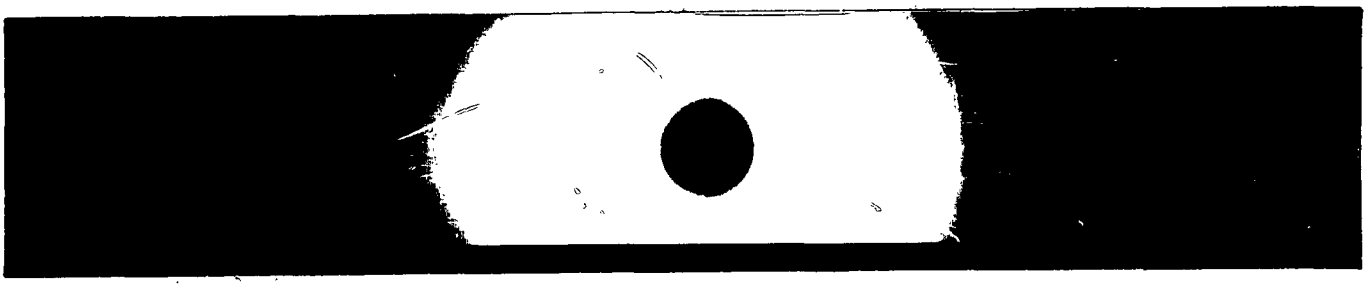

Figure 8. X-ray Powder Pattern of Guar Triacetate Taken from the Large Agglomerate Shown in Fig. 6 and 7. The d-Spacings for this Pattern Are Given in Table IV. Six-Hour Exposure, Copper Target, Nickel Filter, 50 Kilovolts, 20 Milliamperes.

Material from this agglomerate was also investigated by electron microscopy. A small amount of a water slurry of the guar triacetate was placed on a collodion grid. After evaporation of the water, the material was palladium shadowed at an angle of 30°. An R.C.A. electron microscope, Type EMU-3F operated at 50 kilovolts and a magnification of 11,500X was used to view the material deposited on the grid. Although a number of relatively large pieces could be seen, a certain amount of the material had the appearance of a number of particles that are joined into a twisted coil as shown in Fig. 9 and 10 which are enlarged three times from the initial photograph. This is similar in appearance to the crystalline hemicellulose from Indian bamboo obtained by Karnik, Morak, and Ward (51). Very close examination of

TABLE IV

RESULTS OF THE X-RAY POWDER PATTERN ON MATERIAL FROM AN AGGLOMERATE OF GUAR TRIACETATE [THE VALUES OBTAINED BY PALMER AND BALLANTYNE (8) ON STRETCHED FILMS OF UNACETYLATED GUAR GUM ARE INCLUDED FOR COMPARISON]

(Intensities are relative values determined by visual observation)

Guar Triacetate		Guar Gum, stretched film (8)	
Approximate d-Spacings, A.	Intensity	Observed d-Spacings, A.	Intensity
--	--	15.45	Strong
--	--	9.89	Very weak
--	--	8.65	Medium
7.7	Medium	7.72	Medium
7.4	Medium	--	--
--	--	6.17	Medium
--	--	5.19	Weak
--	--	5.16	Medium strong
4.4	Strong	4.39	Medium strong
--	--	4.31	Very very strong
--	--	4.02	Medium weak
3.75	Very weak	3.86	Medium
--	--	3.62	Medium weak
--	--	3.40	Medium
--	--	3.16	Medium
3.05	Medium	--	--
2.82	Medium	2.79	Weak
2.68	Medium	2.64	Weak
2.48	Very weak	2.47	Very weak
--	--	2.30	Weak
2.23	Very weak	2.20	Very weak
--	--	2.18	Weak
2.07	Very weak	--	--
1.90	Very weak	1.94	Very weak
4.5 to 3.5	Most intense halo	--	--
3.5 to 2.5	Less intense halo	--	--

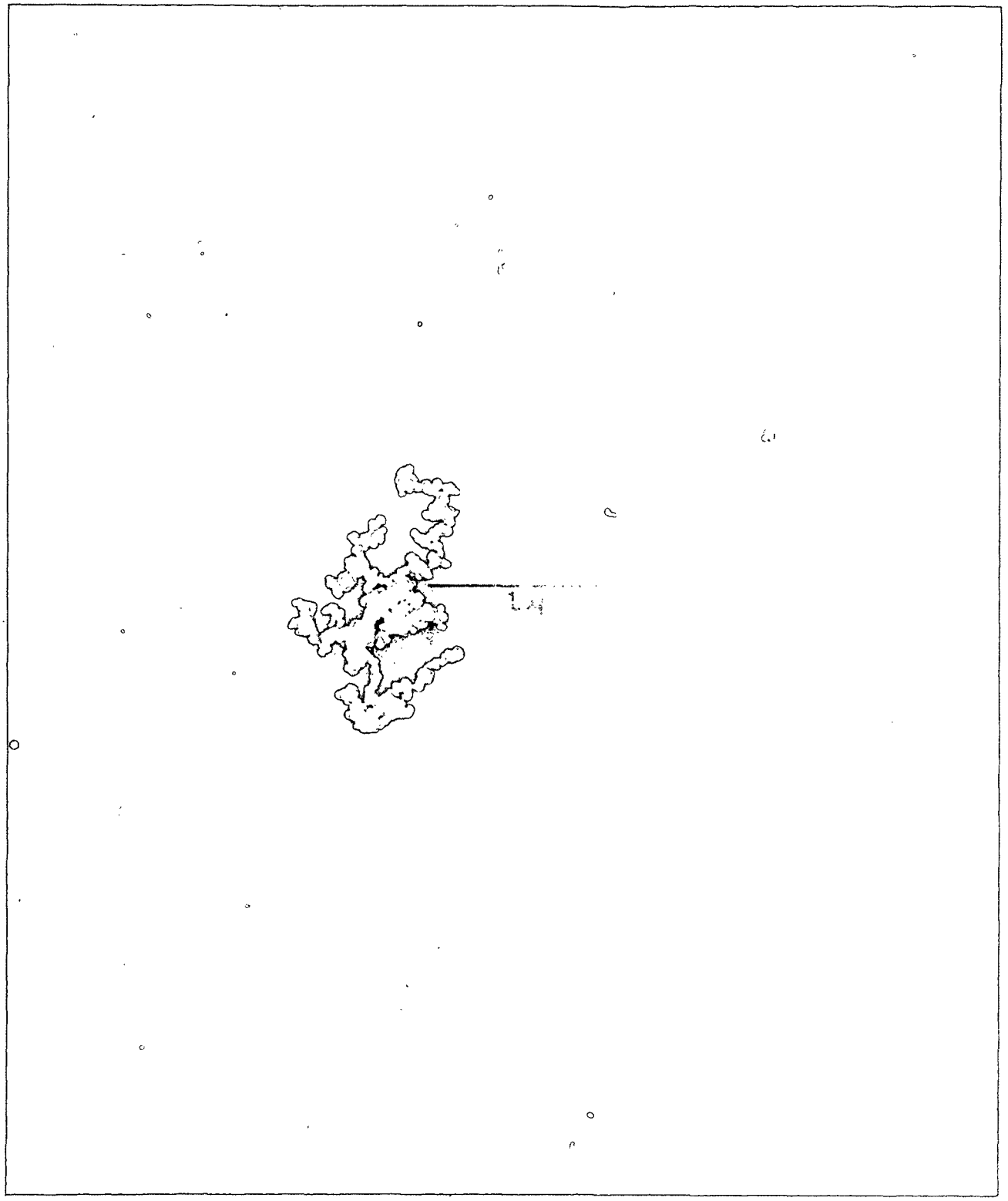

Figure 9. Electron Photomicrograph of Crystalline Guar Triacetate, Palladium Shadowed at 30° (34,500X)

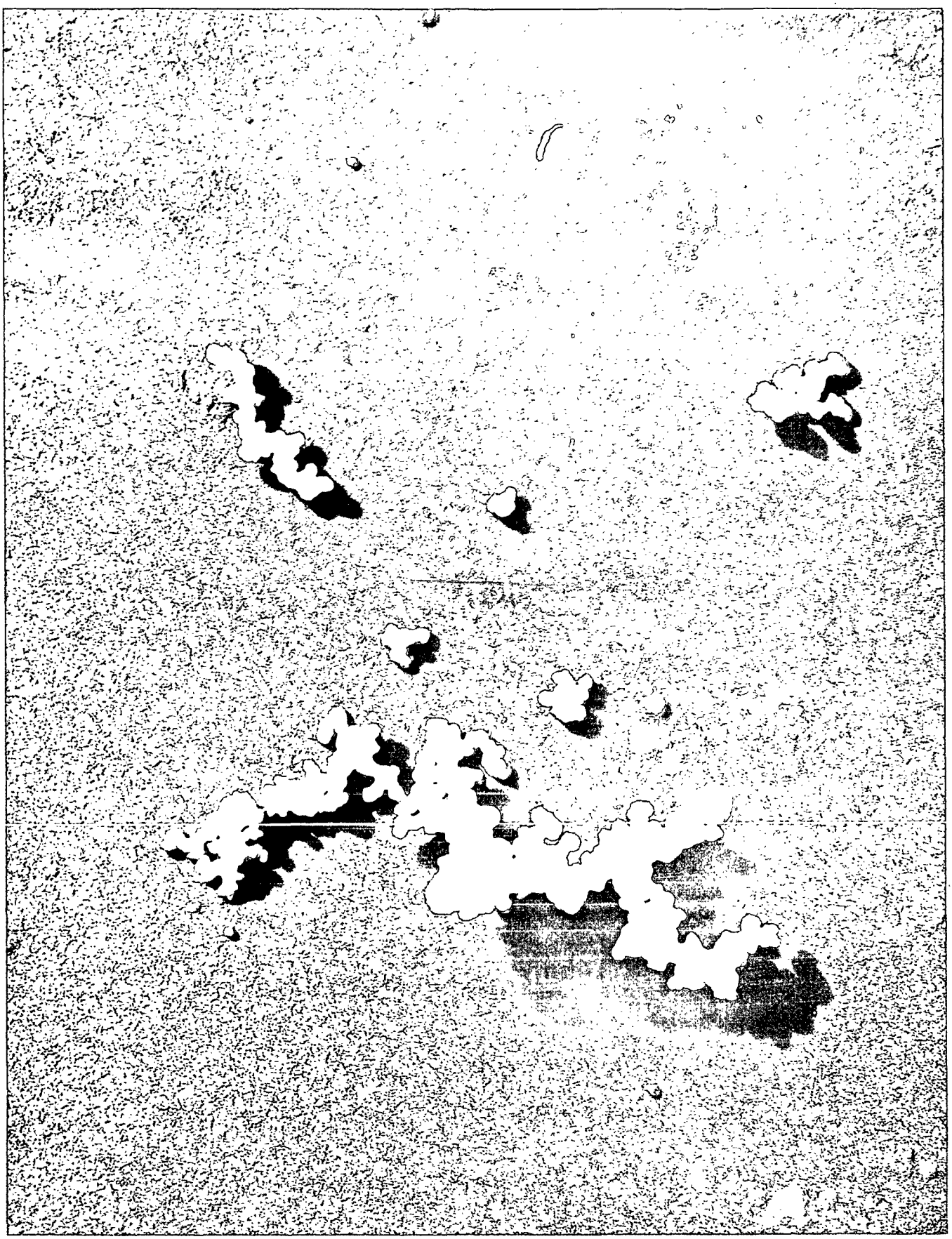

Figure 10. Electron Photomicrograph of Crystalline Guar Triacetate, Palladium Shadowed at 30° (34,500X)

Fig. 9 shows that the particles seem to be thin platelets, certain of which have a more or less regular shape that appears to be hexagonal. (It should be kept in mind that only a few of the platelets would be in focus in Fig. 9, since the twisted coil is at approximately right angles to the electron beam as evidenced by the shadow.) An enlargement of Fig. 9 is shown in Fig. 11 and shows, in a few instances, the hexagonal shape which is similar to that obtained by Yundt (52) for crystalline xylan from barley straw and by Marchessault (53) for crystalline xylan from esparto grass. The possibility exists that the platelets, or at least a portion of them, may be similar to the layered spherulites obtained by Manley (54) with cellulose triacetate.

INFRARED ANALYSIS OF FRACTIONS

Since none of the other fractions listed in Table III gave a visual indication of crystallinity, an infrared analysis was made on material from Fractions 1 and 4. It should be kept in mind that the slurry containing Fraction 1 had been warmed on a steam bath to concentrate it. Fraction 4 (as well as the other fractions) was not subjected to this heating cycle. The infrared analysis indicated that the two materials were identical from a chemical viewpoint.

PREPARATION AND FRACTIONATION OF GUARAN TRIACETATE

PREPARATION OF GUARAN

Guaran was isolated by preparing a 0.25% solution of guar gum in distilled water. The guar gum used was the previously described material prepared by Haug (44). The water was heated to 75°C. on a steam bath, and the gum was dusted into the rapidly agitated water. The temperature was maintained at 75°C. for one hour, and the resulting solution was then allowed to stand overnight in a constant temperature room (22.2 $\pm$ 0.5°C.).

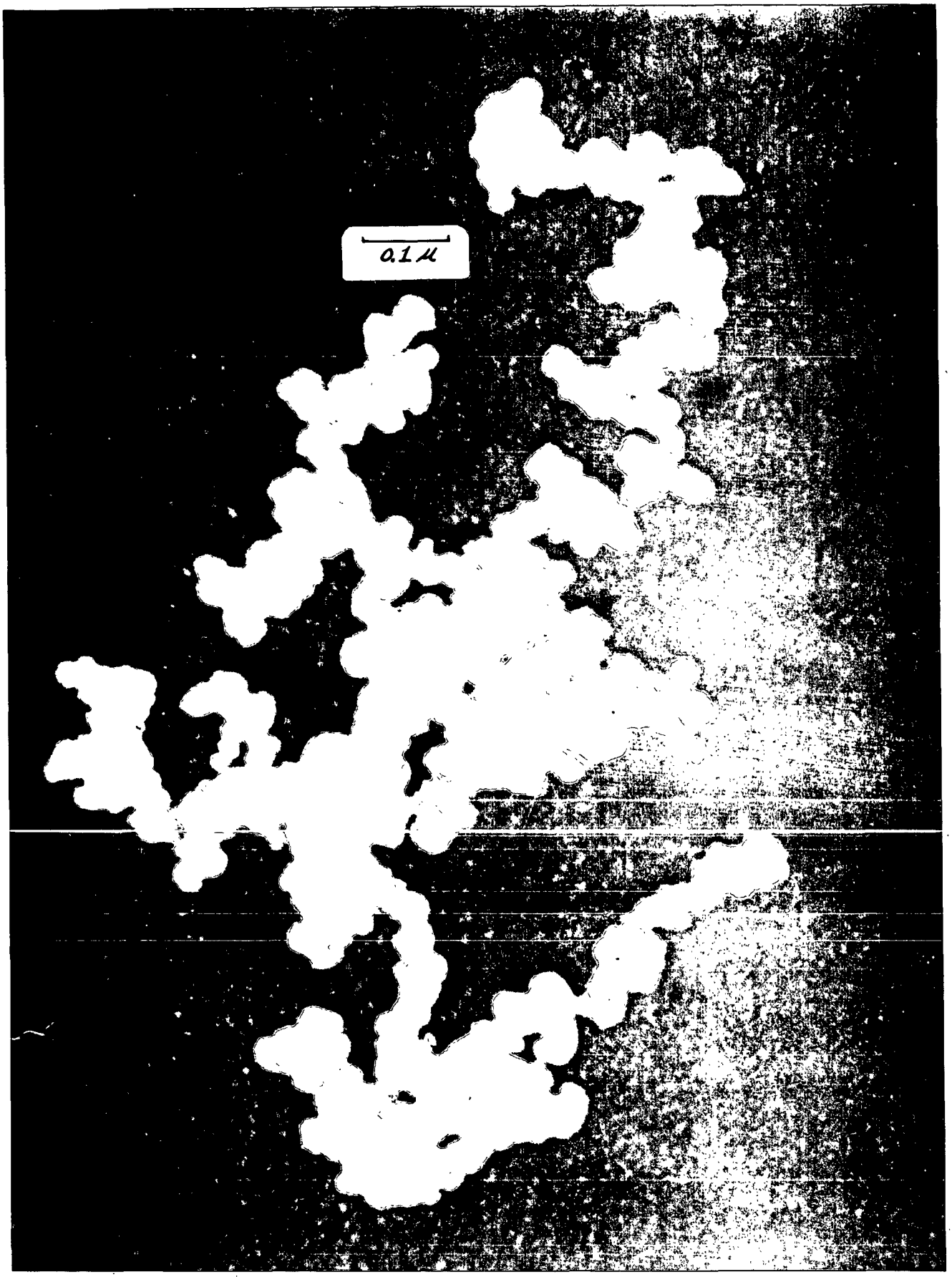

Figure 11. Enlargement of the Particle of Guar Triacetate Shown in Fig. 9 (Scale Indicator Indicates Enlargement)

While rapidly agitating the gum solution, 25% ethanol by volume was slowly added. After standing 24 hours at constant temperature, the suspension was centrifuged in a laboratory centrifuge* at 2400 r.p.m. to remove the precipitated gum. The fraction insoluble in 25% ethanol represented 12.2% of the original gum.

After centrifugation, the concentration of ethanol was increased to 40% by volume in the supernatant liquid to obtain the fraction termed guaran by Heyne and Whistler (3). The suspension was allowed to stand at constant temperature (22.2°C.) for four days to insure complete precipitation. Guaran was removed by centrifugation in a Sharples Super Centrifuge using a rotor speed of 40,000 r.p.m. and a flow rate which yielded a clear supernatant liquid. The precipitate of guaran was filtered and placed in absolute ethanol for six hours to remove residual water. Then the guaran was again filtered and placed in absolute ethyl ether for 14 hours. The ether was removed by filtration and the product was dried in a vacuum desiccator at 22.5°C. Guaran represented 86.0% of the guar gum which agrees favorably with the 86.5% value previously reported (3).

The supernatant liquid was allowed to evaporate to dryness, and the fraction soluble in 40% ethanol was found to represent 2.0% of the guar gum.

PREPARATION OF GUARAN TRIACETATE

Guaran was acetylated by the method of Carson and Maclay (48) as described by McKee (49) and previously designated as Method II. The guaran acetate had an acetyl content of 44.66% as determined by the Eberstadt method (50) indicating that a triacetate had been formed (theoretical value 44.78%). The melting point range

*International Centrifuge, Size 2, Model V. Hereafter when a laboratory centrifuge is specified, this particular one is implied.

was found to be 226-227°C. This compares favorably with the melting point range of 224-226°C. which Heyne and Whistler (3) found for their guaran triacetate.

SOLUBILITY OF GUARAN TRIACETATE

Initially, it was assumed that the usual cellulose acetate solvents could be used for guaran triacetate. However, it was found that the polymer was not completely soluble in a number of these solvents at concentrations high enough to make them readily usable in light-scattering studies. In order to make an intelligent choice of solvent, a systematic approach based on the use of solubility parameters was employed. A brief discussion of the theory behind the use of solubility parameters is given in Appendix I. A more detailed discussion will be found elsewhere (55-58).

Attempts to prepare several solutions of guaran triacetate in various solvents were made by warming approximately 0.5 to 1% solutions for 15-20 minutes in a water bath at 50 to 60°C. The solutions were then placed in a rotary device and rotated for 48 hours at room temperature. The results are shown in Table V along with the appropriate solubility parameters, δ. The value of δ for guaran triacetate was found to be 11.1 when calculated from the polymer's structural formula by means of Small's (56) table of molar attraction constants.

From Table V, it can be seen that the data do not fall into any coherent pattern. These results are similar to those found by Burrell (58) for cellulose acetate and cellulose nitrate. This same author found definite ranges of δ over which solvents could be found for ethyl cellulose and chlorinated rubber.

It was found that if the polymer was first wet with a small amount of non-solvent, such as ethanol, solution could be more readily effected. Therefore, some of the solvents in Table V which showed gel particles probably would not have had

TABLE V

SOLUBILITY PARAMETERS AND SOLVENCY OF GUARAN TRIACETATE, δ = 11.1

Solvent	δ	Solubility by Visual Observation[d]	Solubility by Second Virial Coefficient	Reference for δ
Methanol	14.5	I	--	(57)
Ethanol	12.7	I	--	(57)
Formamide	12.2	G	--	(a)
Acetonitrile	11.9	S	Good Solvent	(57)
n-Propanol	11.9	I	--	(57)
i-Propanol	11.5	I	--	(57)
Cyclohexanol	11.4	G	--	(57)
Nitroethane	11.1	S	--	(58)
Pyridine	10.7	P	--	(55)
Tetrachloroethane	10.2	P	--	(a)
1,1,2-Trichloroethane	10.2	S	Poor Solvent	(a)
Acetone	10.0	P	--	(57)
Dioxane	10.0	P	--	(55)
Ethyl lactate	10.0	P	--	(57)
1,2,3-Trichloropropane	9.8	S	Poor Solvent	(a)
Chloroform	9.7	P	--	(55)
Butyl bromide	9.6	I	--	(a)
Dimethyl formamide	9.6	P	--	(a)
Methyl acetate	9.6	P	--	(57)
Ethyl citrate	9.5	P	--	(b)
Acetyl acetone	9.4	S	--	(a)
Dimethyl phthalate	9.4	P	--	(57)
Phenylacetonitrile	9.4	P	--	(a)
Benzene	9.2	I	--	(57)
Ethyl acetate	9.1	P	--	(57)
Cyclohexylacetate	8.9	I	--	(a)
Carbon tetrachloride	8.6	I	--	(55)
Mesitylene	8.0	G	--	(a)
Triethyl amine	7.6	I	--	(a)
n-Butyl ether	7.4	I	--	(a)
Chloroacetonitrile	--	S	--	(c)
Dimethylsulfoxide	--	S	--	(c)

[a] Calculated from the energy of vaporization (57).
[b] Calculated from molar-attraction constants (56).
[c] Necessary data for calculating δ could not be found.
[d] Visual observation consisted of noting complete solubility of solid, use of ethanol to precipitate polymer from clear solution if some solid remained, or of evaporating clear solution to dryness if ethanol did not precipitate polymer. S = Soluble, I = Insoluble, P = Mostly soluble with a small amount of insoluble gelatinous material, G = Mostly insoluble gelatinous phase with a small amount of soluble polymer.

them present if a preliminary treatment with nonsolvent had been used. Chloroform is one example of this.

Debye and Cashin (59) have pointed out that light-scattering theory is for polymer-single solvent systems and application of the theory to mixed solvent-polymer systems may produce anomalous results. It is for this reason that even the addition of small amounts of a nonsolvent was avoided.

Purification of Acetonitrile

Acetonitrile was chosen as a suitable solvent to use for an investigation of guaran triacetate. The refractive index gradient of the polymer in this solvent is of the proper magnitude for light scattering and ultracentrifugation. In addition, the partial specific volume of the polymer and the density of this solvent are such that the polymer will sediment in the gravitational field of the centrifuge.

Practical-grade acetonitrile obtained from the Matheson, Coleman, and Bell Company was purified by a method described by Vermillion (60). Four liters of acetonitrile are shaken for less than a minute with saturated aqueous potassium hydroxide, stored over anhydrous sodium carbonate for at least 12 hours, and then distilled twice from a small amount of phosphorus pentoxide. The glass distillation column which had a three-fourth inch inside diameter was packed to a height of 61 inches with single-turn 1/4 by 1/32-inch glass helices.

Starting with four liters of practical-grade acetonitrile, which had been given the above preliminary treatment, the distillation was carried out at 95% reflux ratio until approximately 200 ml. of distillate were collected. This first fraction was discarded. Then the distillation was continued at 25% reflux ratio until about three liters were collected for redistillation. The remaining solvent

was discarded. Fresh phosphorus pentoxide was added to the three liters collected for redistillation and the second distillation was begun. Again about 200 ml. were collected at 95% reflux ratio and discarded. Then about two and one-half liters were collected at 25% reflux ratio for use and the remaining residue was discarded. The purified acetonitrile was stored under nitrogen until used.

FRACTIONATION OF GUARAN TRIACETATE

Fractionation procedures are based on the small difference in solubility between molecules of different molecular weight. Fractional precipitation is the most widely used method of fractionation. In this method, a precipitant is slowly added to a dilute polymer solution until a slight turbidity results at the temperature chosen for fractionation. The turbid solution is then warmed to dissolve the precipitate. This warming technique insures equilibrium between the precipitate, when it forms, and the supernatant solution. Then, the solution is allowed to slowly cool with stirring to the fractionation temperature. The supernatant phase is then removed and the polymer in the precipitated phase, the first fraction, is recovered. Precipitant is then added to the supernatant solution until turbidity develops and the procedure is repeated to obtain the next fraction.

Certain conditions must be met to ensure as sharp a fractionation as possible. The polymer solution should be as dilute as practical, and care should be taken that the polymer precipitates in an amorphous state rather than in a semicrystalline state. Inefficient fractionation will result from the high local concentrations of precipitant that exist near the immediate point of precipitant addition. Thus, as mentioned above, the solution must be warmed after the precipitate is formed to yield a homogeneous solution from which precipitation then may take place at the constant temperature used for the fractionation.

The process of precipitation is regarded as a separation of a polymer solution into two liquid phases (24). The phase rich in polymer is termed the precipitate and the other is the supernatant phase. The polymer is partitioned between these two phases with each phase containing all molecular species. However, the smaller molecules will be distributed at more nearly equal concentrations in the two phases. They have fewer units per molecule to be influenced by the less desirable supernatant phase and will show less discrimination than do the large molecules between the two phases. Thus, if the volume of the supernatant phase is made much larger than that of the precipitate, a great deal more of the low molecular weight material will be retained in it. As a result of this, a sharper fractionation will be obtained if the solution is as dilute as possible. From a practical standpoint, a concentration of about one gram per liter should be employed (61).

Two types of equilibrium may exist between the two phases. The supernatant phase may be in equilibrium with a crystalline polymer phase or with a liquid amorphous polymer phase. If the equilibrium is with a crystalline phase, the fractionation is the most selective (13). However, this solution-crystalline polymer equilibrium is very slowly approached, and unless excessive times are employed, the equilibrium will be between solution and a semicrystalline polymer phase. In this latter instance, the fractionation is severely limited. Since equilibrium is easily approached if one phase is in an amorphous state, it is more practical to seek this type of precipitate.

Prior to solution, 9.9 grams of guaran triacetate were placed in a 9-liter pyrex bottle and 300 ml. of 95% ethanol were added. The polymer was allowed to stand in the nonsolvent for 24 hours at room temperature. Then 2900 ml. of chloroform were added to the slurry, and the mixture was agitated for 24 hours to effect solution.

To obtain a fraction, 95% ethanol was slowly added to the rapidly agitated polymer solution until a persistent turbidity was obtained. To ascertain persistent turbidity at the earliest time, the precipitant was added to the solution in a dark room and a penlight flashlight was shone into the solution. The Tyndall effect easily showed the presence of turbidity at the earliest possible time. Just before the condition of constant turbidity was reached, addition of a small amount of precipitant produced a white haze which quickly disappeared. The point of persistent turbidity was taken to be the point where this haze remained after waiting a few minutes to ensure thorough mixing.

Then the solution was heated on a steam bath until a homogeneous solution was again obtained. It never was necessary to heat above 35°C. to effect solution of the precipitate. The warm solution was allowed to slowly cool with stirring at constant temperature (22.2 $\pm$ 0.5°C.) for 24 hours or more. The turbid solution was then centrifuged for 10-15 minutes in a laboratory centrifuge at about 1000 g. to obtain the fraction. The precipitate was then washed from the centrifuge bottles with a chloroform–ethanol mixture that had the same composition as the supernatant solution.

This procedure was repeated until a total of seven fractions was obtained. Then, since the addition of two liters of ethanol produced no precipitate, the solution was evaporated to dryness at room temperature in a hood. The fractions had a transparent "gel-like" appearance after centrifugation and did not show any indications of crystallinity. (When the volume of the solution exceeded the capacity of the 9-liter bottle, a 5-gallon stainless steel container with a friction-fit cover was used as a container.)

Table VI summarizes the results of this fractionation. Fraction 1 was very small and contained mostly dust that had been in the solution. It was not used

TABLE VI

RESULTS OF FRACTIONATION OF GUARAN TRIACETATE FROM A CHLOROFORM SOLUTION BY PRECIPITATION WITH 95% ETHANOL

Fraction No.	Volume of $CHCl_3$, ml.	Volume of Ethanol Added, ml.	Ratio of Polymer to Solution, g./ml.	Weight of Fraction, g.	Fraction of Total Polymer
Initial Solution	2900	300	3.2×10^{-3}	9.90	1.000
1[a]	3100	5450	1.2×10^{-3}	0.03	0.003
2	3130	5980	1.1×10^{-3}	4.42[b]	0.442
2A	1450	2200	1.1×10^{-3}	1.35[b]	0.136
2B	1450	2200	7.2×10^{-4}	2.29[bc]	0.231
2C	1450	2400	8.3×10^{-5}	0.14[b]	0.014
3	3180	6080	6.4×10^{-4}	0.94	0.095
4	3210	6355	5.1×10^{-4}	1.39	0.140
5	3240	6855	3.6×10^{-4}	1.48	0.150
6	3270	7355	2.0×10^{-4}	0.62	0.063
7	3300	7855	1.3×10^{-4}	0.22	0.022
8	3300	9855[d]	9.4×10^{-5}	0.39	0.039

[a]Fraction 1 contained mostly dust that had been in the solution. It was not used in the ensuing work.

[b]Since Fraction 2 was very large, it was refractionated into three fractions, 2A, 2B, and 2C in the above table. 3.92 g. of Fraction 2 was used.

[c]After Fraction 2A was obtained, the solution was warmed to 30°C. and then held at constant temperature for 34 hours. No precipitant was added.

[d]After two liters of ethanol had been added to the supernatant solution from Fraction 7, no cloud point could be observed and the last fraction was obtained by evaporating the solution.

in any of the ensuing work. Fraction 2 was very large, and 3.92 grams of it were refractionated into 3 fractions, 2A, 2B, and 2C, by the method described above. It is noteworthy that after Fraction 2A was obtained, the supernatant solution still had a very slight haze. No precipitant was added to this solution, but it was heated to 30°C. where the haze disappeared. Fraction 2B was obtained by allowing this solution to stand at the constant temperature (22.2°C.) for 34 hours, after which time a very definite precipitate was formed. Fraction 2C was obtained by the conventional method of adding precipitant to the supernatant phase after removal of Fraction 2B.

The amount of chloroform in the solution varied during the fractionation since the precipitated polymer was washed from the centrifuge bottles with small amounts of a chloroform–ethanol mixture that was of the same composition as the supernatant polymer solution. After the precipitate settled to the bottom of the container, this solution was added to the supernatant solution, thereby increasing the amount of chloroform and ethanol present.

ULTRACENTRIFUGATION

EXPERIMENTAL DETERMINATION OF MOLECULAR WEIGHT DISTRIBUTION

It was pointed out previously that the theories on the hydrodynamic properties of polymers assume that all of the molecules in a given fraction have the same molecular weight. Experimentally one must work with fractions that are not homogeneous, and one must make assumptions concerning the molecular weight distribution if a comparison between experiment and theory is to be made. In order to obtain a reliable estimate of the molecular weight distributions of the various fractions of guaran triacetate, a direct determination of the molecular weight distributions for two key fractions was made. The ultracentrifugal procedure used and the resulting

molecular weight distributions of Fractions 2B and 3 are given in the following sections.

SEDIMENTATION VELOCITY ANALYSIS

Molecular weight distributions were determined by the method described by McCormick (62) and in greater detail by Taylor (63). The method is based on a boundary analysis of schlieren photographs taken during a sedimentation velocity experiment performed in an ultracentrifuge. A distribution of sedimentation coefficients is obtained which, after correction for diffusion and concentration-dependent sedimentation, ultimately leads to a distribution of molecular weights. Once the distribution of molecular weights is known, the appropriate molecular weight averages can be obtained by means of a summation procedure based on the definition of the molecular weight average in question.

Experimental Methods and Calculation Procedure

During acceleration of the ultracentrifuge to the speed at which the sedimentation velocity experiment is to be conducted, the gravitational field gradually builds up and sedimentation takes place. To correct for this, the following expression is used,

$$t_e = (1/\omega_f)^2 \int_0^t \omega^2 dt, \tag{56}$$

where t_e is the equivalent time of operation at the desired speed, ω_f, and ω is the angular speed at the time t.

The sedimentation velocity experiment is conducted in a synthetic boundary cell and schlieren photographs are taken at periodic intervals from the time the

boundary is first formed between the solvent and the solution until the molecules have sedimented to the bottom of the cell. The first photograph should be taken before there has been any noticeable movement of the boundary.

The first step in calculation of the data is determination of the apparent distribution function, $g^*(S)$. The apparent distribution function, which yields the relative amount of a molecular species with a sedimentation coefficient S, is given by

$$g^*(S) = (dc/dx)\,\omega^2 t_e x^3/x_o^2 C_o. \tag{57}$$

In this expression, dc/dx is the concentration gradient which is proportional to the height of the schlieren curves (and to the refractive index gradient) at a distance x from the center of rotation, ω is the angular speed of rotation in radians per second, t_e is the time of the particular photo, x_o is the original boundary location, and C_o is the solution concentration in optical units at the time t_e and for the sector cell used is given by

$$C_o = \int_{x_1}^{x_2} (x/x_o)^2 (dc/dx)\,dx. \tag{58}$$

The value of S at the distance x is determined from

$$S = (1/\omega^2 t_e)\ln(x/x_o). \tag{59}$$

The entire distribution curve is obtained by determining $g^*(S)$ values for 20 or more points which describe the refractive index gradient curve and then plotting them against the corresponding sedimentation coefficient.

The apparent distribution function is broadened by diffusion and sharpened by concentration effects. The method for determining the diffusion correction,

which is important in many cases, can be found elsewhere (63, 64). It was negligible for guaran triacetate in acetonitrile.

Correction of the $g(S)$ versus S curve for concentration effects is accomplished by selecting a photograph taken at a time t_e near the middle of the run. (Note that $g(S)$ is the distribution function corrected for diffusion.) From this run one calculates dC/dS from the relation

$$dC/dS = g(S)C_o\exp(-2\omega^2 S t_e). \tag{60}$$

The actual concentration in the cell, C_S, is then calculated as a function of S by means of

$$C_S = k\tan\phi\int_0^S (dC/dS)dS, \tag{61}$$

in which ϕ is the schlieren blade angle at which the photograph was taken and k is a constant for the system that relates the optical units to the actual concentration. The value of k may be determined from

$$k = cA_o\tan\phi, \tag{62}$$

where c is the original concentration of the solution in g./dl. and A_o is the area of the schlieren peak at the time in question and is given by

$$A_o = \int_{x_1}^{x_2} (dc/dx)dx. \tag{63}$$

The concentration dependence of S in the low concentration range may be expressed by

$$S = S^o/(1 + k_s c). \tag{64}$$

In this expression, k_s is obtained from a plot of $(1/S)$ against c, the actual concentration, and S^o is the sedimentation coefficient extrapolated to zero concentration. It is possible to calculate a value of S^o for each value of C_S and S. With S^o known as a function of S the value of dS/dS^o is graphically determined. The frequency function is then corrected by using

$$g(S^o) = g(S)(dS/dS^o). \tag{65}$$

The distribution corrected for diffusion and concentration effects is then plotted as $g(S^o)$ versus S^o.

The $g(S^o)$ versus S^o co-ordinates may be transformed into $f(M)$, the distribution function which yields the relative amount of a molecular species with molecular weight M, versus M co-ordinates in the following manner. First, it is necessary to have a known relationship between S^o and M which is of the form

$$S^o = k'M^d, \tag{66}$$

where k' is the proportionality constant. This expression will transform S^o into M. To transform $g(S^o)$ into $f(M)$, the following relation is applied (62),

$$f(M) = g(S^o)(dS^o/dM) = g(S^o)(k')^2/2S^o. \tag{67}$$

To make these transformations, the exponent in Equation (66) should equal 0.5 (62).

Determination of Average Molecular Weights

With $f(M)$ and M known, the various average molecular weights may be determined by a summation process and application of the following definitions for the various averages.

$$M_n = \int_0^\infty f(M)dM \Big/ \int_0^\infty [f(M)/M]dM \tag{68}$$

$$M_w = \int_0^\infty f(M)MdM \Big/ \int_0^\infty f(M)dM \tag{69}$$

$$M_z = \int_0^\infty f(M)M^2dM \Big/ \int_0^\infty f(M)MdM \tag{70}$$

Since $\underline{f(M)dM}$ represents the weight fraction of material with molecular weight between $\underline{M}$ and $\underline{M} + \underline{dM}$, $\int_0^\infty \underline{f(M)dM} = 1$. These expressions may be written in terms of $\underline{S}^o$ and $\underline{g}(\underline{S}^o)$ by using Equation (67) to transform the various terms.

$$M_n = (k')^{-2} \Big/ \int_{S_1}^{S_2} [g(S^o)/(S^o)^2]dS^o \tag{71}$$

$$M_w = (k')^{-2} \int_{S_1}^{S_2} (S^o)^2 g(S^o)dS^o \tag{72}$$

$$M_z = (k')^{-2} \int_{S_1}^{S_2} (S^o)^4 g(S^o)dS^o \Big/ \int_{S_1}^{S_2} (S^o)^2 g(S^o)dS^o \tag{73}$$

RESULTS

Sedimentation velocity data were obtained in acetonitrile at 25.0°C. in a Spinco Model E Ultracentrifuge operating at 56,100 r.p.m. utilizing a single sector, synthetic boundary cell and the schlieren optical system. The molecular weight distribution was determined on unfractionated guaran triacetate and on Fractions 2B and 3 of this polymer. The molecular weight distribution of Fraction 3 should be the broadest since it lies at the head of the Fraction 3 to 8 sequence. Since

the fractionation solution became more dilute as each succeeding fraction was removed, the sharpness of the fractionation should increase somewhat as one proceeds down the sequence. Fraction 2B will be broader than 2C, but narrower than 2A.

The concentration dependence of the sedimentation coefficient was determined from sedimentation velocity runs made on Fraction 2B in the concentration range of 0.5 to 0.05 g./dl. Figure 12 is a plot of $1/\underline{S}$ versus $\underline{c}$, the concentration in g./dl., and indicates that over the concentration range covered, Equation (64) does not represent the data and the equation should be in the form

$$S = S^{o}/(1 + k_s c + k'_s c^2 + \ldots). \qquad (74)$$

However, at the lower concentrations Equation (64) is sufficient as indicated by the linear extrapolation. The equation of this line is $\underline{S} = \underline{S}^{o}/(1 + 10\underline{c})$.

The run made at a concentration of 0.128 g./dl. was used to evaluate the molecular weight distribution for Fraction 2B. Values of $\underline{g}^*(\underline{S})$, $\underline{g}^*(\underline{S})/\underline{g}^*(\underline{S})_{max}$, and $\underline{S}$ were calculated, and by using the previously mentioned procedure, the diffusion correction was found to be negligible. A photo taken at 954 seconds, which was near the middle of the run, was selected to use for the concentration correction. Since the diffusion correction was negligible, $\underline{g}^*(\underline{S}) = \underline{g}(\underline{S})$. The plot of $\underline{g}(\underline{S})$ versus $\underline{S}$ is shown in Fig. 13.

For the appropriate values of $\underline{g}(\underline{S})$ and $\underline{S}$, values of $\underline{dC}/\underline{dS}$ were calculated and are shown in Fig. 14. With $\underline{dC}/\underline{dS}$ known, values of $C_{\underline{S}}$ were calculated for each value of $\underline{S}$, and the value of $\underline{S}^{o}$ was determined from $\underline{S}^{o} = \underline{S}(1 + 10C_{\underline{S}})$. Figure 15 is a plot of $\underline{S}$ versus $\underline{S}^{o}$ from which $\underline{dS}/\underline{dS}^{o}$ was graphically determined to use in Equation (65) for calculation of the true distribution function $\underline{g}(\underline{S}^{o})$. The true distribution of sedimentation coefficients is shown in Fig. 16. The $\underline{g}(\underline{S}^{o})$ versus

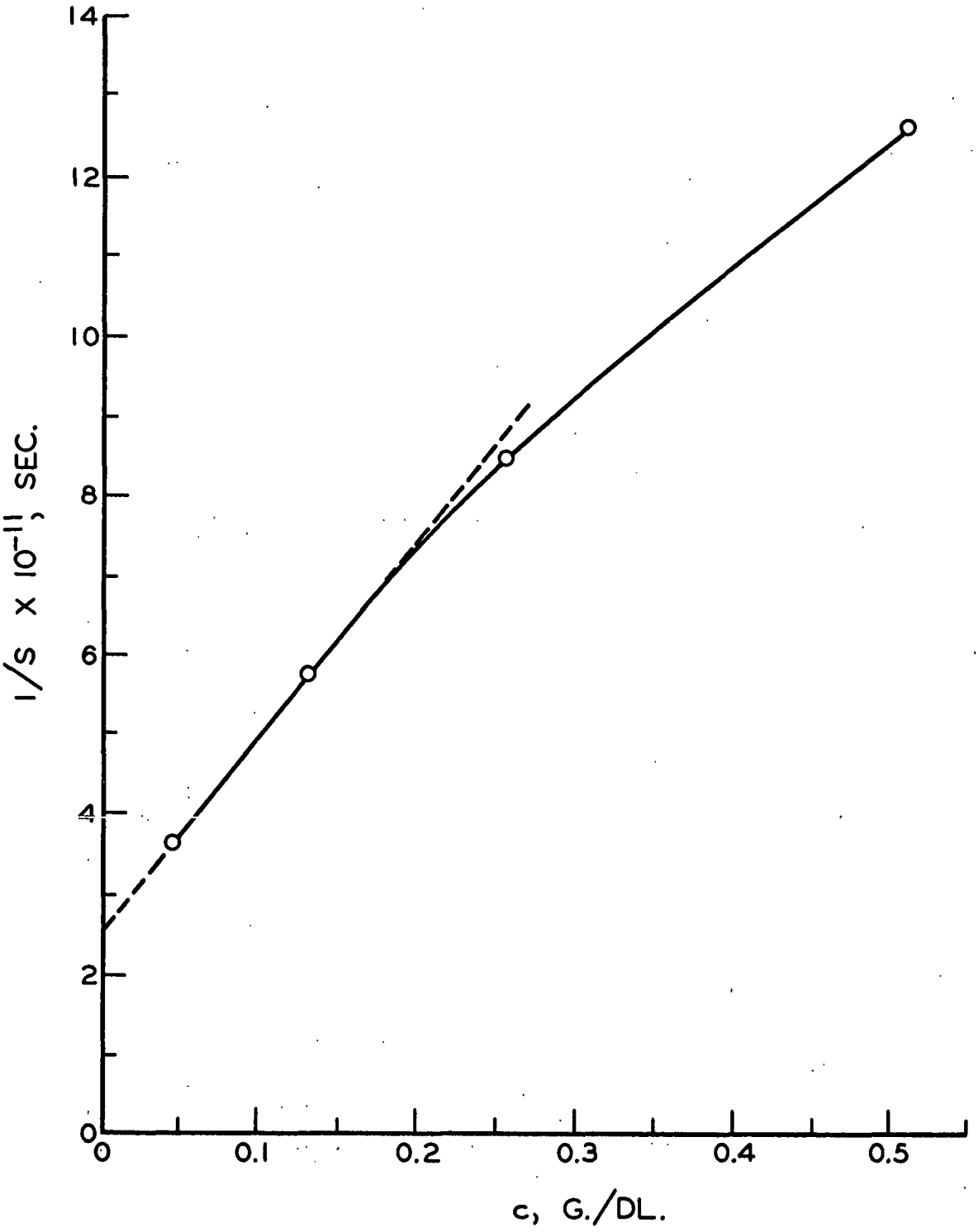

Figure 12. Concentration Dependence of the Sedimentation Coefficient Determined from the Maximum Ordinate. Fraction 2B, Guaran Triacetate in Acetonitrile, 25.0°C. Schlieren Blade Angle, 70°. Linear Portion of the Curve is Expressed by $\underline{S} = (40 \times 10^{-13})/(1 + 10\underline{c})$.

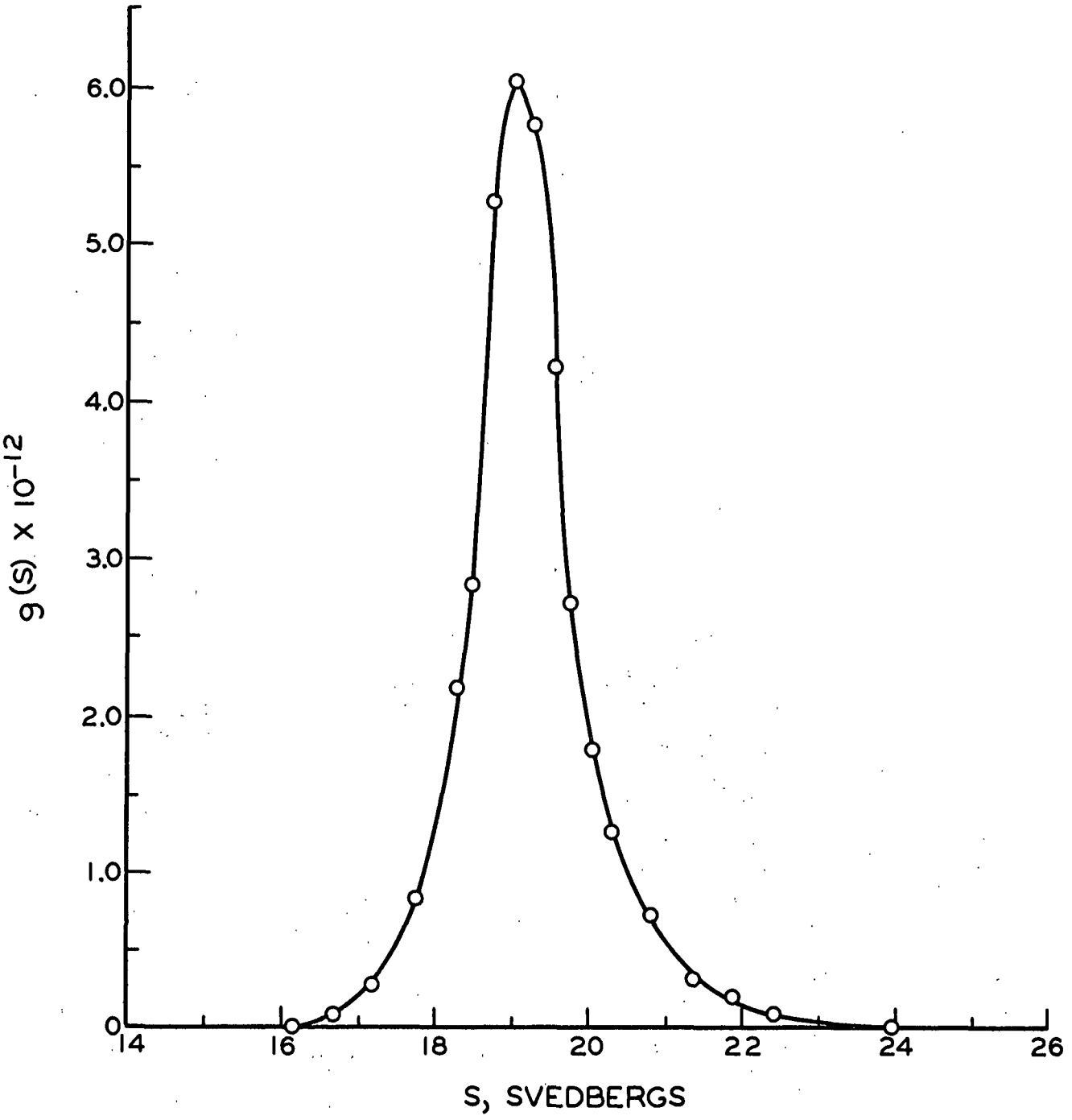

Figure 13. Distribution Function, $g(S)$ Versus the Sedimentation Coefficient, S. Fraction 2B, Guaran Triacetate in Acetonitrile, 25.0°C., c = 0.128 g./dl., 954 Seconds at 56,100 r.p.m.

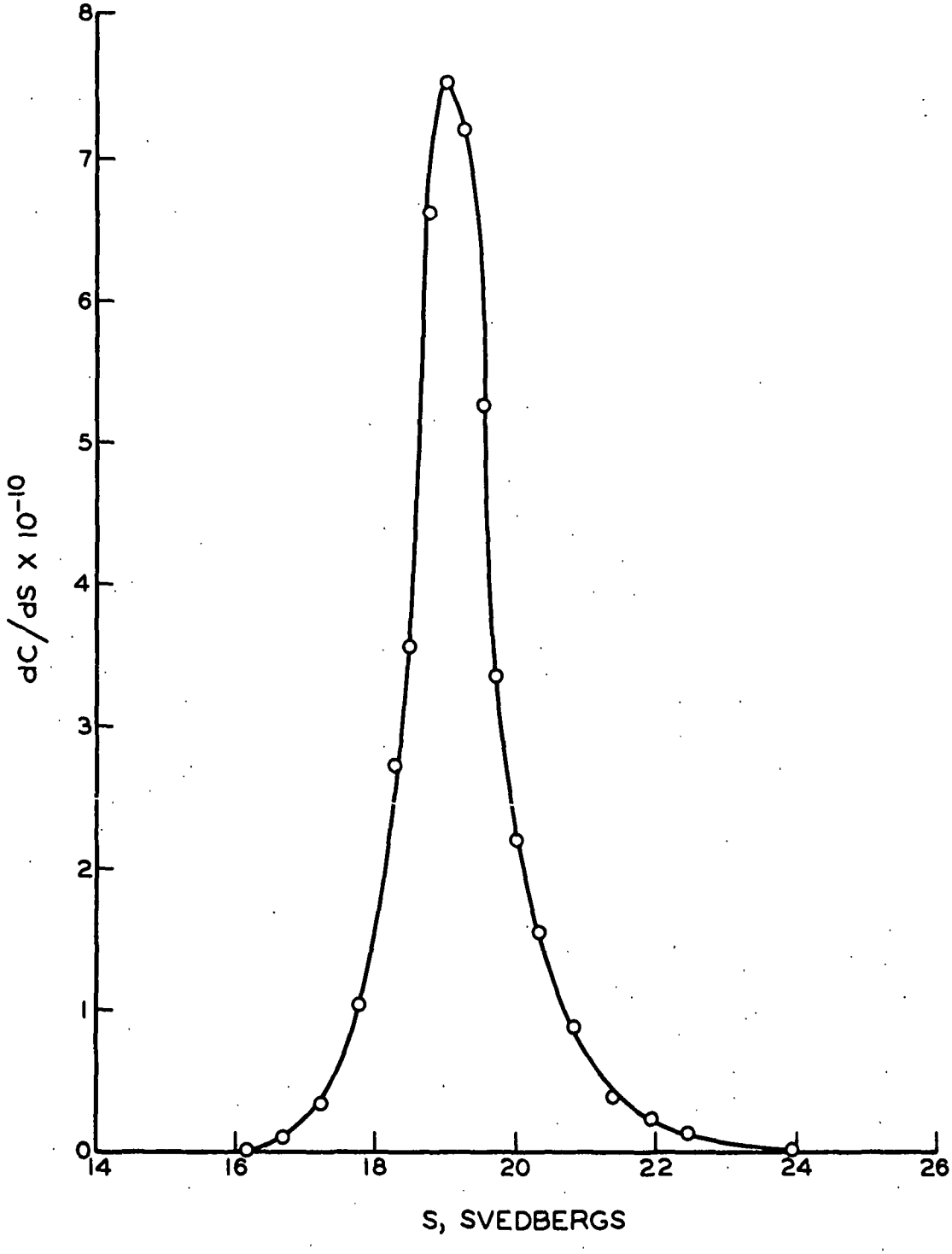

Figure 14. Calculated Values of dC/dS as a Function of Sedimentation Coefficient. Fraction 2B, Guaran Triacetate, Determined in Acetonitrile at 25.0°C.

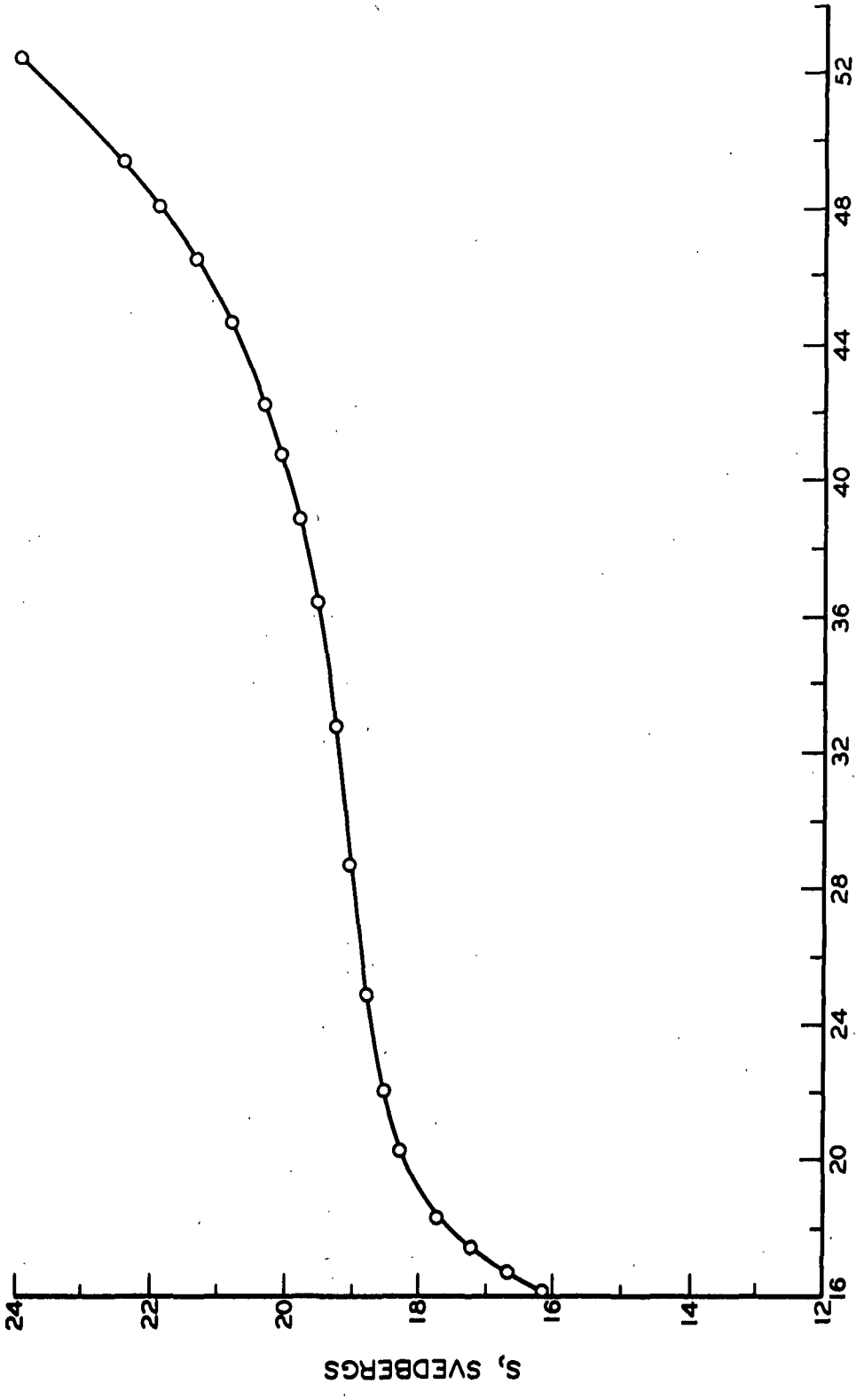

Figure 15. Apparent Sedimentation Coefficient, $\underline{S}$, as a Function of the Sedimentation Coefficient Corrected for Concentration Effects, $\underline{S}^{o}$, Used in Graphically Determining $d\underline{S}/d\underline{S}^{o}$. Fraction 2B, Guaran Triacetate Determined in Acetonitrile at $\bar{2}\bar{5}.\bar{0}^{o}\bar{C}$.

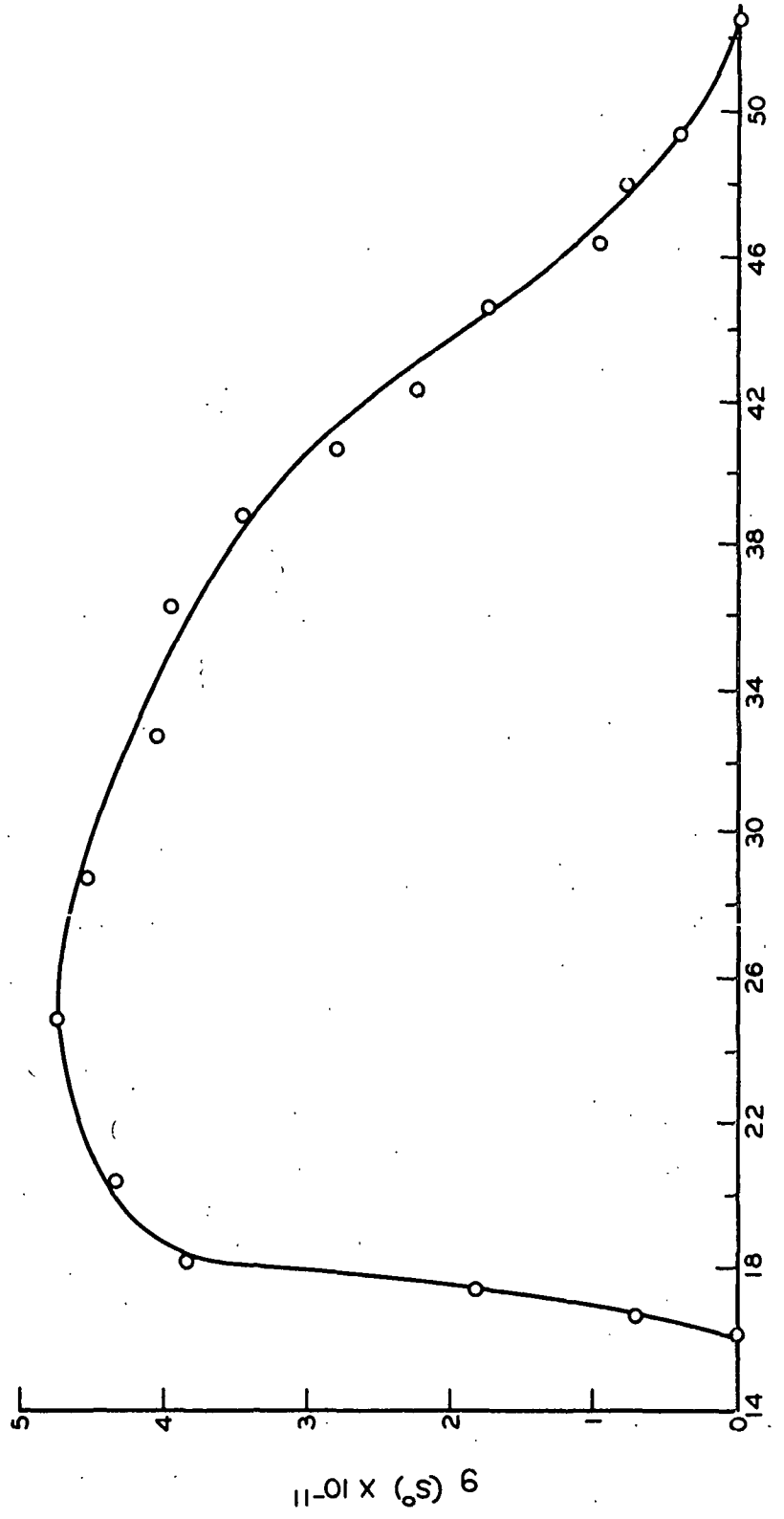

Figure 16. True Distribution of Sedimentation Coefficients for Fraction 2B, Guaran Triacetate. Determined in Acetonitrile at 25°C.

$\underline{S}^{\circ}$ co-ordinates were transformed into $\underline{f}(\underline{M})$ versus $\underline{M}$ co-ordinates as shown in Fig. 17. To accomplish this transformation, it was assumed that the exponent in Equation (66) was equal to 0.5. The basis for this assumption was the small value of the second virial coefficient and the exponent in the equation $[\eta] \sim \underline{M}^{0.52}$ which fits the fractions investigated (these facts will be brought out in the ensuing work).

For Fraction 3 and for the unfractionated polymer, the sedimentation velocity runs were made at a concentration of 0.109 g./dl. The photographs selected for evaluation of the concentration correction were taken at 629 seconds for Fraction 3 and at 528 seconds for the unfractionated guaran triacetate. The diffusion correction was assumed negligible on the basis of the work done on Fraction 2B. Figures 18 and 19 show the distribution of sedimentation coefficients and of molecular weights for Fraction 3, and Fig. 20 and 21 show the same characteristics for the unfractionated polymer.

The value of $\underline{k}'$ in Equation (66) was found to be 1.55×10^{-15} by utilizing the weight average molecular weight of Fraction 2B obtained from light-scattering measurements. The mean sedimentation coefficient corrected for concentration effects, $\overline{\underline{S}}^{\circ}$, was obtained by means of the expression

$$\overline{S}^{\circ} = \int g(S^{\circ}) S^{\circ} dS^{\circ}. \qquad (74)$$

The value of $\overline{\underline{S}}^{\circ}$ was found to be 35.5 svedbergs, 34.1 svedbergs, and 27.0 svedbergs and $\underline{M}_{\underline{z}}:\underline{M}_{\underline{w}}:\underline{M}_{\underline{n}}$ was 2.7:1.8:1.0, 1.9:1.7:1.0, and 2.1:1.6:1.0 for the unfractionated polymer, for Fraction 2B, and for Fraction 3, respectively. The ratio of weight average to number average molecular weight indicates that the fractions are quite polydisperse and a sizable correction will be required in certain of the following work.

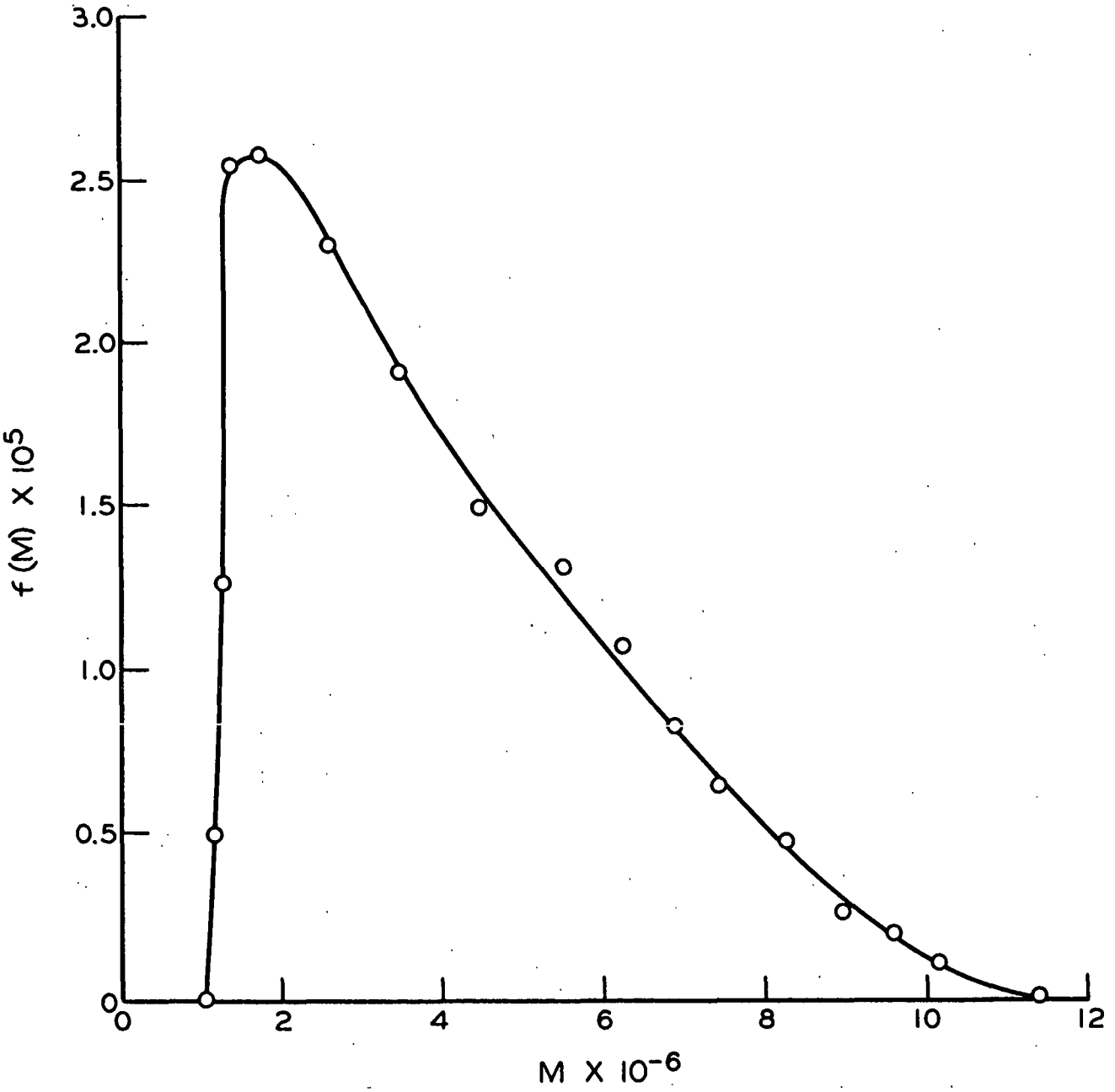

Figure 17. Molecular Weight Distribution of Fraction 2B, Guaran Triacetate. Determined in Acetonitrile at 25.0°C.

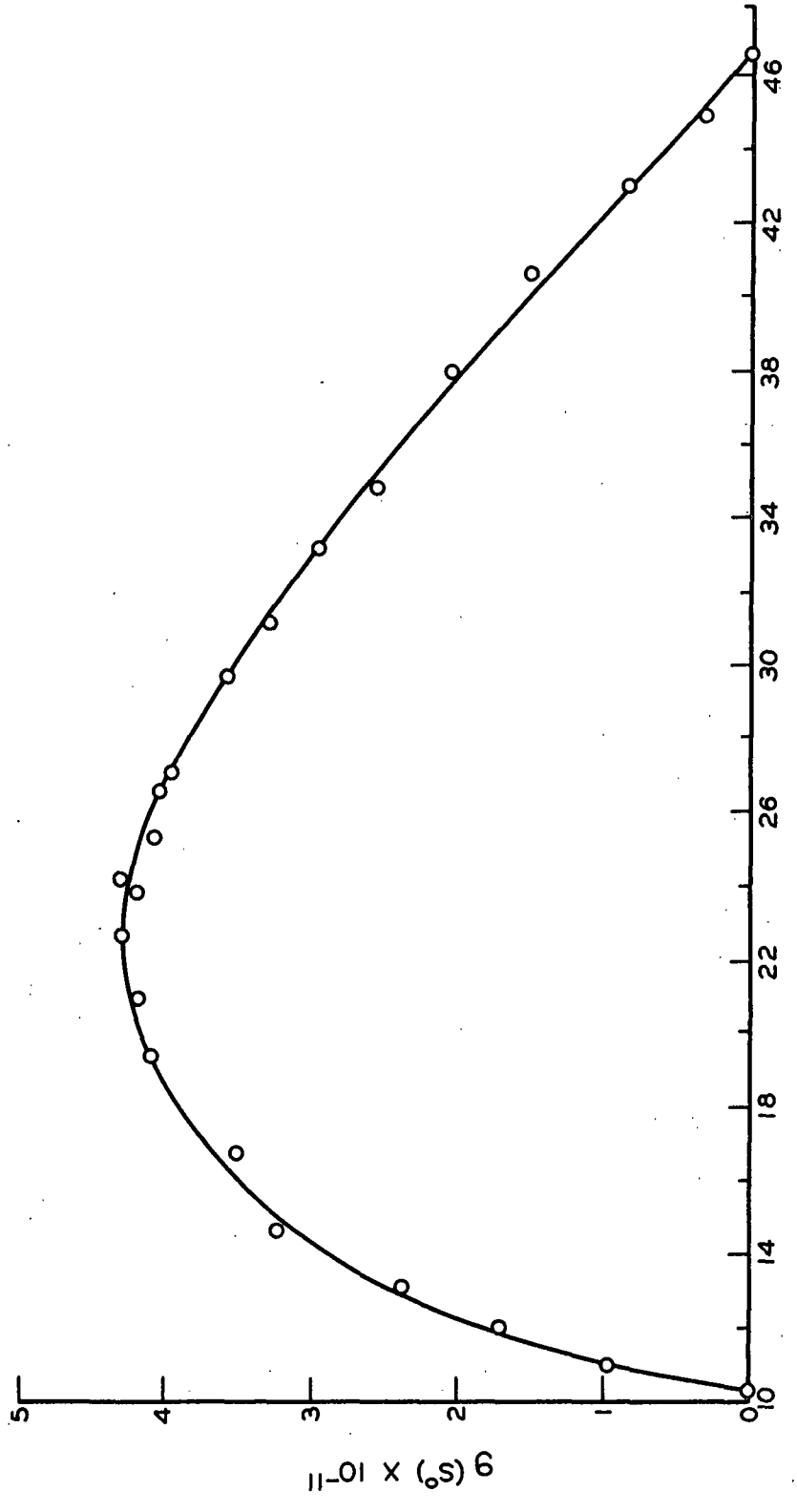

Figure 18. True Distribution of Sedimentation Coefficients for Fraction 3, Guaran Triacetate. Determined in Acetonitrile at 25.0°C.

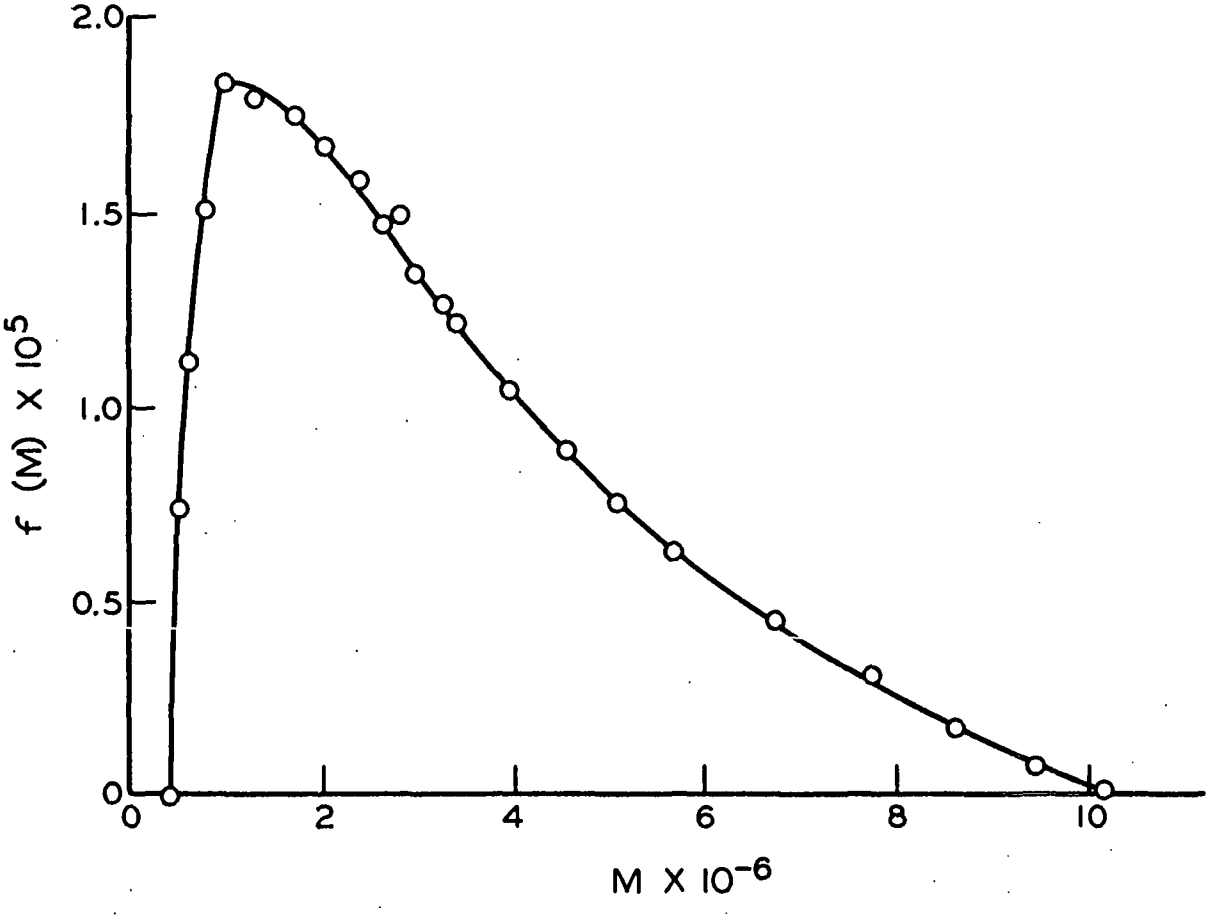

Figure 19. Molecular Weight Distribution of Fraction 3, Guaran Triacetate. Determined in Acetonitrile at 25.0°C.

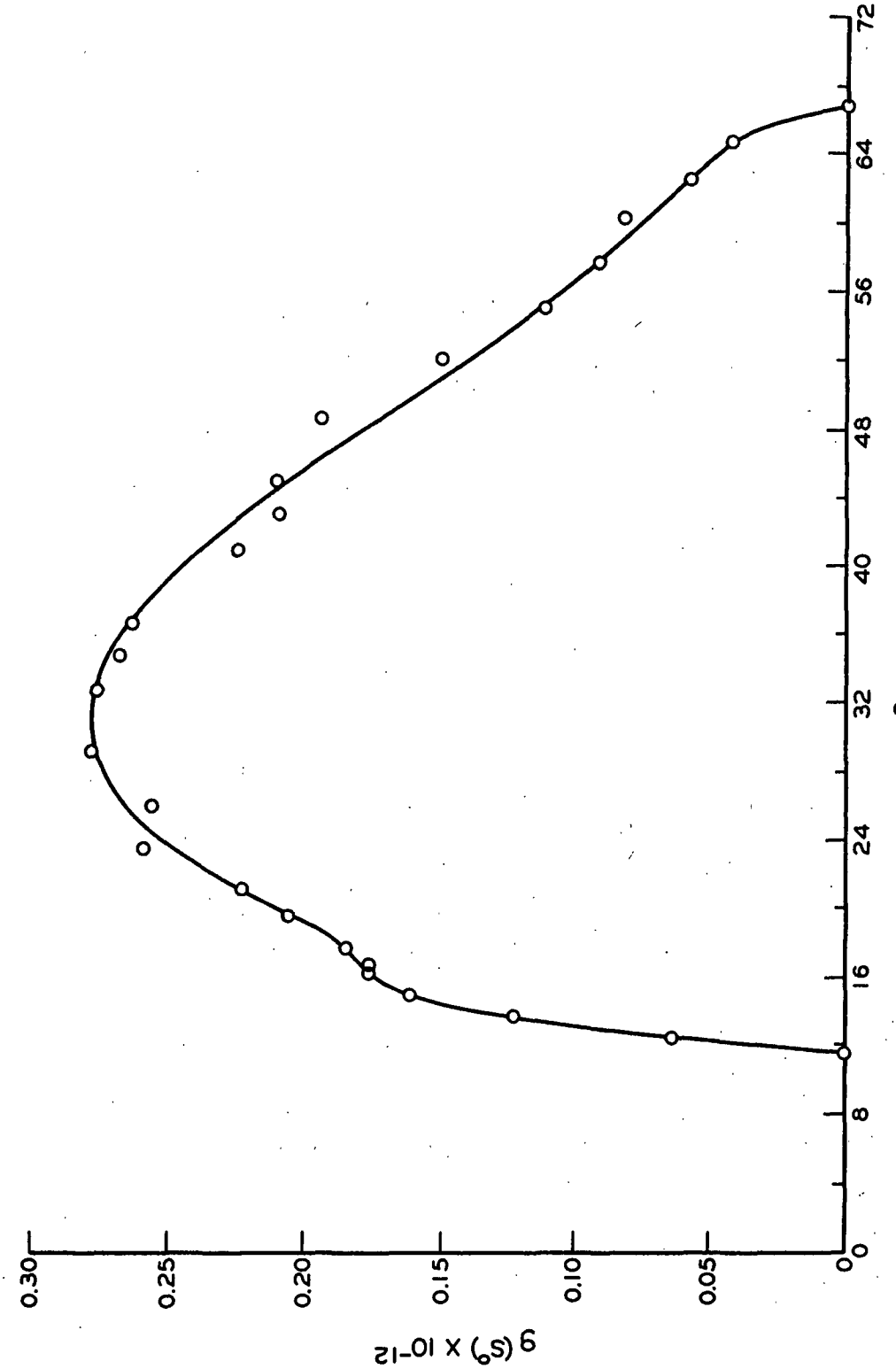

Figure 20. True Distribution of Sedimentation Coefficients for Unfractionated Guaran Triacetate. Determined in Acetonitrile at 25.0°C.

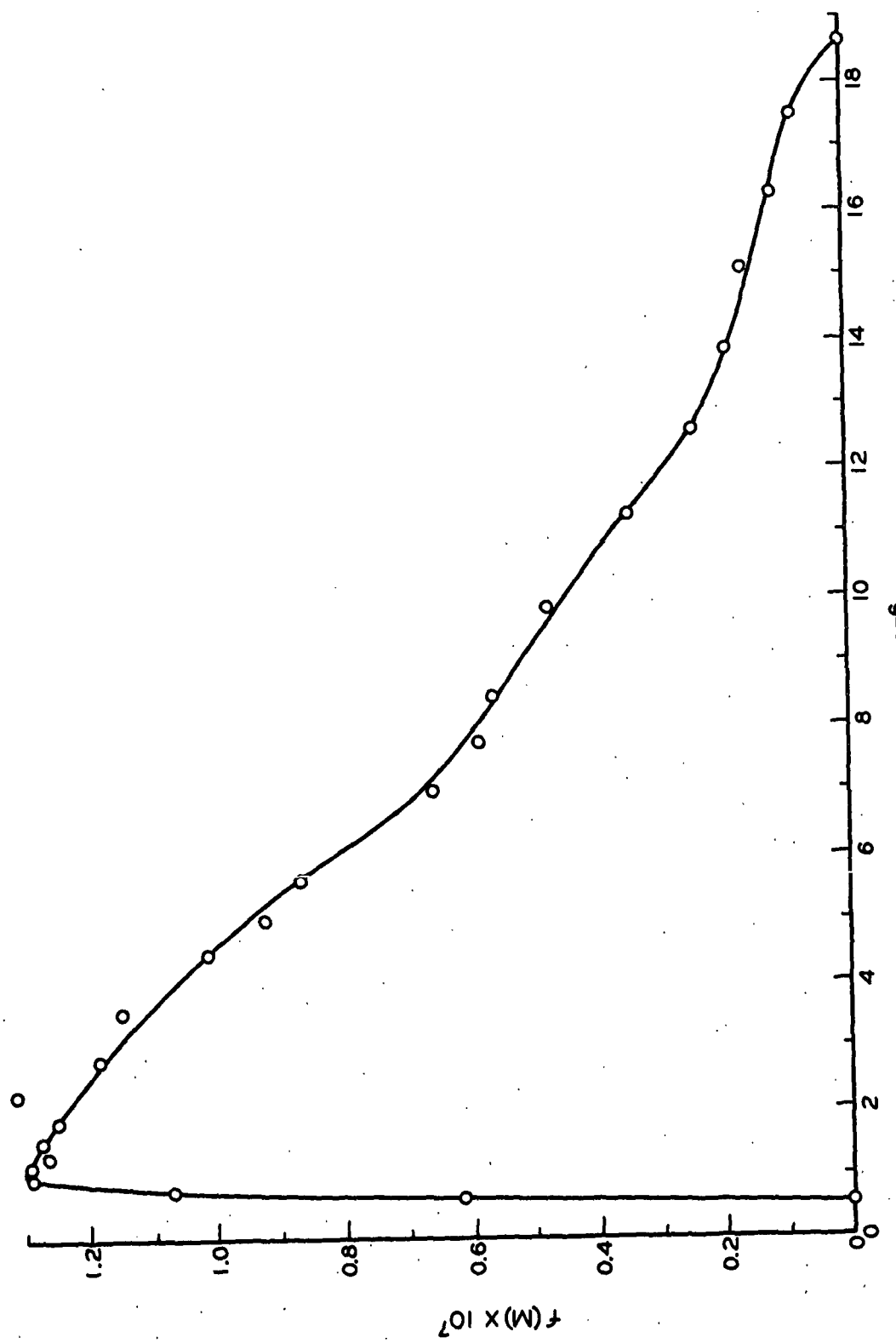

Figure 21. Molecular Weight Distribution of Unfractionated Guaran Triacetate. Determined in Acetonitrile at 25.0°C.

It should be noted that in determining the true distribution of sedimentation coefficients, the value for k_s, see Equation (64), of 10 dl./g. was used to evaluate S^o from the value of S. This value of k_s was determined from the concentration dependence of the maximum ordinate sedimentation coefficient for Fraction 2A. Yamakawa (65) recently has shown that k_s is proportional to the intrinsic viscosity, and therefore it is proportional to the square root of the molecular weight. Thus, actually k_s varies according to the molecular weight at a given point within the distribution of sedimenting molecules. However, for the two fractions investigated, it is felt that this correction to the shape of the distribution curves will not greatly alter the ratio of $M_z:M_w:M_n$. For the unfractionated polymer which undoubtedly has a broader distribution of molecular weights than the fractions, the correction will be sizable and the ratio of the various molecular weight averages could be significantly disturbed. Therefore, the true distributions and ratios given for the unfractionated polymer should be regarded as a first approximation of the true values for these quantities.

LIGHT SCATTERING

THEORETICAL BASIS OF THE METHOD

The manner in which the intensity of light scattered by a dilute polymer solution depends on its concentration and on the angle of observation has been developed by Debye (66) and by Zimm (39, 67). It has been found that the reciprocal absolute turbidity, $1/\tau$, of the solution is represented by

$$(Hc/\tau) = [1/M_w P(\theta)] + 2A_2 c + \ldots \qquad (75)$$

where H is a constant, c is the concentration in g./ml., M_w is the weight average molecular weight, $P(\theta)$ is a function of the scattering angle θ and is termed the

particle scattering factor (66, 68), and A_2 is the second virial coefficient which is a measure of the polymer-solvent interaction.

To determine the molecular weight, the size and shape of the molecules in solution, and the polymer-solvent interaction coefficient, values of Hc/τ are plotted as a function of $\sin^2(\theta/2)$ and concentration as described by Zimm (39, 67). For the Brice-Phoenix instrument, the value of the absolute turbidity, τ, is obtained from the expression

$$\tau = [16TD/3(1.045)h][n_o^2 R_w/R_c]\,(a)(r/r')[\sin\theta/(1+\cos^2\theta)]\,x$$
$$[(FG_\theta/G_0)_{solution} - (FG_\theta/G_0)_{solvent}], \qquad (76)$$

where

- TD = experimentally determined product of the diffuse transmittance of an opal glass reference standard and a diffuser correction factor
- h = diaphragm width
- a = working standard constant
- n_o = refractive index of the solvent
- R_w/R_c = correction factor for incomplete compensation of refraction effects
- r/r' = calibration factor for narrow slit system and circular cell
- $\sin\theta$ = correction factor for the volume change on viewing the solution at different angles
- $1/(1+\cos^2\theta)$ = correction factor applied when unpolarized light is used
- F = filter factor
- G_θ = galvanometer reading at angle θ
- G_0 = galvanometer reading at angle $\theta = 0°$.

The constant H embodies a number of optical terms and is obtained from

$$H = 32\pi^3 n_o^2 (dn/dc)^2 / 3\lambda^4 N_A, \qquad (77)$$

where

dn/dc = specific refractive index gradient

λ = wavelength of light used

N_A = Avogadro's number.

Values of Hc/τ are determined as a function of angle at a number of concentrations. Extrapolations are then made at constant scattering angle to zero concentration to determine $(Hc/\tau)_{\theta,c=0}$ by plotting $(Hc/\tau)_{\theta,c}$ versus concentration, and at constant concentration to zero scattering angle to determine $(Hc/\tau)_{\theta=0,c}$ by plotting $(Hc/\tau)_{\theta,c}$ versus $\sin^2(\theta/2)$. The values of $(Hc/\tau)_{\theta,c=0}$ and $(Hc/\tau)_{\theta=0,c}$ are in turn extrapolated to zero angle and zero concentration, respectively, to determine $(Hc/\tau)_{\theta=0,c=0}$. The data may be summarized by plotting the values of Hc/τ as a function of $\sin^2(\theta/2) + kc$, where k is an arbitrary constant chosen so as to make the concentration values suitably spread out. The resulting Zimm plot is a gridlike graph with two limiting lines—$(Hc/\tau)_{\theta,c=0}$ versus $\sin^2(\theta/2)$ and $(Hc/\tau)_{\theta=0,c}$ versus kc. A typical Zimm plot is shown in Fig. 22.

Determination of Weight Average Molecular Weight and z-Average Radius of Gyration

The zero concentration curve of the Zimm plot obtained from Equation (75) is described by

$$(Hc/\tau)_{\theta,c=0} = 1/\bar{M}_w P(\theta). \qquad (78)$$

The angular dependence of light scattering, $P(\theta)$, due to the interference of electromagnetic waves in the molecular domain of a molecule with N links and $N+1$ scattering centers (monomeric units) is given by the expression (69)

$$P(\theta) = (2/(N+1)^2) \sum_i \sum_j \sin(\mu r_{ij})/(\mu r_{ij}). \qquad (79)$$

with $\mu = (4\pi/\lambda')\sin(\theta/2)$. The wavelength of light in the medium used is given by $\lambda/n_o = \lambda'$. The distance between pairs of the scattering centers is denoted by r_{ij}. For molecules having the shape of spheres, Gaussian coils, or rods this expression reduces to simple analytical expressions. For molecules that are between a rod and a Gaussian coil, i.e., those which are non-Gaussian coils, Benoit and Doty (69) show that the sine in Equation (79) may be expanded into an equation of the form

$$P(\theta) = 1 - (A\mu^2/3) + (B\mu^4/60) - (C\mu^6/2520) + \ldots , \qquad (80)$$

where A can be shown to be the mean-square radius of gyration of the molecule about its center of gravity, $(\bar{s}^2)$.* Zimm (39) shows that the particular averaging in this expression results in the z-average mean-square radius of gyration, $(\bar{s}^2_z)$. If the reciprocal of $P(\theta)$ is expanded and only the lower angles are considered, that is for small values of μ, the expansion is given by

$$1/P(\theta) = 1 + (\bar{s}^2_z)\mu^2/3, \qquad (81)$$

with the higher terms being negligible. Thus, the second term in the expansion of $1/P(\theta)$ measures the radius of gyration for a particle of any shape. On substitution of Equation (81) into Equation (78) and substituting for μ the following expression is obtained,

$$(Hc/\tau)_{\theta,c=0} = (1/M_w)[1 + (16\pi^2/3(\lambda')^2)(\bar{s}^2_z)\sin^2(\theta/2)]. \qquad (82)$$

Therefore, the intercept of the zero concentration line, $(Hc/\tau)_{\theta=0,c=0}$, is equal

*Benoit and Doty (69) have listed the expressions for A, B, and C and the derivation showing A to be the mean-square radius of gyration.

to the reciprocal of the weight average molecular weight, and the initial slope of this line yields $(\overline{s}_z^2)$ by means of the relationship

$$(\overline{s}_z^2) = [3(\lambda')^2/16\pi^2][(\text{Initial Slope})_{\theta, c=0}/(\text{Intercept})_{\theta=0, c=0}]. \quad (83)$$

It should be kept in mind that the radius of gyration of the molecule determined in this manner is universal and independent of coil structure or model (69, 70). Kurata, Yamakawa, and Teramoto (35) examined the effect of excluded volume on $(\overline{s}_z^2)^{1/2}$ determined by this angular variation and concluded that it yields the true $(\overline{s}_z^2)^{1/2}$ irrespective of the excluded volume.

Determination of Weight Average Molecular Weight and Second Virial Coefficient

The zero angle curve of the Zimm plot obtained from Equation (75) is described by

$$(Hc/\tau)_{\theta=0, c} = (1/\overline{M}_w) + 2A_2c, \quad (84)$$

which is identical to Equation (75) except for the $P(\theta)$ term which becomes unity at $\theta = 0$. The intercept of this line, $(Hc/\tau)_{\theta=0, c=0}$, is again the reciprocal of the weight average molecular weight and the slope is equal to twice the second virial coefficient.

Dissymmetry Methods (71)

The Zimm method is useful when the root-mean-square (RMS) end-to-end distance, $(\overline{r}^2)^{1/2}$, is greater than about 1000 A. When these limits are not met, the dissymmetry method first introduced by Debye (72) is usually used. This method allows determination of the weight average RMS end-to-end separation, $(\overline{r}_w^2)^{1/2}$, M_w, and A_2 with the limitations noted below.

The dissymmetry, $\underline{Z}$, is defined as the ratio of the scattering intensities at two angles which are symmetrical about 90°. Usually the angles of 45° and 135° are chosen, since the term $(\sin\theta/1 + \cos^2\theta)$ in Equation (76) can be ignored, and the value of $\underline{Z}$ is obtained from

$$Z = \left\{ \frac{(G_{45}F/G_0)_{solution} - (G_{45}F/G_0)_{solvent}}{(G_{135}F/G_0)_{solution} - (G_{135}F/G_0)_{solvent}} \right\} . \qquad (85)$$

Since the dissymmetry depends on concentration, its value at zero concentration (the intrinsic dissymmetry, $[\underline{Z}]$) must be evaluated by plotting either $\underline{Z}$ or $1/(\underline{Z} - 1)$ against concentration and extrapolating to zero concentration.

Equation (75) may be rewritten as

$$(Hc/\tau) = [1/M_w P(90°)] + 2A_2 c. \qquad (86)$$

When $(\underline{Hc}/\tau)$ determined from the 90° scattering intensity is plotted against concentration, the intercept, $(\underline{Hc}/\tau)_{90°,\underline{c}=0}$, is equal to the reciprocal of $\underline{M}_{\underline{w}}\underline{P}(90°)$. It was noted in the above that Equation (79) for $\underline{P}(\theta)$ reduces to simple analytical expressions for particles of definite shape. These expressions have been evaluated by Beattie and Booth (40, 73) and values of $\underline{P}(90°)$ and $(\underline{\bar{r}^2_w})^{1/2}$ have been tabulated in terms of the dissymmetry for disks, spheres, coils, and rods. However, to utilize these tables one must either know the shape of the molecule in solution beforehand or assume a molecular shape (which must, of course, be one for which the various values have been determined). In addition, the tables for coils are applicable only for $[\underline{Z}] \leq 2$. Above this value, the tables are restricted to measurements made on flexible linear polymers dissolved in theta solvents. Kurata, Yamakawa, and Teramoto (35) examined the effect of excluded volume on dissymmetry calculations and concluded that the values of $\underline{P}(90°)$ and $[\underline{Z}]$ do deviate from their true values as a result of this effect. However, the deviation is small and within experimental

error. They conclude that near the theta temperature the dissymmetry provides a reliable measure of $(\bar{r}^2)^{1/2}$.

The second virial coefficient, A_2, may be estimated from the slope of this line; however, it should be noted that this value is determined from the 90° scattering angle. The more rigorous method of extrapolating to zero angle is preferred to this method for evaluating A_2.

EXPERIMENTAL

Light-Scattering Apparatus and Working Equations

Light-scattering measurements were made using a Brice-Phoenix Universal Light Scattering Photometer (Series 1937). For the particular instrument used, Equation (76) becomes (75)

$$\tau = 1.14(n_o^2 R_w/R_c)a(r/r')[\sin\theta/(1+\cos^2\theta)][(FG_\theta/G_0)_{solution} - (FG_\theta/G_0)_{solvent}] \quad (87)$$

at wavelength 4358 A. and

$$\tau = 1.21(n_o^2 R_w/R_c)a(r/r')[\sin\theta/(1+\cos^2\theta)][(FG_\theta/G_0)_{solution} - (FG_\theta/G_0)_{solvent}] \quad (88)$$

at wavelength 5461 A. The value of a was found to be 0.0397 at 4358 A. and 0.0508 at 5461 A., (r/r') was equal to 1.232 at both wavelengths, and the appropriate value of $(n_o R_w/R_c)$ was obtained from the Brice-Phoenix operation manual (74).

Performance of Light-Scattering Apparatus

The performance of the light-scattering photometer was checked by evaluating the Rayleigh ratio, $R_{90} = (3\tau/16\pi)$, for benzene and for toluene and the excess turbidity, τ, of a 0.5% solution of Cornell standard polystyrene (75) in toluene at 22.5°C. At wavelengths of 4358 A. and 5461 A., the respective values for the

Rayleigh ratio, R_{90}, were 47.9×10^{-6} cm.$^{-1}$ and 16.8×10^{-6} cm.$^{-1}$ in benzene, 62.4×10^{-6} cm.$^{-1}$ and 20.4×10^{-6} cm.$^{-1}$ in toluene, and for the turbidity of the Cornell standard polystyrene the respective τ_{90} values were 3.50×10^{-3} and 1.37×10^{-3} cm.$^{-1}$. These are in good agreement with the published values (76). Appendix II contains data on the B-6 polystyrene of McCormick (62) and serves as a further check on the performance of the apparatus.

Solvent

Acetonitrile, purified by the previously mentioned method, was the primary solvent used for the light-scattering investigation. Before the solvent was used in light scattering, it was filtered through 2500 A. pore size solvent-resistant Polypore filters under nitrogen pressure directly into the light-scattering cell and its dissymmetry was checked. It was then refiltered in the same manner and the dissymmetry rechecked. The dissymmetry of the solvent (and the solutions) was constant after five filtrations. Therefore, the solvent was always filtered five times before being used for dilution or other purposes in light scattering. The density of acetonitrile is 0.7798 at 22.5°C. and 0.7770 at 25.0°C. (77). The refractive index is 1.3532 at 4358 A. and 1.3475 at 5461 A. (78).

A small amount of work on the unfractionated polymer was done using 1,2,3-trichloropropane and 1,1,2-trichloroethane. However, the refractive index gradient of the polymer in these latter solvents was very small and a large error could have been introduced by using them. In addition, their density was not of such a nature as to make them amenable to ultracentrifugation.

Solutions

Solutions of the fractions of guaran triacetate in acetonitrile were made up by weight and the appropriate concentration in g./ml. was calculated from the

density at the temperature used assuming that the density of the solution was identical to the density of the solvent. The dust was removed from Fractions 2A through 4 by centrifuging in specially designed dust exclusion cells (79) in a laboratory centrifuge equipped with a high-speed head* at 16,500 r.p.m., approximately 16,000 g., for 1-1/2 hours in a helium atmosphere. Fractions 5 through 8 were filtered through 4500 A. solvent-resistant Polypore filters under nitrogen pressure five times after which the dissymmetry was constant. Both clarification methods provided adequate dust removal without changing the solution concentration. The solution was transferred to the light-scattering cell, Brice-Phoenix C-101, with a syringe. Sufficient solution for viscometry was clarified at the same time. Dilution was accomplished by adding filtered solvent to the cell from a separatory funnel.

Refractive Index Gradient Measurements

The refractive index gradient, $\underline{dn}/\underline{dc}$, was measured for the guaran triacetate solutions on a Rayleigh interferometer (Baird Associates, Cambridge, Mass.). Interference fringes were matched at various concentrations of polymer solution, and $\underline{dn}/\underline{dc}$ was calculated from the relation

$$dn/dc = [(D - D_o)/47]\ \lambda/cL, \qquad (89)$$

where

$\underline{D}$ = instrument drum reading for the solution

$\underline{D}_o$ = instrument drum reading for the solvent

λ = wavelength of light used, 5.461×10^{-5} cm.

$\underline{c}$ = solution concentration, g./ml.

$\underline{L}$ = length of the optical path through the solution, 1.00 cm.

$(\underline{D} - \underline{D}_o)/47$ = number of interference fringes.

*International Equipment Company part No. 296, 4 place, 40° angle head. Maximum radius 6.4 cm., minimum radius 2.5 cm., average radius 4.95 cm.

The refractive index gradient had the value of 0.120 ml./g. for guaran triacetate in acetonitrile.

Depolarization Correction

The depolarization correction accounts for the additional scattering that arises from the differences in polarizability along different axes of the molecule, that is, for the molecules anisotropy (80). The correction for this effect has been related to the depolarization ratio, ρ_u, by Cabannes and Rocard (81) through the following ratio

$$C_u = (6 - 7\rho_u)/(6 + 6\rho_u) \tag{90}$$

where C_u, the Cabannes factor, is multiplied times the observed molecular weight to obtain the true average molecular weight. The depolarization ratio is given by

$$(\rho_u)_c = \left\{ \frac{(FG^H_{90}/G^H_0)_{solution} - (FG^H_{90}/G^H_0)_{solvent}}{(FG^V_{90}/G^V_0)_{solution} - (FG^V_{90}/G^V_0)_{solvent}} \right\} \tag{91}$$

where $(\rho_u)_c$ is the value at a given concentration and must be extrapolated to zero concentration to obtain ρ_u. The superscripts H and V, respectively, refer to the horizontal and the vertical components of the scattered light. They are measured by placing a polaroid lens in the proper position between the cell and the photomultiplier tube.

The value of C_u for all fractions of guaran triacetate in acetonitrile was 0.89 ± 0.03.

Light-Scattering Measurements

The unfractionated polymer was examined using light of 4358 A. and 5461 A. wavelength. Since the results were in close agreement, the 4358 A. wavelength

was used to examine the various fractions of guaran triacetate, since it produced higher scattering intensities and the depolarization correction was smaller than at 5461 A. Fluorescence was negligible at both wavelengths.

Results

The results of the experimental light-scattering investigation are presented in the form of Zimm plots* in Fig. 22 through 31. Fraction 8 was not handled in this manner and the results obtained with it will be given in the ensuing work. For Fractions 6 and 7, see Fig. 30 and 31, the (Hc/τ)-axes had to be expanded a great deal to obtain the required separation for the scattering intensities as a function of angle. Consequently, the data showed a great deal of scatter and in some instances overlapped as is shown by the few angles for which the data points were plotted. The data for Fraction 8 differed by less than 10% over the range of 45 to 135° which is about the limit of accuracy for the parameters obtained by this method, and no attempt was made to use the Zimm method for characterizing this fraction. The values of M_w and $(\overline{s^2}_z)^{1/2}$ obtained for Fractions 6 and 7 from the Zimm method could involve considerable error. As will be seen, the values for these parameters fall below the limits for which the Zimm method should be used.

For this reason, the molecular weight and radius of gyration were determined from dissymmetry data and 90° scattering values for Fractions 6, 7, and 8 using a rigid rod model. (The reason for choosing this model will become apparent in the ensuing work on particle scattering factors.) Figure 32 is a plot of $(Hc/\tau)_{90°}$ against concentration for these fractions from which M_w may be obtained from the

*In all instances where extrapolations were required or where data were fitted to a straight line for the results contained in this thesis, the method of least squares was used to find the appropriate slope and intercept.

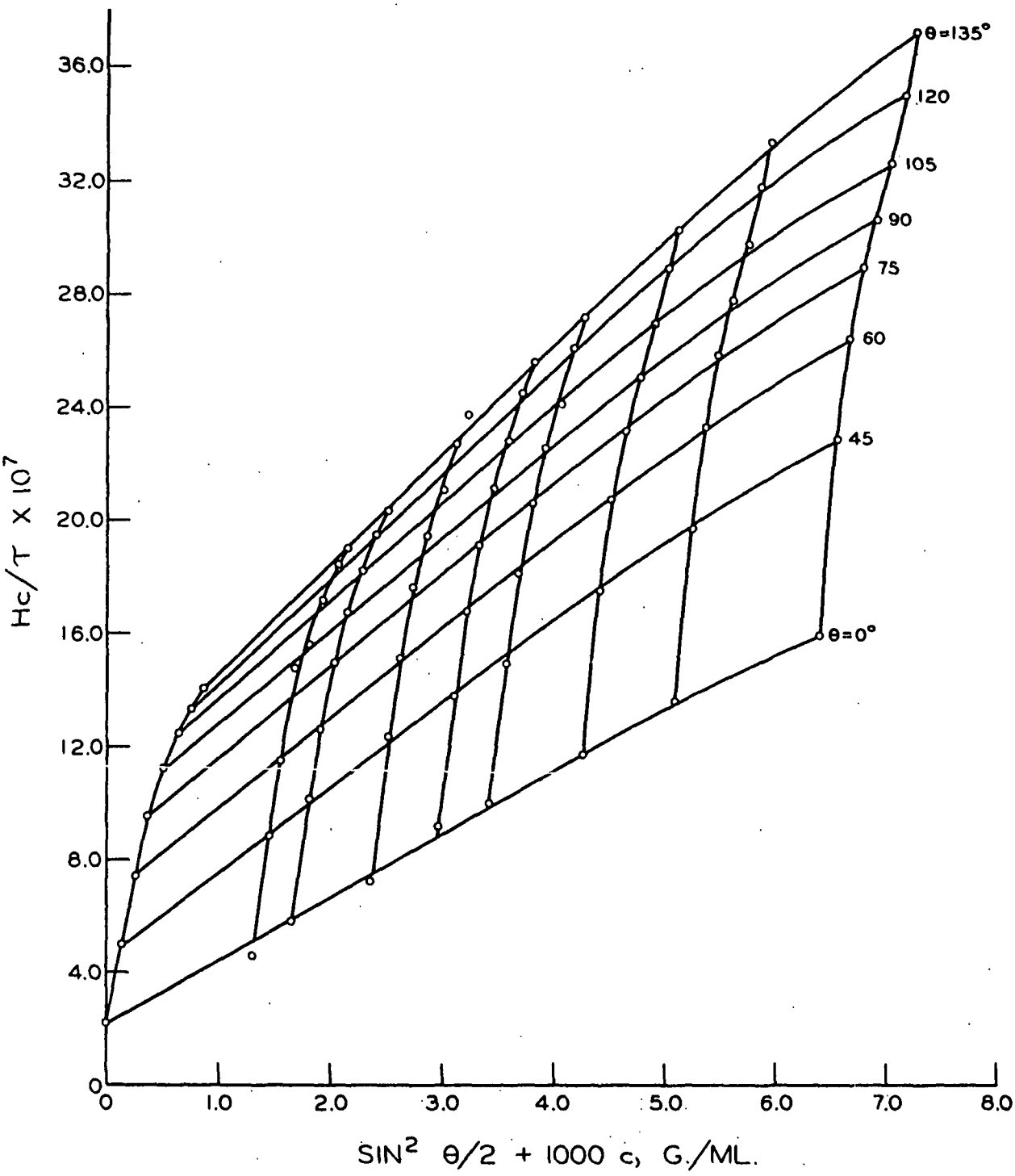

Figure 22. Zimm Plot for Guaran Triacetate, Unfractionated Polymer in Acetonitrile at 22.5°C. λ = 4358 A. $\underline{M}_w$ = 3.87 x 10^6, $(\overline{\underline{s}^2}_z)^{1/2}$ = 1240 A., $\underline{A}_2$ = 1.11 x 10^{-4} Moles cc. $g.^{-2}$

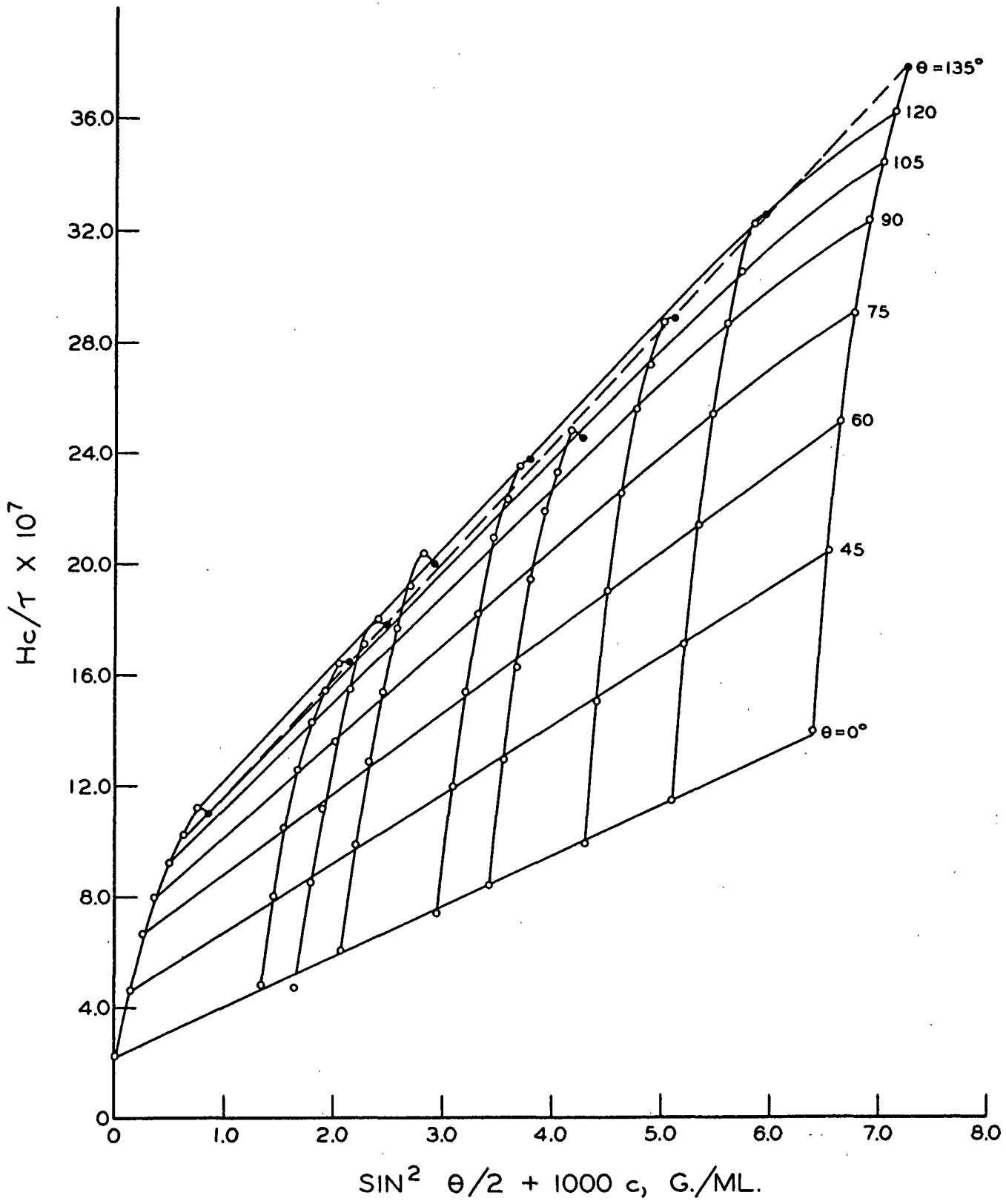

Figure 23. Zimm Plot for Guaran Triacetate, Unfractionated Polymer, in Acetonitrile at 22.5°C. λ = 5461 A. $\underline{M}_w$ = 4.01 x 10^6, $(\underline{\overline{s}}_z^2)^{1/2}$ = 1470 A., $\underline{A}_2$ = 0.91 x 10^{-4} Moles cc. $g.^{-2}$

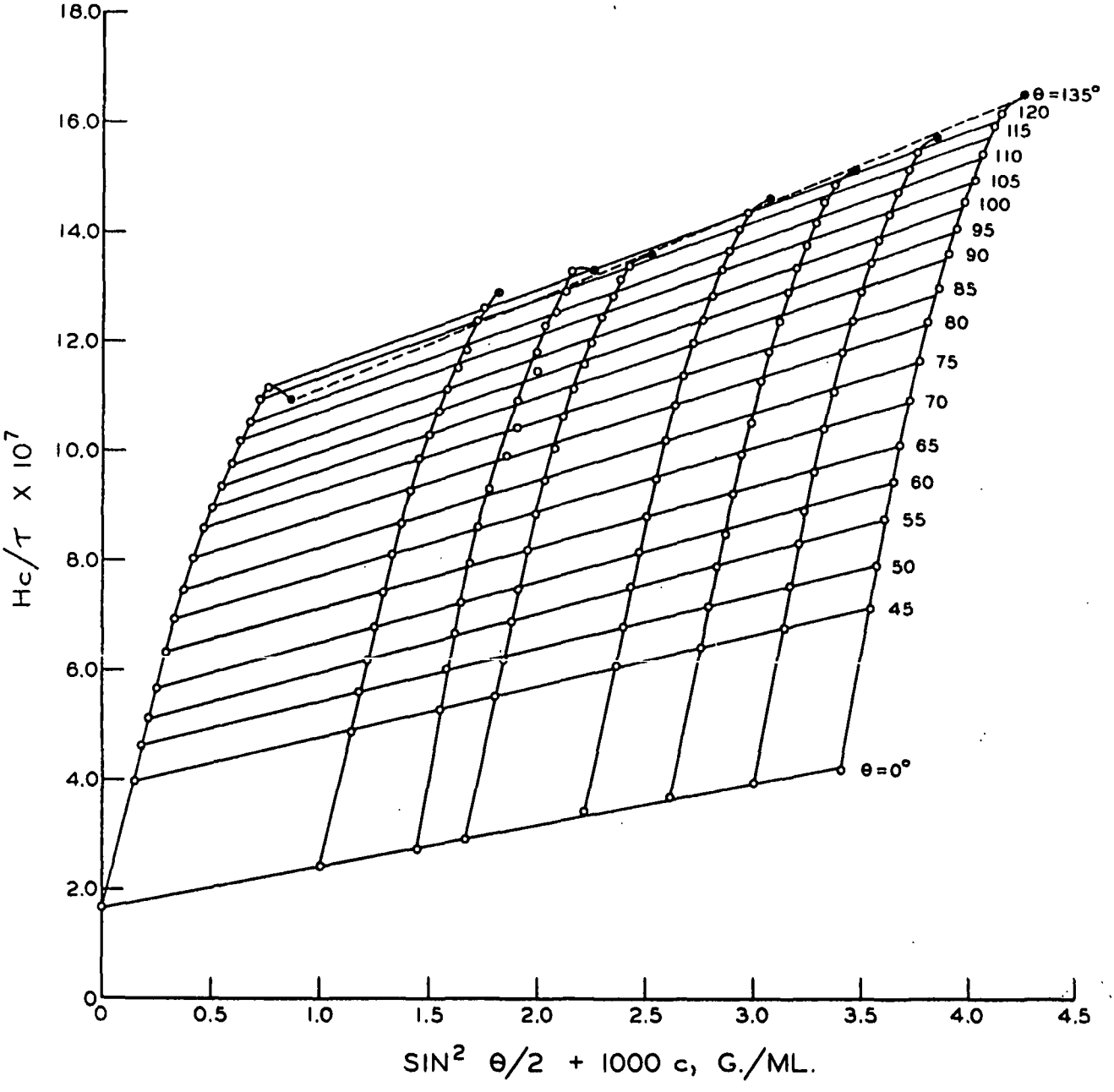

Figure 24. Zimm Plot for Guaran Triacetate, Fraction 2A, in Acetonitrile at 22.5°C. $\lambda = 4358$ A. $\underline{M}_w = 5.34 \times 10^6$, $(\underline{s}_z^{-2})^{1/2} = 1303$ A., $\underline{A}_2 = 0.38 \times 10^{-4}$ Moles cc. g.$^{-2}$

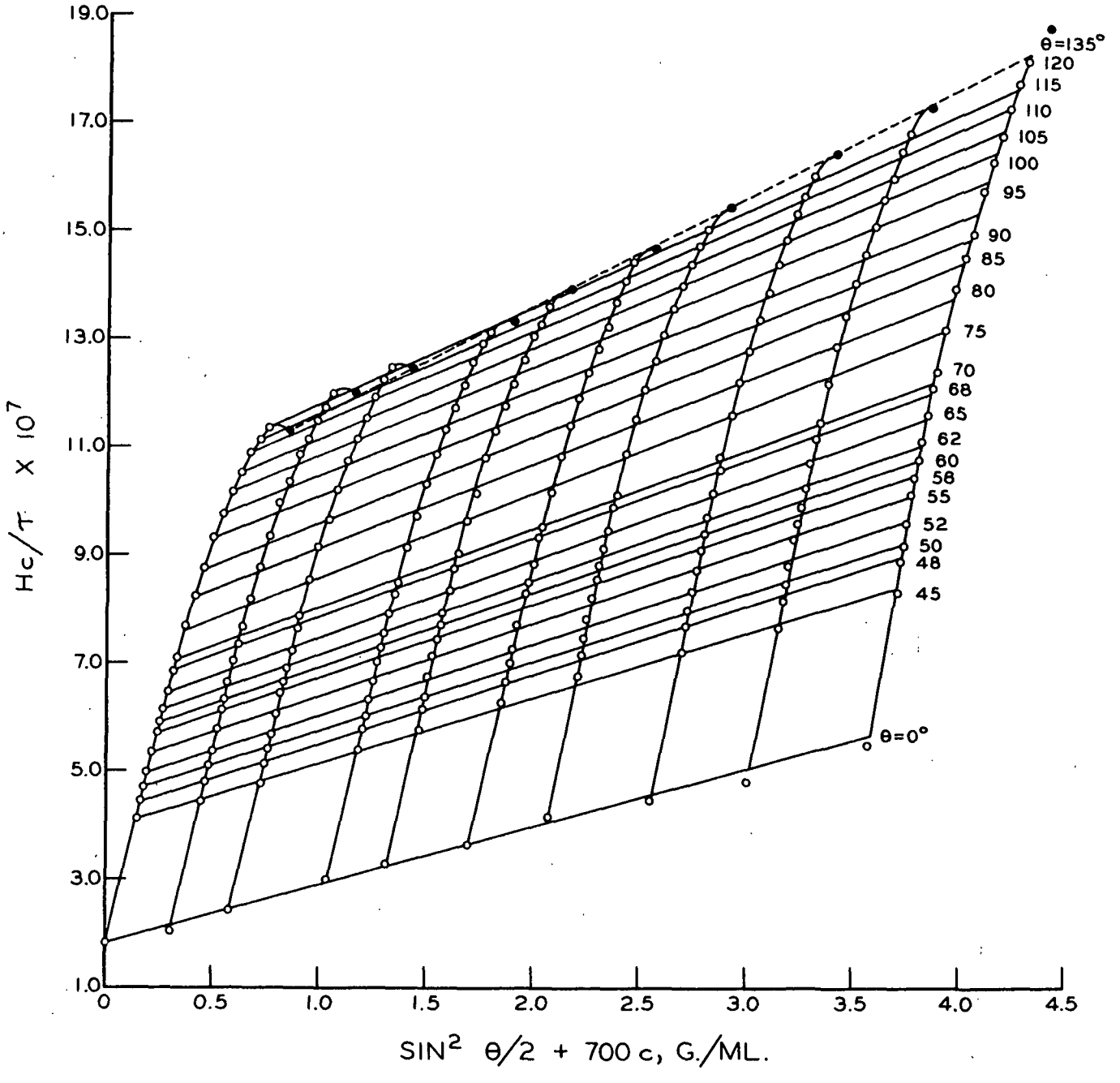

Figure 25. Zimm Plot for Guaran Triacetate, Fraction 2B, in Acetonitrile at 22.5°C. λ = 4358 A. $\underline{M}_{\underline{w}}$ = 4.84 x 10^6, $(\underline{s}^{-2}_{\underline{z}})^{1/2}$ = 1252 A., $\underline{A}_2$ = 0.38 x 10^{-4} Moles cc. $g.^{-2}$

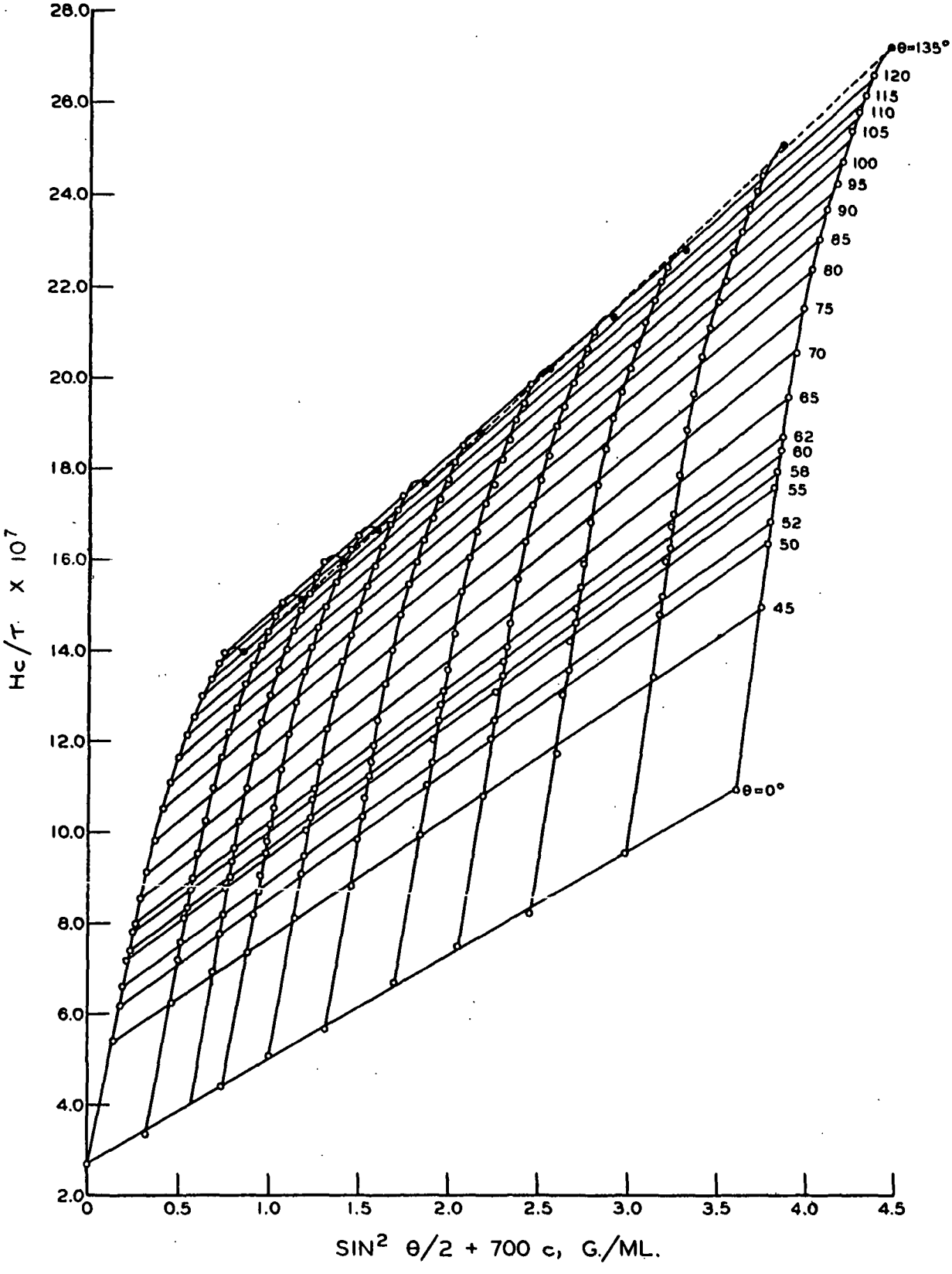

Figure 26. Zimm Plot for Guaran Triacetate, Fraction 3, in Acetonitrile at 22.5°C. λ = 4358 A. $\underline{M}_w$ = 3.30 x 10^6, $(\underline{s}^{-2}_z)^{1/2}$ = 1155 A., $\underline{A}_2$ = 0.81 x 10^{-4} Moles cc. g.$^{-2}$

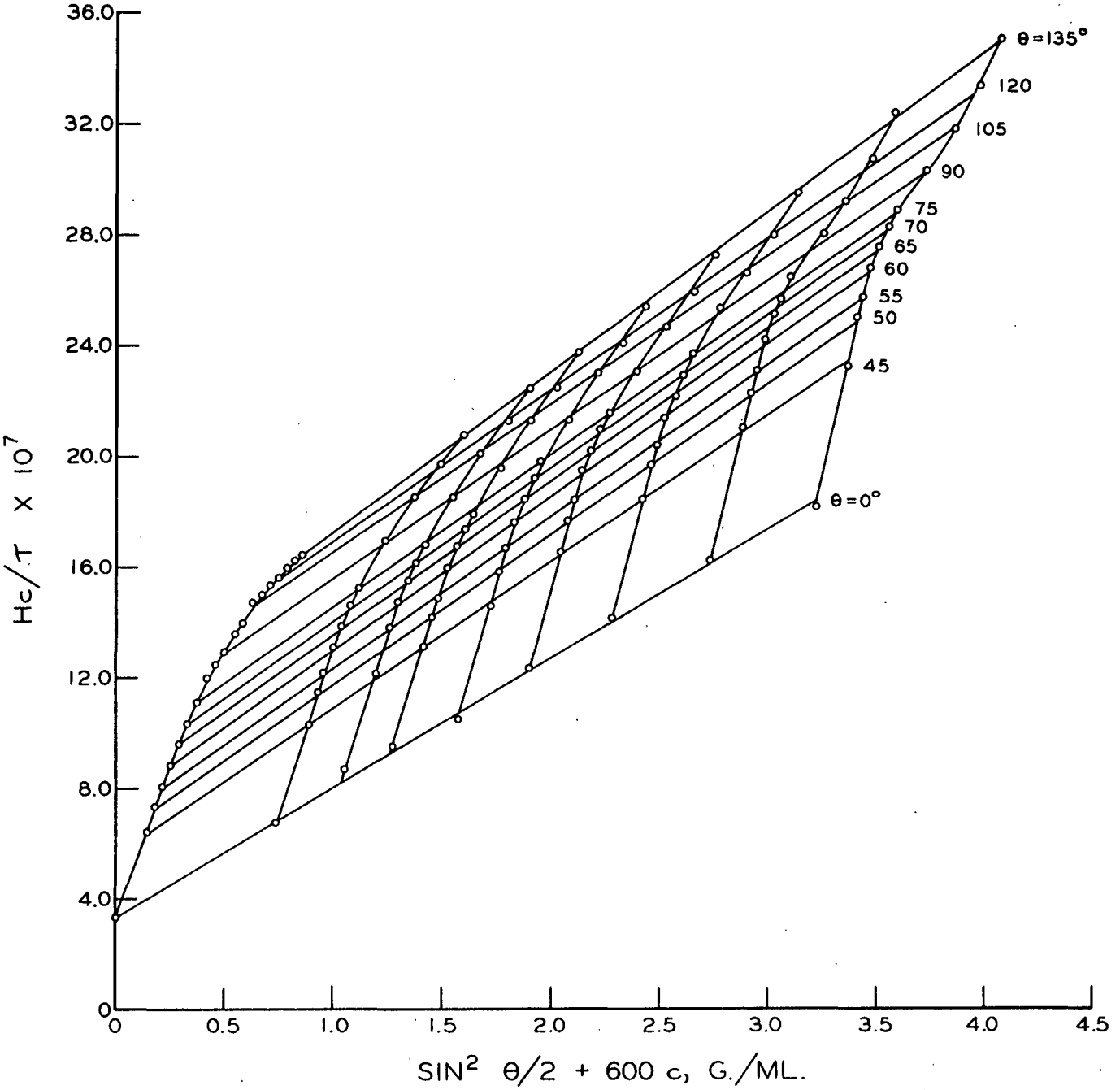

Figure 27. Zimm Plot for Guaran Triacetate, Fraction 4, in Acetonitrile at 22.5°C. λ = 4358 A. $\underline{M}_w$ = 2.86 x 10^6, $(\underline{s}^{-2}_z)^{1/2}$ = 1050 A., $\underline{A}_2$ = 1.42 x 10^{-4} Moles cc. $g.^{-2}$

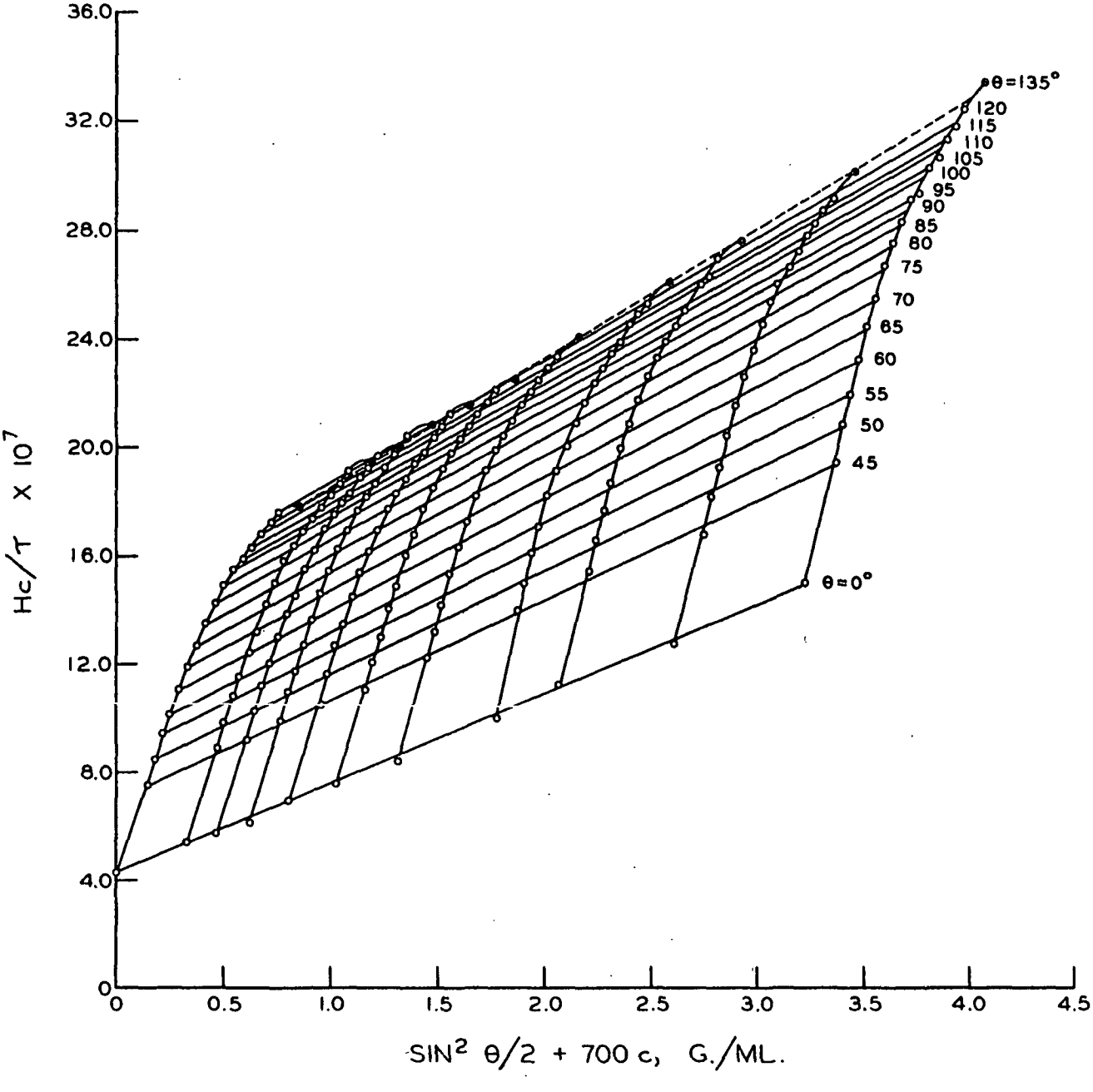

Figure 28. Zimm Plot for Guaran Triacetate, Fraction 2C, in Acetonitrile at 22.5°C. λ = 4358 A. $\underline{M}_w$ = 2.06 x 10^6, $(\underline{s}^{-2}_z)^{1/2}$ = 976 A., $\underline{A}_2$ = 1.40 x 10^{-4} Moles cc. $g.^{-2}$

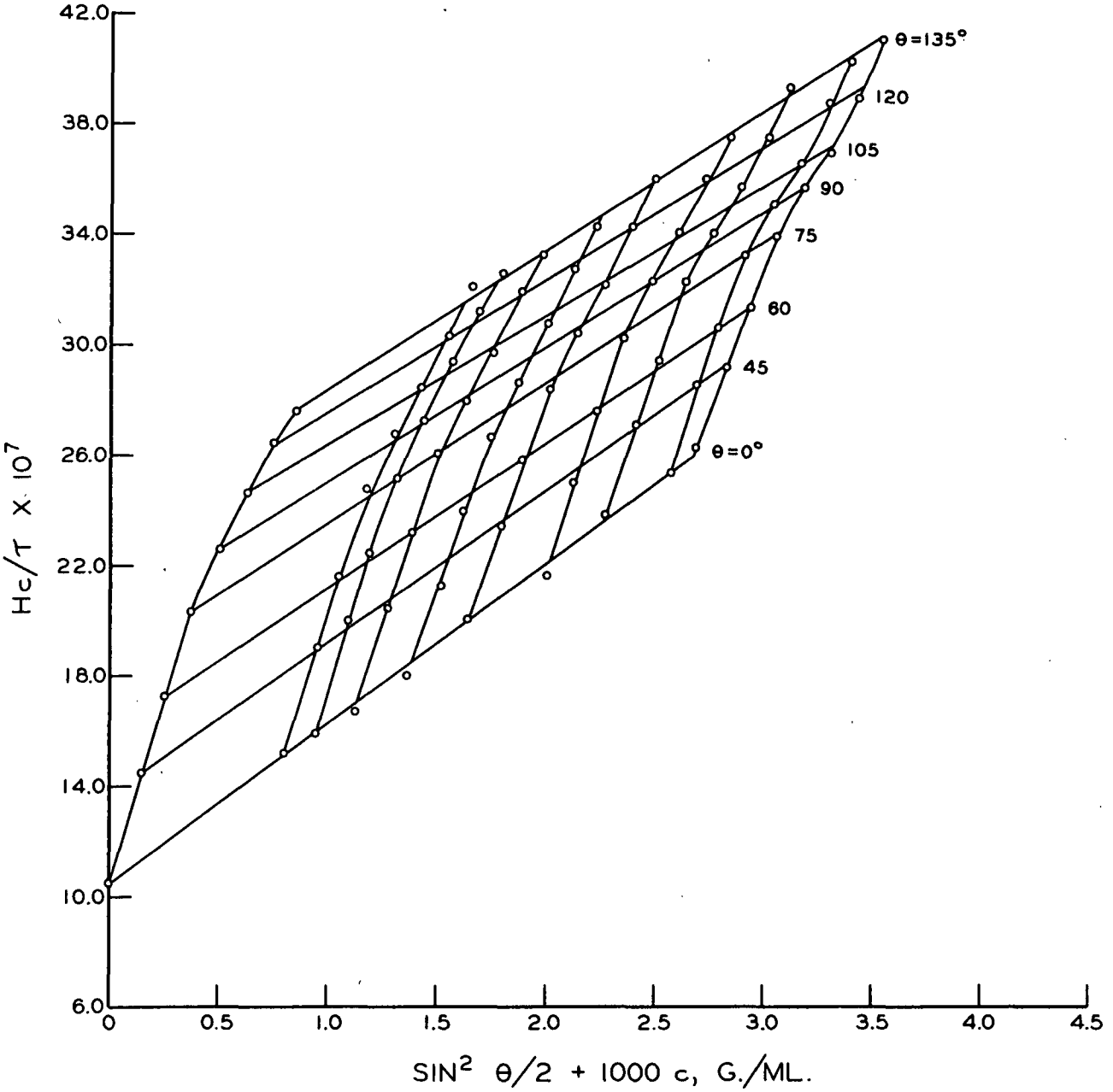

Figure 29. Zimm Plot for Guaran Triacetate, Fraction 5, in Acetonitrile at 22.5°C. λ = 4358 A. $\underline{M}_{\underline{w}}$ = 0.85 x 10^6, $(\underline{\overline{s}^2_z})^{1/2}$ = 680 A., $\underline{A}_2$ = 2.90 x 10^{-4} Moles cc. $g.^{-2}$

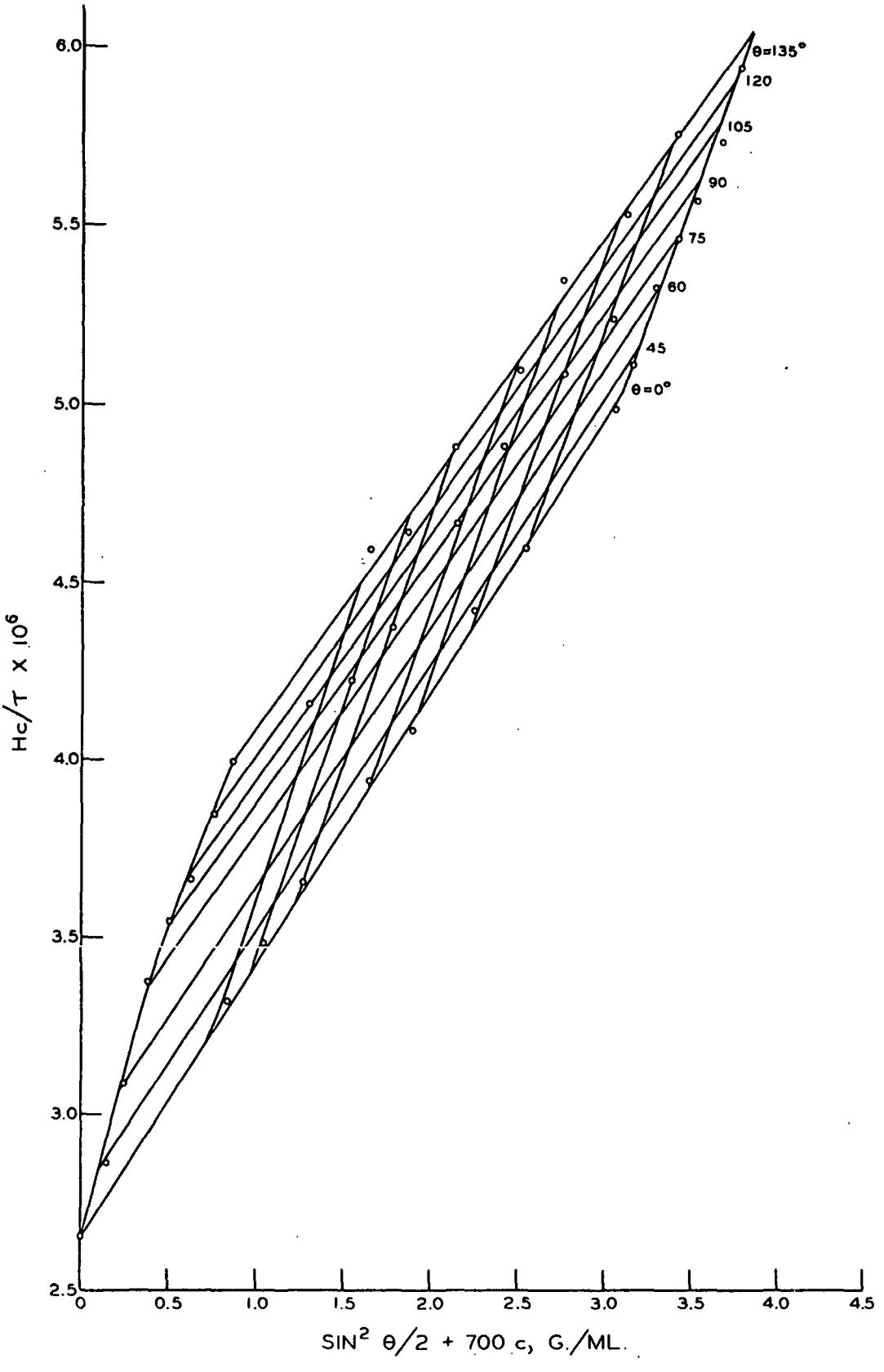

Figure 30. Zimm Plot for Guaran Triacetate, Fraction 6, in Acetonitrile at 22.5°C. λ = 4358 A. $\underline{M}_w$ = 0.33 x 10^6, $(\underline{s}^{-2}_z)^{1/2}$ = 470 A., $\underline{A}_2$ = 2.48 x 10^{-4} Moles cc. $g.^{-2}$

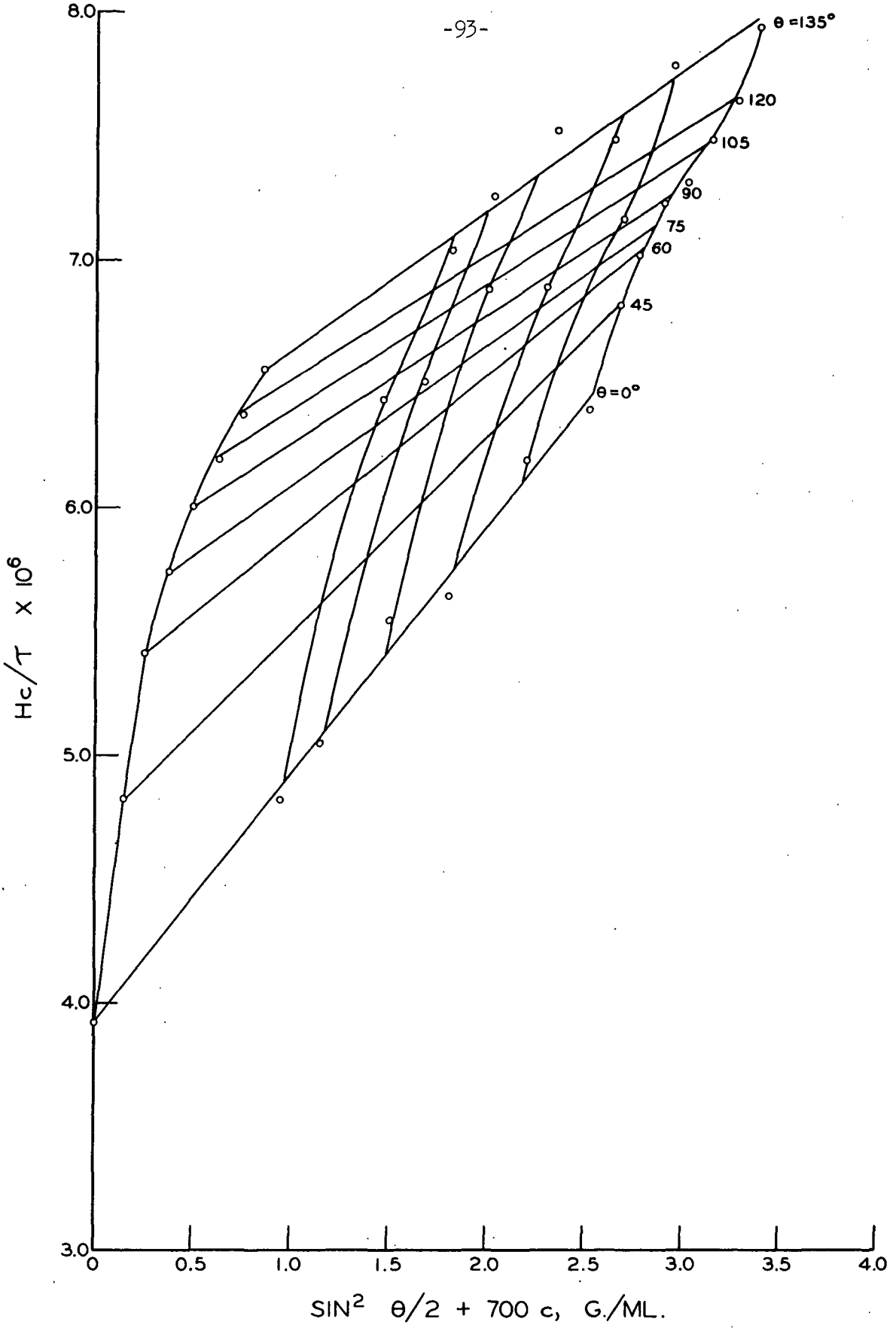

Figure 31. Zimm Plot for Guaran Triacetate, Fraction 7, in Acetonitrile at 22.5°C. λ = 4358 A. $\underline{M}_w$ = 0.23 x 10^6, $(\underline{\overline{s}^2}_z)^{1/2}$ = 440 A., $\underline{A}_2$ = 3.91 x 10^{-4} Moles cc. $g.^{-2}$

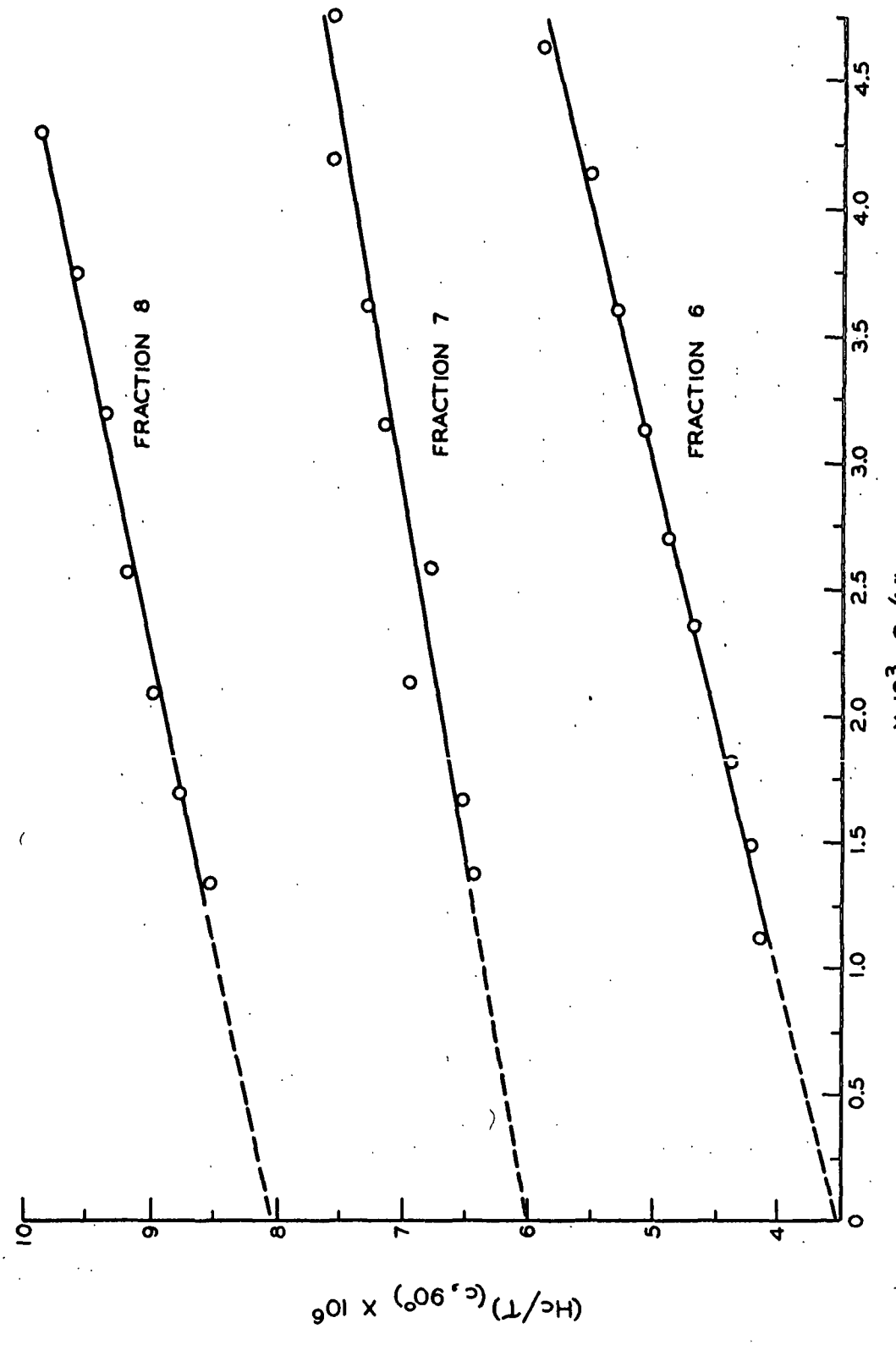

Figure 32. Light-Scattering Data at 90°, Guaran Acetate in Acetonitrile, 22.5°C.

intercept as shown by Equation (86). For Fractions 6 and 7 the value of $\underline{M}_{\underline{w}}$ determined by the two methods agreed to within about 3% for the former and 9% for the latter fraction (Fraction 6, $\underline{M}_{\underline{w}} = 3.3 \times 10^5$ and 3.4×10^5; Fraction 7, $\underline{M}_{\underline{w}} = 2.3 \times 10^5$ and 2.1×10^5 as determined by the Zimm method and the dissymmetry method, respectively). Since the values agreed this well, the values determined by the Zimm method will be reported for they are checked by two different extrapolations (one to zero angle at zero concentration and the other to zero concentration at zero angle). For Fraction 8 the dissymmetry method was used to obtain the molecular weight. The values of $1/\underline{P}(\theta)$ needed to obtain the stated values of molecular weight were obtained from the dissymmetry as described below.

Values of $[1/(\underline{Z} - 1)]$ were plotted for Fractions 6 and 7 as a function of concentration and extrapolated to zero concentration as shown in Fig. 33. The intrinsic dissymmetry, $[\underline{Z}]$, was 1.47 and 1.42 for the respective fractions. The values of $[1/(\underline{Z} - 1)]$ for Fraction 8 showed considerable scatter. Therefore, values of the dissymmetry, $\underline{Z}$, were plotted as a function of concentration to determine $[\underline{Z}]$, which had a value of 1.14, as shown in Fig. 34. By means of the tables of Beattie and Booth (73) and using a rigid rod model, the values of $1/\underline{P}(\theta)$ and of $(\overline{\underline{s}^2_{\underline{z}}})^{1/2}$ were found to be 1.379 and 470 A. for Fraction 6, 1.314 and 440 A. for Fraction 7, and 1.097 and 253 A. for Fraction 8. The values of $(\overline{\underline{s}^2_{\underline{z}}})^{1/2}$ were calculated from the values of $(\overline{\underline{r}^2_{\underline{w}}})^{1/2}$ which are obtained from the cited tables (73) by means of the relation

$$(L^2) = 12(\overline{s^2}), \qquad (92)$$

where $\underline{L}$ is the length of the rod. Then assuming that the distribution of molecular weights obtained by ultracentrifugation was identical to the distribution of radii of gyration, the ratio of $\underline{M}_{\underline{z}}/\underline{M}_{\underline{w}}$ was used to correct $(\overline{\underline{s}^2_{\underline{w}}})^{1/2}$ to $(\overline{\underline{s}^2_{\underline{z}}})^{1/2}$. It was previously ascertained that $\underline{M}_{\underline{z}}/\underline{M}_{\underline{w}} = 2.1/1.6$ for Fraction 3. Although the

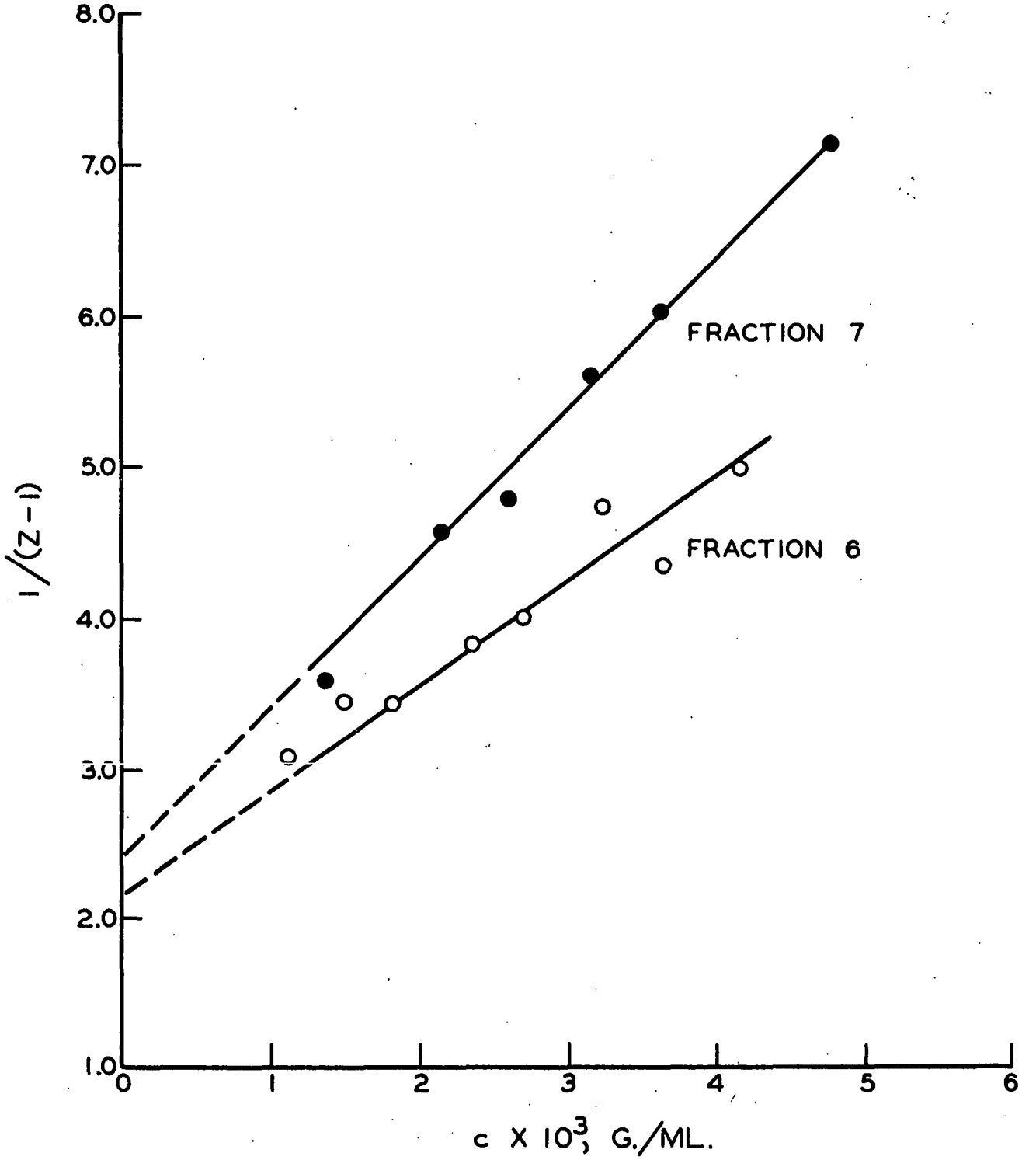

Figure 33. Values of $1/(Z-1)$ as a Function of Concentration for Determination of the Intrinsic Dissymmetry

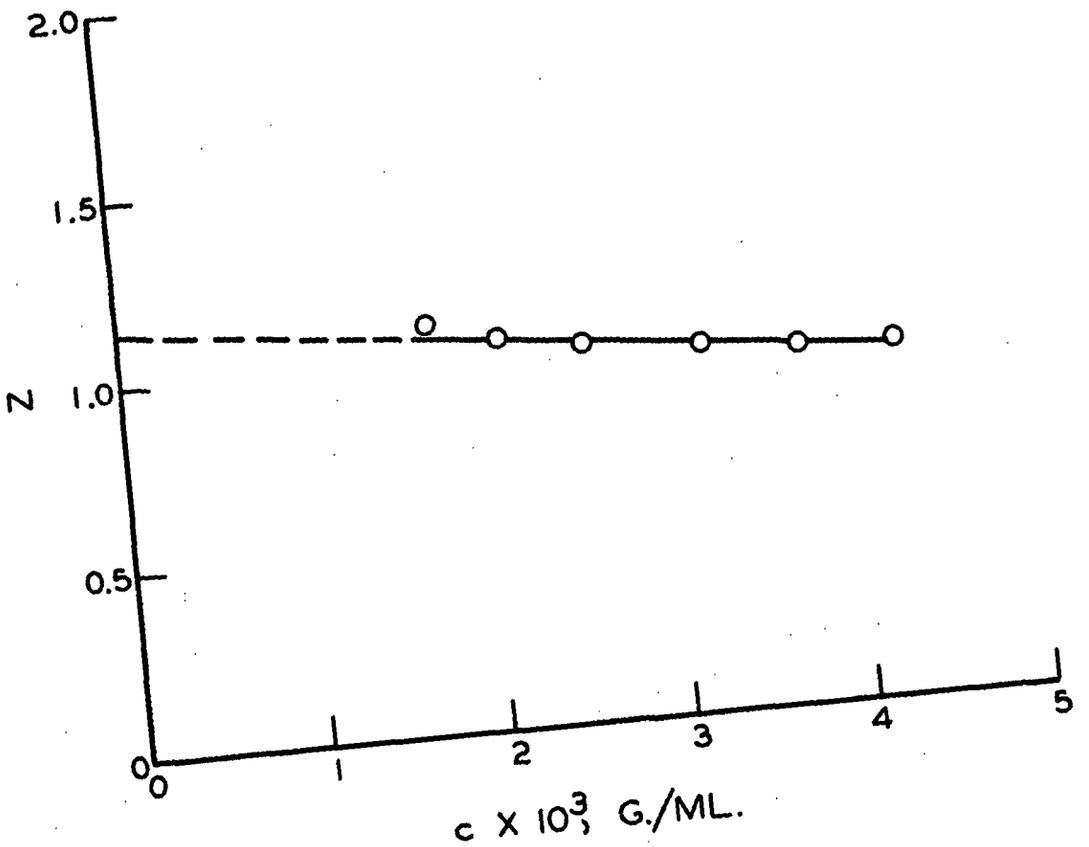

Figure 34. Values of the Dissymmetry as a Function of Concentration for Fraction 8 of Guaran Triacetate in Acetonitrile. Intercept is the Intrinsic Dissymmetry

manner in which removal of a given fraction affected the sharpness of succeeding fractions was not known, this ratio is assumed to be approximately correct for Fractions 3 through 8.

The value for $(\overline{s}_z^2)^{1/2}$ for Fraction 6 was 407 A. and for Fraction 7 it was 530 A. when determined by the Zimm method. Since these values of $(\overline{s}_z^2)^{1/2}$ were not in agreement with the other data, the values determined by the dissymmetry method using a rigid rod model will be reported. Note that these values of $(\overline{r}^2)^{1/2}$ are near the limits at which the Zimm method is difficult to apply (see the Dissymmetry Methods section of this thesis). In addition, the scatter of the data for Fractions 6 and 7 which was mentioned previously, could have caused considerable error which did not allow an accurate slope to be measured from the Zimm plots at zero concentration.

The results are summarized in Table VII using the particular values described above for Fractions 6, 7, and 8. The degree of polymerization, D.P., was calculated using a monomer weight of 432. The value of 432 for the monomer weight, M_o, was calculated in the following manner.

$$M_o = [(\text{Weight of a 2,3-di-O-acetyl-anhydromannose unit}) + (\text{Weight of a 2,3,6-tri-O-acetyl-anhydromannose unit}) + (\text{Weight of a 2,3,4,6-tetra-O-acetylanhydrogalactose unit})]/2 = (245 + 288 + 331)/2 = 864/2 = 432. \quad (93)$$

Light-scattering data yields a relation which is of interest in connection with the configuration of polymer molecules. This relation is the reciprocal of the previously discussed particle scattering factor, $P(\theta)$. The value of $1/P(\theta)$ can be obtained by dividing the intercept of a given angular extrapolation line with the zero concentration line in a Zimm plot, $(Hc/\tau)_{\theta, c=0}$, by the intercept of the zero angle line with the zero concentration line, $(Hc/\tau)_{\theta=0, c=0}$ (82), that is,

TABLE VII

SUMMARY OF RESULTS OBTAINED FROM LIGHT-SCATTERING MEASUREMENTS AT 4358 A. UNLESS OTHERWISE NOTED

Fraction	$\underline{M}_w \times 10^{-6}$ [a]	$(\overline{\underline{s}^2}_z)^{1/2}$, A.	$\underline{A}_2 \times 10^4$ moles cc. $g.^{-2}$	D.P. [b]
Whole Polymer, 5461 A.	4.01	1470	0.91	9,290
Whole Polymer	3.87	1240	1.11	8,950
2A	5.34	1303	0.38	12,361
2B	4.84	1252	0.38	11,204
3	3.30	1155	0.81	7,639
4	2.68	1050	1.42	6,204
2C	2.06	976	1.40	4,769
5	0.85	680	2.90	1,968
6	0.33	470	2.48	764
7	0.23	440	3.91	532
8	0.074	253	4.70 [c]	171

[a] These molecular weights have been corrected for depolarization using an average value of 0.89 for the Cabannes factor.

[b] Determined using a monomer weight of 432.

[c] The value of $\underline{A}_2$ for Fraction 8 was approximated by plotting $\underline{A}_2$ as a function of molecular weight and extrapolating.

$$1/P(\theta) = (Hc/\tau)_{\theta,c=0}/(Hc/\tau)_{\theta=0,c=0} \tag{94}$$

The values of $1/\underline{P}(\theta)$ for a given polymer molecule may be compared to the values that would be obtained if the molecule were a sphere, a monodisperse coil, a polydisperse coil, or a rigid rod by employing the tables of Doty and Steiner (68) for $\underline{P}(\theta)$ and $\underline{x}$, where $\underline{x}$ is defined by the following expressions for the indicated models,

$$\text{Sphere:}\quad P(\theta) = [(3/x^3)(\sin x - x\cos x)]^2, \tag{95}$$

where $\underline{x} = \mu\underline{d}/2$,

$$\text{Coil:}\quad P(\theta) = (2/x^2)\,[\exp(-x) - (1 - x)], \tag{96}$$

where $\underline{x} = \mu^2(\overline{\underline{r}^2})/6$,

$$\text{Rigid Rod:}\quad P(\theta) = (1/x)\int_0^{2x} [(\sin v)/v]\,dv - [(\sin x)/x]^2, \tag{97}$$

where $\underline{x} = \mu\underline{L}/2$. In these expressions, $\underline{d}$ is the diameter of a sphere, $\underline{L}$ is the length of a rod, and μ has been previously defined as $(4\pi/\lambda')\sin(\theta/2)$. These equations are the analytical expressions for a particular model which may be obtained from the general equation, Equation (79). The above expressions assume the polymer is monodisperse. Significant deviations result for broad molecular weight distributions. In the case of the random coil, the expression for polydisperse coils has been evaluated by Doty and Steiner (68) to be

$$P(\theta) = (1 - x)/(2 + x) \tag{98}$$

where $\underline{x}$ has the same meaning as in Equation (97).

From the cited tables, for a given value of $\underline{P}(\theta)$ a value of $\underline{x}$ is known for the various models. Since $\underline{x}$ is a function of either the diameter, the end-to-end

separation, or the length if the model is a sphere, a coil, or a rod and of $\sin(\theta/2)$, one may calculate the value of $\sin(\theta/2)$. This is accomplished by assuming the radius of gyration obtained by light scattering is the radius of gyration for the appropriate model. Then, the radius of gyration is related to the dimension of the model by the following expressions,

$$\text{Sphere:} \quad (\bar{s}^2) = 3d^2/20 \tag{99}$$

$$\text{Coil:} \quad (\bar{s}^2) = \bar{r}^2/6 \tag{100}$$

$$\text{Rod:} \quad (\bar{s}^2) = L^2/12 \tag{101}$$

With the appropriate dimension known, it is a simple matter to evaluate $\sin(\theta/2)$ from $\underline{x}$ at the given value of $\underline{P}(\theta)$.

Figures 35 and 36 are plots of $1/\underline{P}(\theta)$ against $\sin(\theta/2)$ for the fractions of guaran triacetate in acetonitrile. The theoretical curves for a sphere, polydisperse coil, monodisperse coil, and rigid rod are shown for comparison. (Appendix III contains the tabulated values of $1/\underline{P}(\theta)$ and $\sin(\theta/2)$ for the various fractions of guaran triacetate.) At high molecular weights the guaran triacetate molecules are somewhat like a random coil and at the lower molecular weights similar to a rigid rod. (It is for this reason that the rigid rod model was used in evaluating the configurational parameters from dissymmetry.) Since the variable angle data for Fractions 6 and 7 were not considered reliable, these fractions were not examined by this method.

Figure 37 is the $1/\underline{P}(\theta)$ versus $\sin(\theta/2)$ plot for unfractionated guaran triacetate in acetonitrile. The plot indicates that the unfractionated polymer is also between a rod and a coil model as would be expected from the results for the fractions of guaran triacetate. It is interesting to note that the curve is

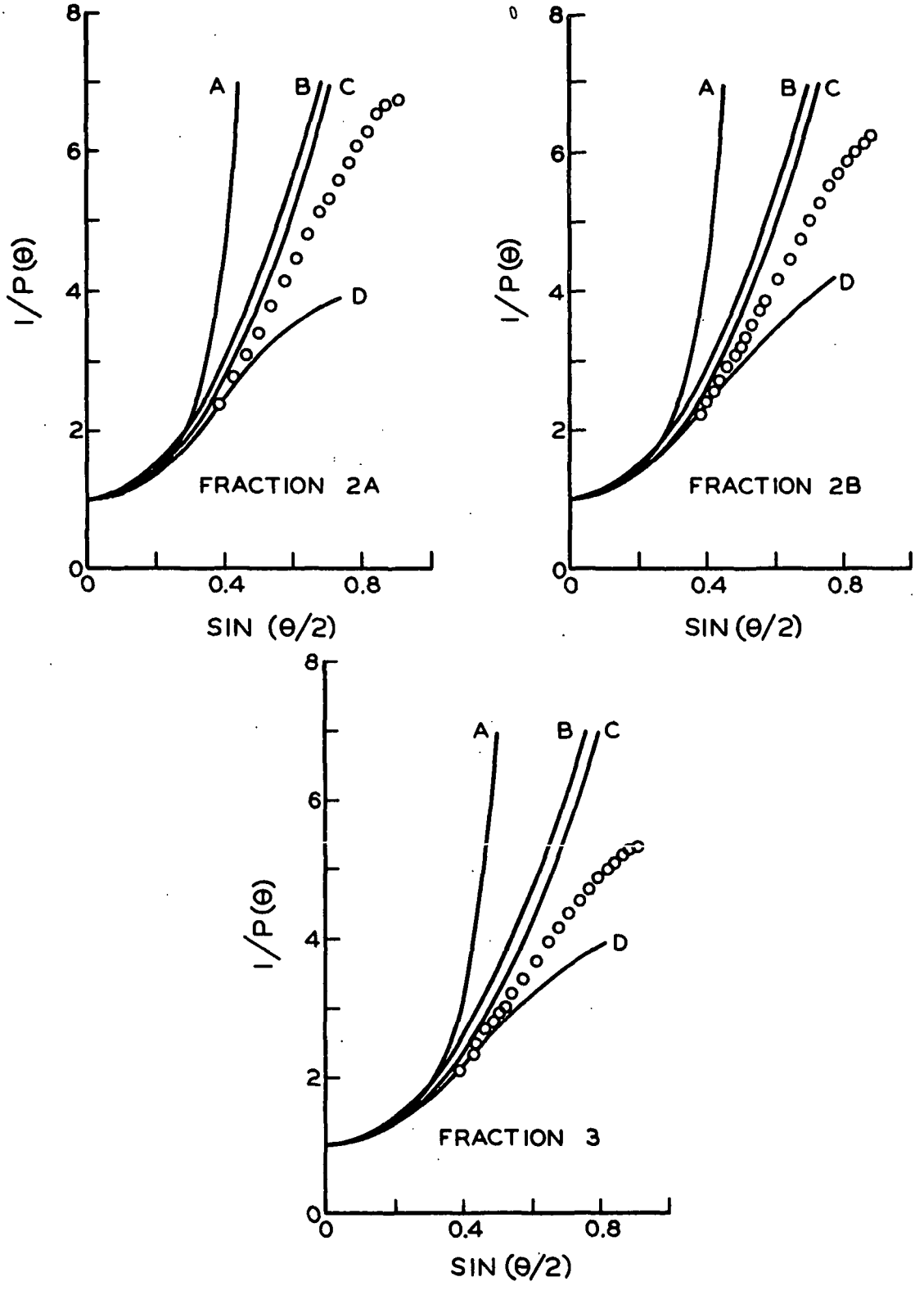

Figure 35. Plots of $1/\underline{P}(\theta)$ as a Function of $\sin(\theta/2)$ for Guaran Triacetate in Acetonitrile. Solid Lines are the Theoretical Curves for A, a Sphere; B, a Polydisperse Coil; C, a Monodisperse Coil; and D, a Rigid Rod. The Open Circles are Experimental Data Points

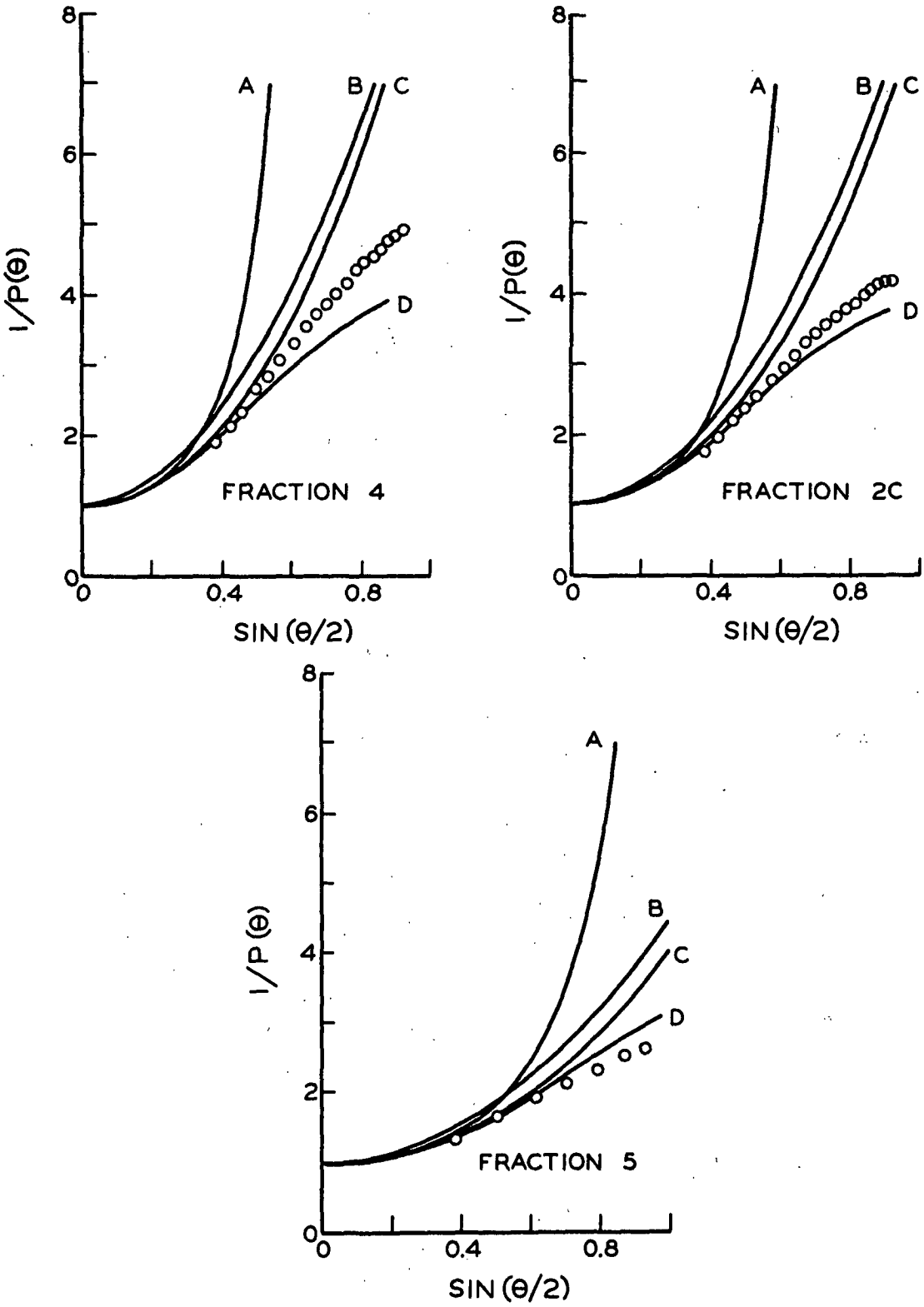

Figure 36. Plots of $1/\underline{P}(\theta)$ as a Function of $\sin(\theta/2)$ for Guaran Triacetate in Acetonitrile. Solid Lines are the Theoretical Curves for A, a Sphere; B, a Polydisperse Coil; C, a Monodisperse Coil; and D, a Rigid Rod. The Open Circles are Experimental Data Points

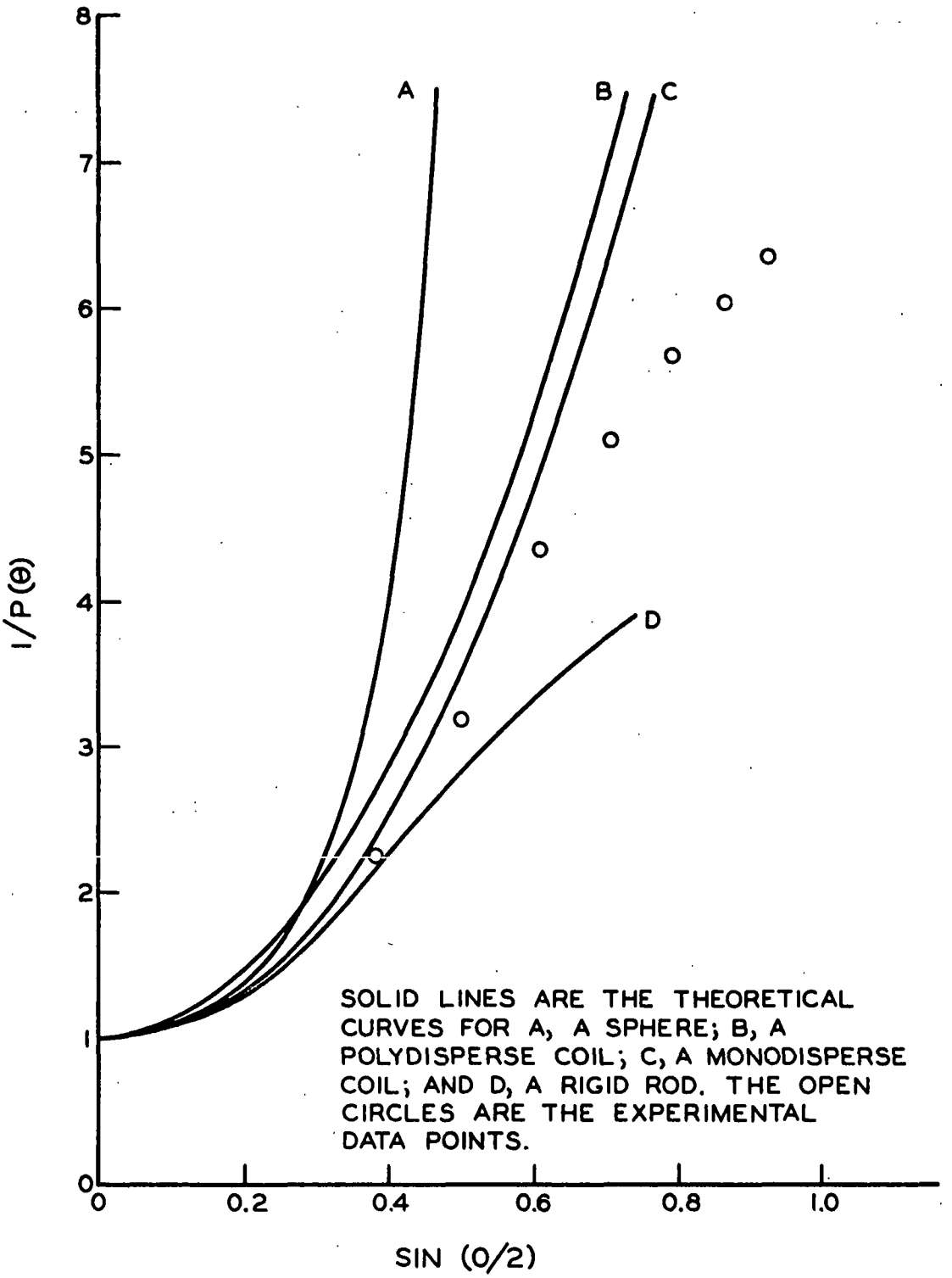

Figure 37. Plots of $1/\underline{P}(\theta)$ Versus $\sin(\theta/2)$ for Unfractionated Guaran Triacetate in Acetonitrile

similar in character to that of Fraction 3, Fig. 35, which has an intrinsic viscosity and molecular weight near that of the unfractionated polymer.

Everett and Foster (82) find that the $1/\underline{P}(\theta)$ versus $\sin(\theta/2)$ curves for fractions of amylose in dimethyl sulfoxide approximate a random coil quite well for molecular weights between 1.52×10^5 and 2.22×10^6. Another example of this type of analysis is given by Gueidushek and Doty (83) who find that sodium deoxyribonucleate is more rodlike than coil-like.

Thus, in summary, it may be said that when the reciprocal particle scattering factors for fractionated guaran triacetate are compared with various models, the molecules best fit a random coil model at high molecular weights and a rigid rod model at low molecular weights.

VISCOSITY

EXPERIMENTAL PROCEDURES

The intrinsic viscosity, $[\eta]$, of a solution can be defined in the following manner,

$$[\eta] = \lim_{c \to 0}(\eta_{sp}/c) = \lim_{c \to 0}(\eta_{rel} - 1)/c = \lim_{c \to 0}[(\ln \eta_{rel})/c], \qquad (102)$$

where the relative viscosity, η_{rel}, is the ratio of the efflux time of the solution, $\underline{t}$, to that of the solvent, $\underline{t}_o$. The specific viscosity, η_{sp} is given by

$$\eta_{sp} = (\eta_{rel} - 1) = (t - t_o)/t_o. \qquad (103)$$

The concentration, $\underline{c}$, is expressed in grams per deciliter of solution. Therefore, by extrapolation of $\eta_{sp}/\underline{c}$ or $(\ln \eta_{rel})/\underline{c}$ as a function of concentration to zero concentration the intrinsic viscosity may be determined. Quite often the

concentration dependence of η_{sp}/c is of such a nature that it is necessary to plot $\log(\eta_{sp}/c)$ rather than η_{sp}/c against concentration in order to obtain a linear plot. Flory (24) notes that $(\ln \eta_{rel})/c$ changes less rapidly with concentration and is usually linear to higher concentrations than either η_{sp}/c or $\log(\eta_{sp}/c)$ which would make it the preferred method of extrapolation.

Kinetic Energy Correction

A correction should be applied to the flow times to account for the kinetic energy loss which is due to the fact that the liquid is flowing at a finite velocity when it leaves the capillary. This correction may be applied to the specific viscosity by using the following relationship which is cited by Timell (84).

$$\eta_{sp} = \eta'_{sp} \left\{[F_o/(1 - F_o)]\ [(t + t_o)/t] + 1\right\} . \qquad (104)$$

In this expression, η_{sp} is the corrected specific viscosity, η'_{sp} is the observed specific viscosity, and F_o is defined as

$$F_o = m_e \rho_o V/8\pi \eta_o t_o L, \qquad (105)$$

where m_e is the kinetic energy coefficient or end correction, ρ_o is the solvent density, V is the bulb volume, η_o is the absolute solvent viscosity expressed in poises, and L is the length of the capillary.

Non-Newtonian Behavior

Non-Newtonian behavior of a polymer solution must be accounted for if it exists, since it will cause a decrease in the intrinsic viscosity determined. Therefore, one must extrapolate and determine $[\eta]$ at zero shear stress. The shear stress, τ_R, can be defined as (85)

$$\tau_R = h\rho gR/2L, \tag{106}$$

where ρ is the solution density, g is the gravitational constant, R is the capillary radius, and h is the mean hydrostatic head which may be determined from Meissner's equation (86).

$$h = (m_1 - m_2)/\ln(m_1/m_2). \tag{107}$$

In this relationship, m_1 is the initial distance (top mark on a bulb) and m_2 is the final distance (bottom mark on a bulb) between the top level of the liquid and the lower end of the capillary. For a given capillary viscometer and a particular bulb, Equation (106) reduces to

$$\tau_R = (\text{Constant})\ \rho. \tag{108}$$

When capillary viscometers are employed, viscosity values are determined at fixed values of shear stress (assuming that the density of the dilute solutions is equal to the density of the solvent), but each viscosity value is determined at a different rate of shear. When it is desired, the rate of shear, $\dot{\epsilon}$, for a capillary viscometer can be obtained from

$$\dot{\epsilon} = h\rho gR/2L\ \eta_o\ \eta_{rel} = \tau_R/\eta_o\eta_{rel} = K/\eta_{rel}, \tag{109}$$

where K is a constant for a given bulb and a particular solvent and η_o is the absolute viscosity, in poises, of the solvent. The absolute viscosity of a solvent, η_x, can be determined from

$$\eta_x = (\rho_w/\rho_x)(t_x/t_w)\ \eta_w, \tag{110}$$

where the subscript w refers to water and the subscript x refers to the solvent in question (87).

EXPERIMENTAL METHODS AND CALCULATION PROCEDURE

A modified Ubbelohde variable shear viscometer, Cannon 47-A1, was used. This viscometer is described in detail in Appendix IV. The viscometric determinations were carried out at 25.00 ± 0.02°C. The maximum kinetic energy corrections were found to be less than 1% and were neglected.

For those fractions which did not exhibit shear dependence, the equations

$$\eta_{sp}/c = [\eta] + pc \tag{111}$$

and

$$(\ln \eta_{rel})/c = [\eta] + qc \tag{112}$$

were applied to obtain the intrinsic viscosity. In these expressions p and q, respectively, are the slopes of a plot of η_{sp}/c and $(\ln \eta_{rel})/c$ against c.

For the fractions which exhibited shear dependence, determination of the intrinsic viscosity at zero shear stress proceeded in the following manner. For each concentration η_{sp}/c was plotted against the shear stress calculated from Equation (106). Flow times for water and acetonitrile are listed in Appendix IV which will allow calculation of the rate of shear if it should be desired. The intercept of this plot is the value of η_{sp}/c at zero shear stress. Figure 38 is an example of this type of plot. The values of $(\eta_{sp}/c)_{\tau_R=0}$ were then plotted as a function of concentration to obtain the value of $[\eta]_{\tau_R=0}$ from Equation (111).

RESULTS

Unfractionated Guaran Triacetate

The dependence of the intrinsic viscosity on shear stress for unfractionated guaran triacetate was examined in acetonitrile at 25.00 ± 0.02°C. In this solvent

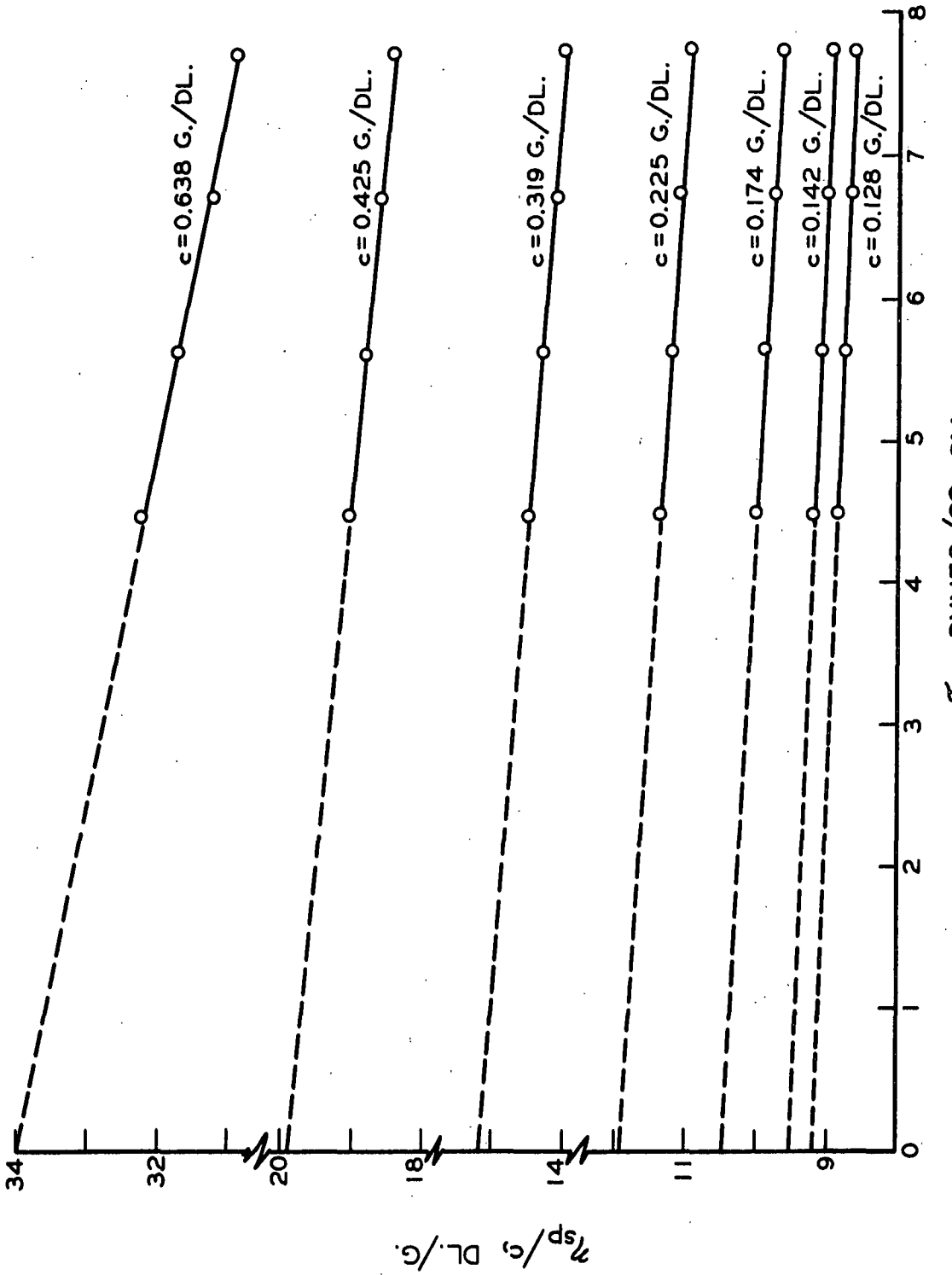

Figure 38. Guaran Triacetate in Acetonitrile, Unfractionated Polymer 25.00°C.

the non-Newtonian behavior (shear dependence) was readily detected. Values of $(\eta^*_{sp}/\underline{c})$ were extrapolated to zero shear stress and zero concentration in the manner described previously. An example of this type of plot is shown in Fig. 39. The parameter $(\eta^*_{sp}/\underline{c})$ is the apparent reduced viscosity at a particular shear stress (89). At zero shear stress $\eta^*_{sp}/\underline{c} = \eta_{sp}/\underline{c}$. The equations for these lines are given in Table VIII. The intrinsic viscosity as a function of shear stress for unfractionated guaran triacetate is shown in Fig. 40. At zero shear stress the intrinsic viscosity has a value of 6.62 dl./g.

TABLE VIII

LEAST SQUARE LINES FOR $\log(\eta^*_{sp}/\underline{c}) = \underline{m}\underline{c} + \log(\eta^*_{sp}/\underline{c})_{\underline{c}=0}$
UNFRACTIONATED GUARAN TRIACETATE IN ACETONITRILE AT 25.00°C.

Shear Stress, dynes/sq.cm.	$\underline{m}$	$\log(\eta^*_{sp}/\underline{c})_{\underline{c}=0}$
7.76	1.097	0.791
6.74	1.109	0.792
5.64	1.113	0.797
4.49	1.115	0.804
0.0	1.159	0.821

Fractionated Guaran Triacetate

The shear dependence of the apparent reduced viscosity of the fractions of guaran triacetate in acetonitrile at 25.00 ± 0.02°C. was determined. Guaran triacetate exhibited shear dependence above $\underline{M}_w = 2 \times 10^6$ in the low range of shear investigated, 4.49-7.76 dynes/sq. cm.

Plots of $(\eta_{sp}/\underline{c})$ and $(\ln \eta_{rel})/\underline{c}$ against concentration for those fractions which did not exhibit shear dependence are shown in Fig. 41. Table IX contains the equations for these lines.

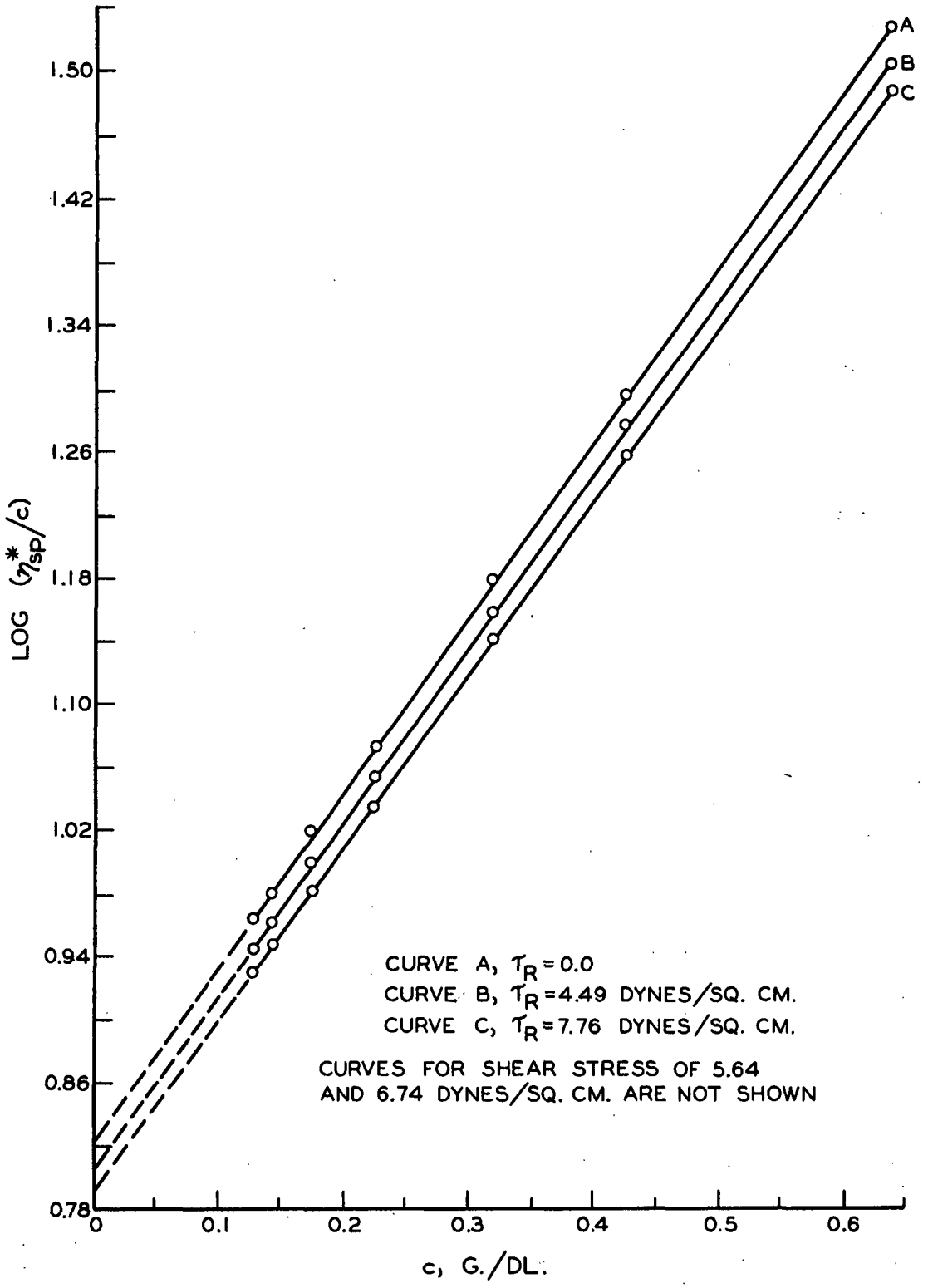

Figure 39. Log $\eta^*_{sp}/\underline{c}$ versus $\underline{c}$ for Unfractionated Guaran Triacetate in Acetonitrile, 25.00 ± 0.02°C.

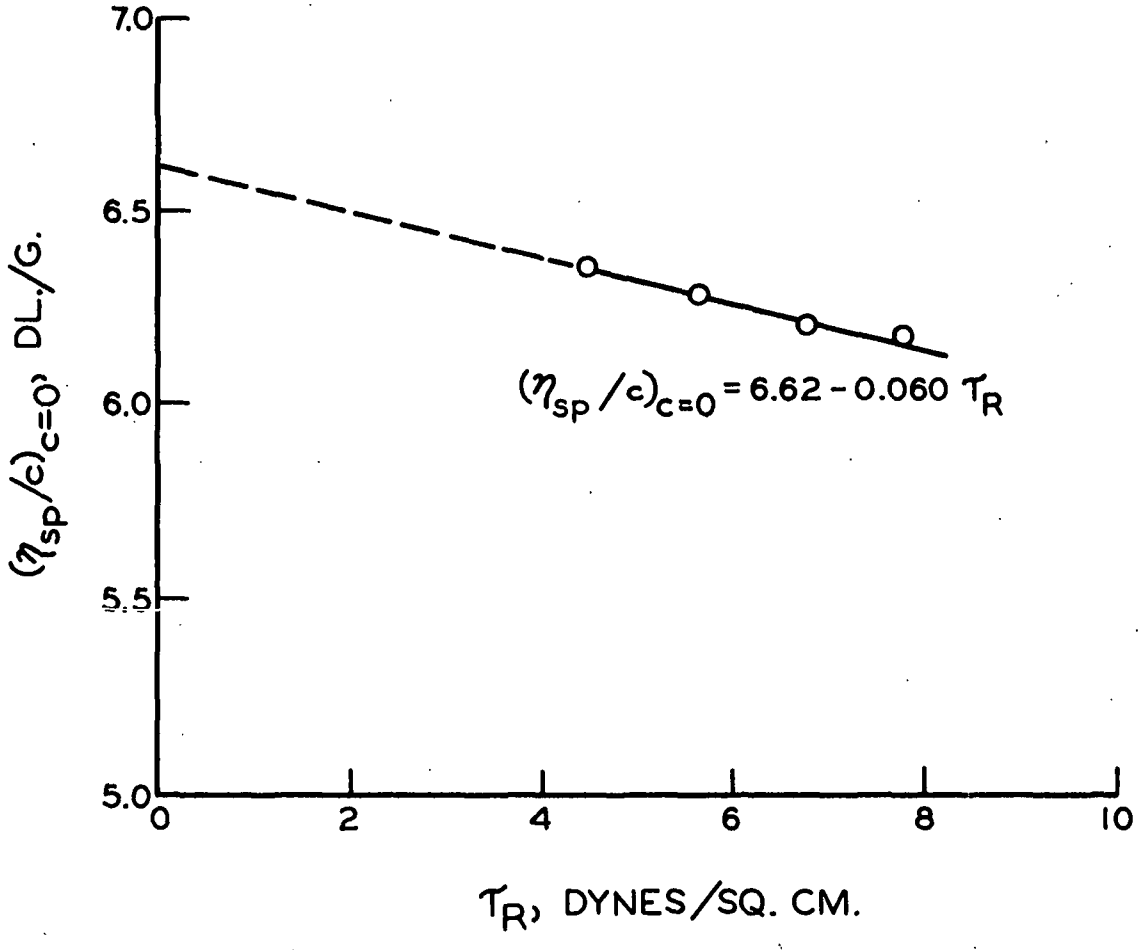

Figure 40. Apparent Reduced Viscosity at Zero Concentration as a Function of Shear Stress, Unfractionated Guaran Triacetate in Acetonitrile at 25.00 ± 0.02°C.

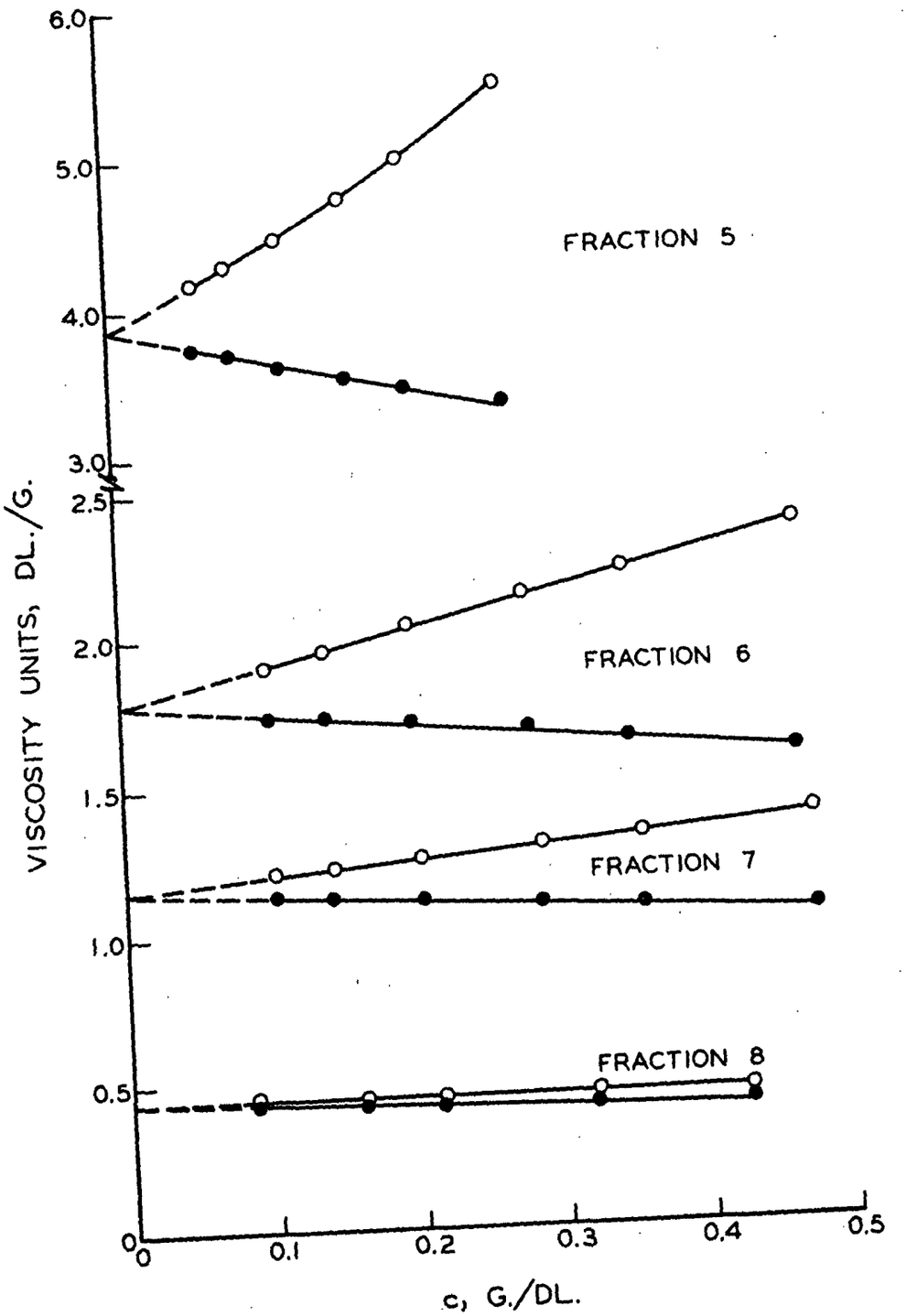

Figure 41. Viscosity as a Function of Concentration, Guaran Triacetate in Acetonitrile, 25.00 ± 0.02°C. These Fractions did not Exhibit Shear Dependence. Open Circles are η_{sp}/c Values and Solid Circles are $(\ln \eta_{rel})/c$ Values

TABLE IX

LEAST SQUARE LINES FOR VISCOSITIES INDEPENDENT OF SHEAR STRESS. GUARAN TRIACETATE IN ACETONITRILE, 25.00 ± 0.02°C.

Fraction	$\underline{M}_w \times 10^{-6}$	$(\eta_{sp}/\underline{c}) = \underline{p}\underline{c} + [\eta]$ $\underline{p}$	$[\eta]$	$(\ln \eta_{rel})/\underline{c} = \underline{q}\underline{c} + [\eta]$ $\underline{q}$	$[\eta]$
5	0.85	--	3.87	-2.04	3.87
6	0.33	1.27	1.79	-0.40	1.79
7	0.23	0.47	1.16	-0.21	1.16
8	0.074	0.064	0.44	-0.031	0.44

Figures 42 and 43 are plots of $\log(\eta^*_{sp}/\underline{c})$ as a function of concentration at given shear stresses for those fractions which exhibited shear dependence. For simplicity only the maximum, minimum, and zero shear stress lines are shown in these figures. Table X is a summary of all the least square lines for these curves. Figure 44 is a plot of apparent reduced viscosity as a function of shear stress. The intercepts of these lines are intrinsic viscosities.

Intrinsic Viscosity-Molecular Weight Relationships

When a log-log plot is made of the intrinsic viscosity against the weight average molecular weight as in Fig. 45, the data fit the equation

$$[\eta] = (2.37 \times 10^{-4})(M_w)^{0.69}. \qquad (113)$$

However, closer examination of the data indicates that the plot actually is a curve that probably is second degree. Badgley and Mark (89) find that cellulose acetate in acetone follows this type of relationship, $[\eta] = (2.09 \times 10^{-5})\underline{M}_n - (0.315 \times 10^{-10})\underline{M}_n^2$, for molecular weights between 3×10^4 and 3×10^5. However, as pointed out by Holtzer, Benoit and Doty (90), the fact that viscosity measurements were not

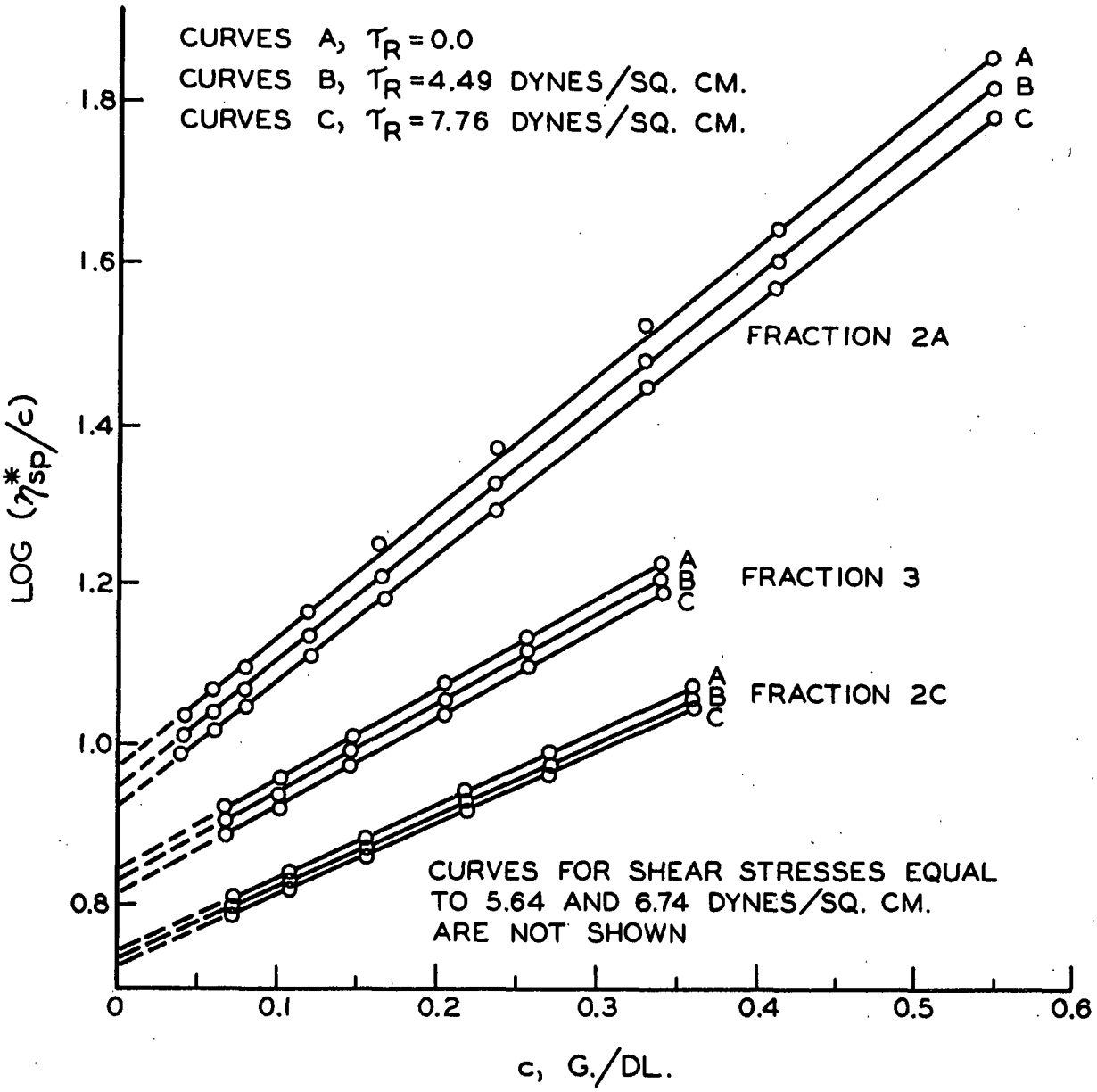

Figure 42. Log $\eta^*_{sp}/\underline{c}$ vs. $\underline{c}$ for Guaran Triacetate Fractions in Acetonitrile, 25.00 ± 0.02°C.

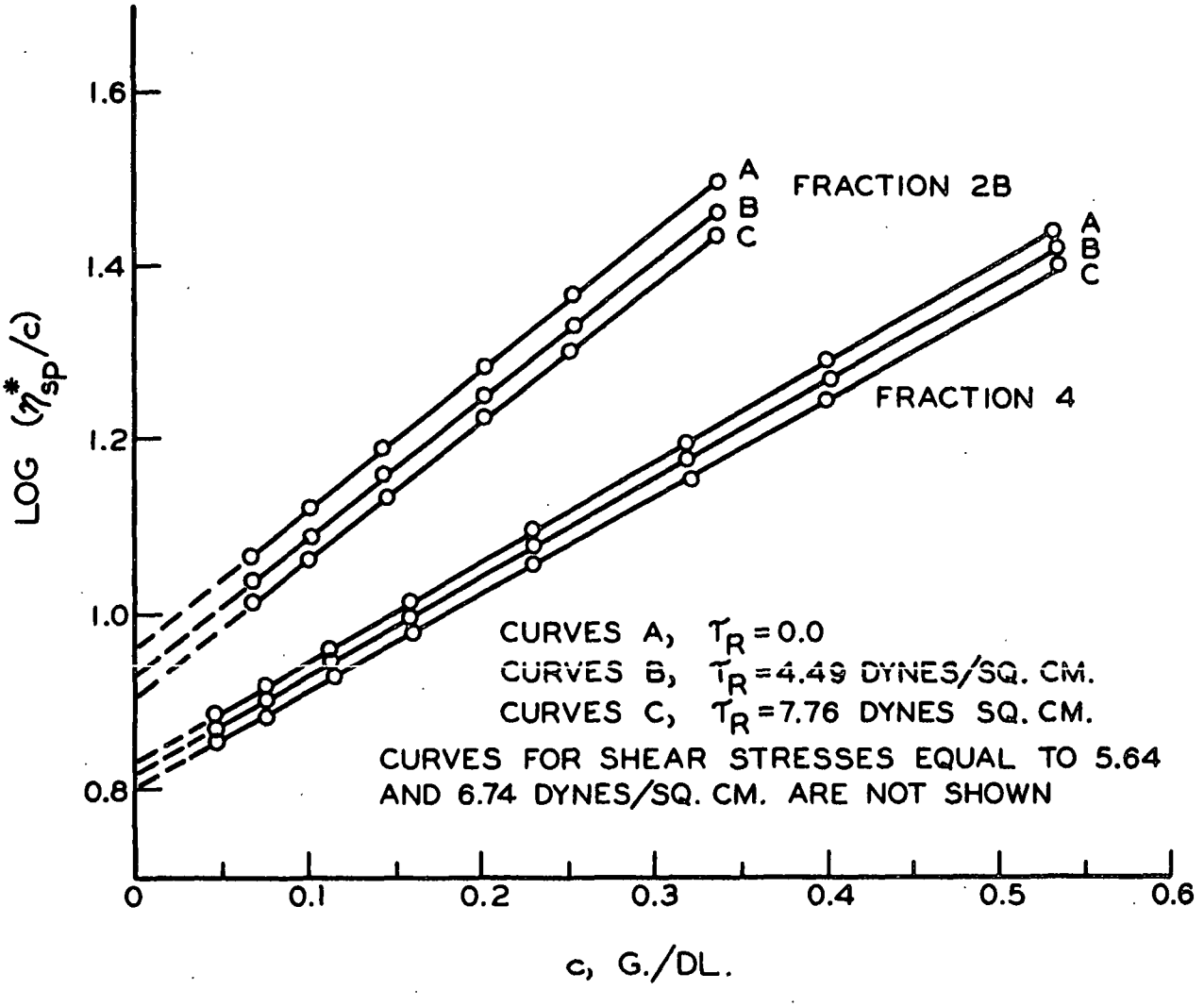

Figure 43. Log η^*_{sp}/c vs. c for Guaran Triacetate Fractions in Acetonitrile, 25.00 ± 0.02°C.

TABLE X

LEAST SQUARE LINES FOR $\log (\eta^*_{sp}/\underline{c}) = \underline{m}\underline{c} + \log (\eta_{sp}/\underline{c})_{\underline{c}=0}$.
GUARAN TRIACETATE FRACTIONS IN ACETONITRILE, 25.00 ± 0.02°C.

Fraction	$\bar{M}_w \times 10^{-6}$	τ_R = 7.76 dynes/sq.cm.		τ_R = 6.74 dynes/sq.cm.		τ_R = 5.64 dynes/sq.cm.		τ_R = 4.49 dynes/sq.cm.		τ_R = 0	
		$\underline{m}$	$\log(\eta_{sp}/\underline{c})_{\underline{c}=0}$	$\underline{m}$	$\log(\eta_{sp}/\underline{c})_{\underline{c}=0}$	$\underline{m}$	$\log(\eta_{sp}/\underline{c})_{\underline{c}=0}$	$\underline{m}$	$\log(\eta_{sp}/\underline{c})_{\underline{c}=0}$	$\underline{m}$	$\log[\eta]$
2A	5.34	1.570	0.9258	1.594	0.9314	1.601	0.9387	1.605	0.9464	1.628	0.9756
2B	4.84	1.582	0.9021	1.583	0.9167	1.589	0.9223	1.577	0.9318	1.608	0.9598
3	3.30	1.091	0.8188	1.100	0.8203	1.095	0.8263	1.096	0.8307	1.123	0.8470
4	2.68	1.105	0.8056	1.117	0.8089	1.122	0.8128	1.127	0.8164	1.146	0.8318
2C	2.06	0.889	0.7300	0.891	0.7325	0.890	0.7360	0.897	0.7372	0.903	0.7481

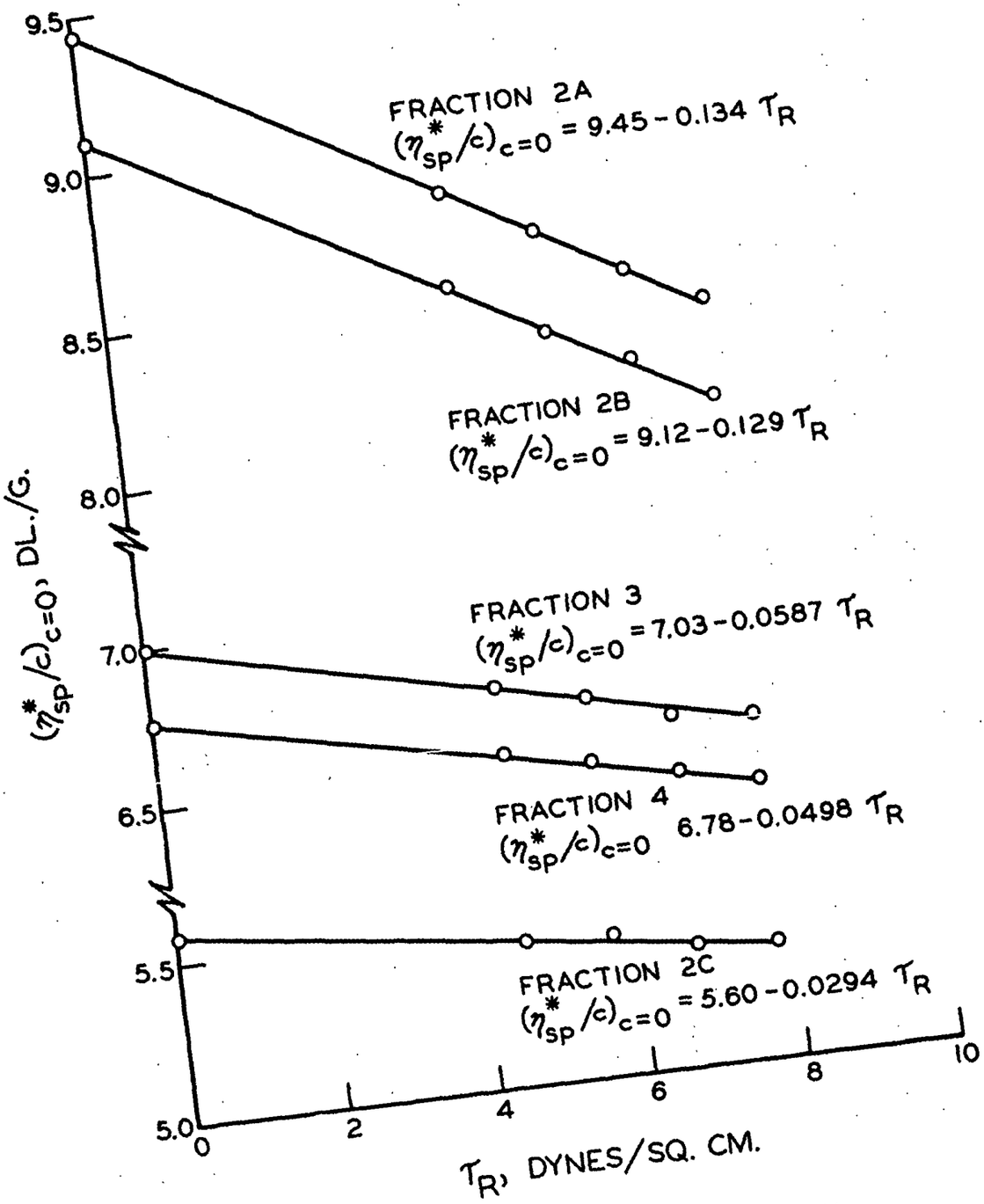

Figure 44. Dependence of Apparent Reduced Viscosity at Zero Concentration on Shear Stress, Guaran Triacetate in Acetonitrile, 25.00 + 0.02°C. Equations Are of the Form $(\eta^*_{sp}/\underline{c})_{\underline{c}=0} = [\eta] - \underline{M}\ \tau_{\underline{R}}$

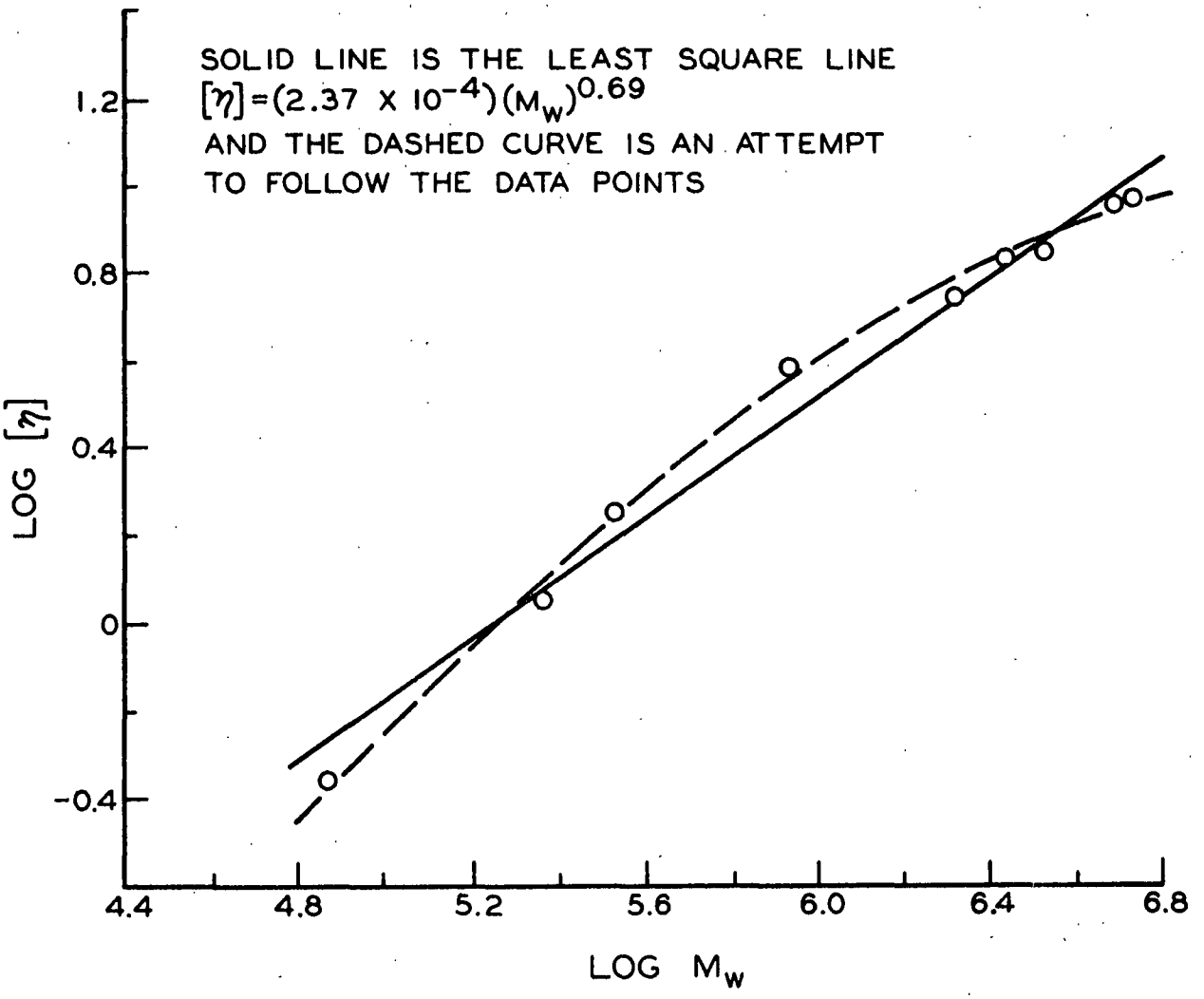

Figure 45. Intrinsic Viscosity-Molecular Weight Curve for Guaran Triacetate Fractions in Acetonitrile at 25.00 ± 0.02°C.

made as a function of shear and were not extrapolated to zero shear stress may have been responsible for these results. These same workers (90) also point out that Munster's (91) curves for cellulose nitrate in acetone, which show a similar curvature, were not studied as a function of shear. Since the viscosities of the guaran triacetate fractions were studied as a function of shear and extrapolated to zero shear, it would seem that the $[\eta]$-$\underline{M}$ relationship actually does show curvature. Hunt, et al. (92) note that the straight lines obtained from plots of intrinsic viscosity against molecular weight should be regarded as tangents to curves whose shape could be more reliably described by covering a wider range of molecular weights.

A better fit than a single straight line for the data is obtained if the data are divided into two parts and two straight lines are used as shown in Fig. 46 and 47. For the lower molecular weights the equation is

$$[\eta] = (2.62 \times 10^{-5})(M_w)^{0.87}, \qquad (114)$$

and for the higher molecular weights the equation is

$$[\eta] = (3.11 \times 10^{-3})(M_w)^{0.52}, \qquad (115)$$

with the standard error* for each exponent equal to $\pm$ 0.03.

Recently Marx-Figini and Schulz (94) consolidated intrinsic viscosity and molecular weight data obtained by various workers on cellulose nitrate. It was

*The standard error of the regression coefficient was calculated from

$$\text{Standard Error} = \left\{\Sigma(\underline{y} - \underline{Y})^2/(\emptyset - 2)\right\}^{1/2} / \left\{\Sigma\underline{x} - [(\Sigma\underline{x})^2/\emptyset]\right\}^{1/2}$$

where $\underline{y}$ is the observed value of the dependent variable, $\underline{Y}$ is the calculated value of the dependent variable, $\underline{x}$ is the value of the independent variable, and $\emptyset$ is the number of observations (93).

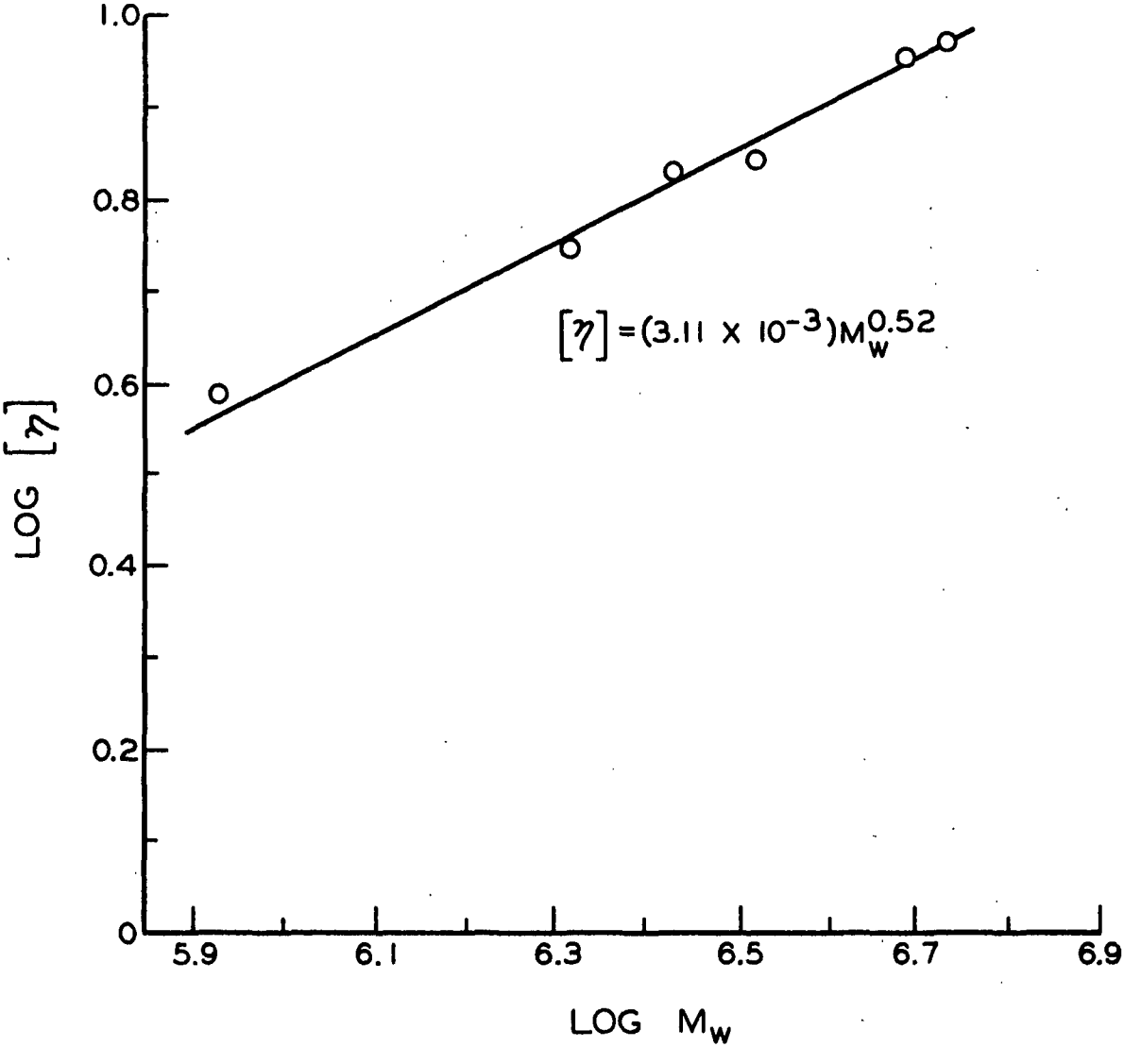

Figure 46. Intrinsic Viscosity-Molecular Weight Curve for the High Molecular Weight Fractions of Guaran Triacetate in Acetonitrile at 25.00 ± 0.02°C.

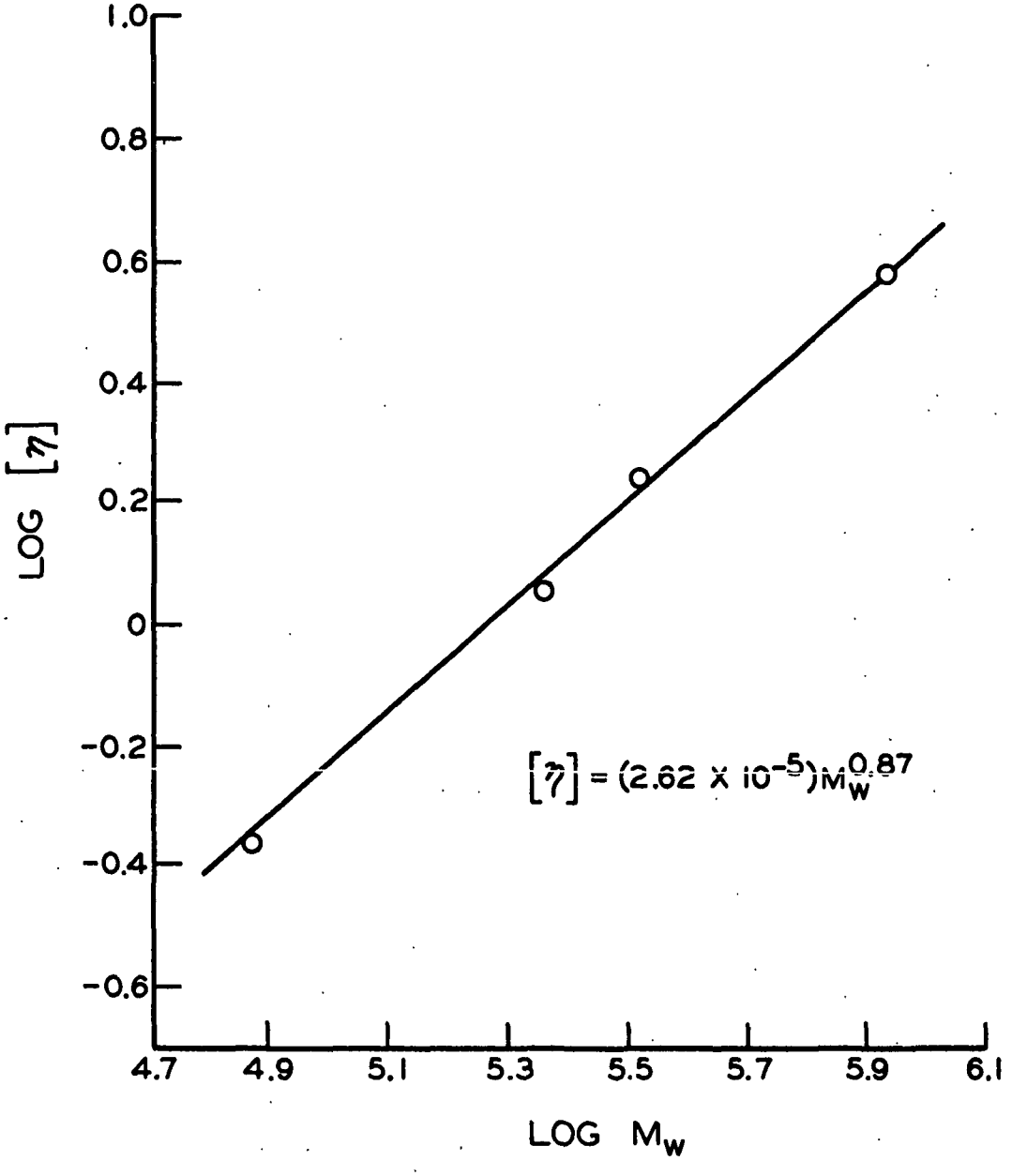

Figure 47. Intrinsic Viscosity-Molecular Weight Curve for the Low Molecular Weight Fractions of Guaran Triacetate in Acetonitrile at 25.00 ± 0.02°C.

found that although the data of each investigator approximates a linear relationship, when examined as a whole the data actually follow a curve. These data also may be expressed as two straight lines on a log-log plot, $[\eta] \sim \underline{M}_{\underline{w}}^{1.0}$ and $[\eta] \sim \underline{M}_{\underline{w}}^{0.76}$, which is similar to the behavior of guaran triacetate in acetonitrile.

DISCUSSION

CONFIGURATIONAL PARAMETERS

INTRODUCTION

To compare the measured values of the RMS radius of gyration, $(\overline{s}^2)^{1/2}$, with molecular models, it is necessary to have the RMS radius of gyration of the unperturbed molecule, $(\overline{s}^2)_o^{1/2}$. Equation (49), $(\overline{s}^2)^{1/2} = \alpha\,(\overline{s}^2)_o^{1/2}$, relates these two dimensional parameters by means of the molecular expansion factor, α. In the following work, the second virial coefficient obtained from light scattering will be used to estimate α.

SECOND VIRIAL COEFFICIENT

The concentration dependence of oxmotic pressure can be expressed in a series expansion as

$$\pi/cRT = (1/M_n) + A_2'c, \tag{116}$$

where π is the osmotic pressure and R is the gas constant. An analogous expression can be written for light scattering as

$$Hc/\tau = (1/M_w) + 2A_2c \tag{117}$$

at zero scattering angle. The second virial coefficients A_2' and A_2 in Equations (116) and (117) are identical for homogeneous polymers. For heterogeneous polymers they depend on molecular weight distribution and they differ from one another in a manner that depends on the particular distribution involved.

For the present analysis, the polymer will be considered to be homogeneous. The second virial coefficient is given, in general, by (42)

$$A_2 = N_A u/2M^2, \tag{118}$$

where u is the excluded volume, N_A is Avogadro's number, and M is the molecular weight. The excluded volume is the volume which is effectively excluded to a given molecule by the presence of another molecule. To see how A_2 depends on molecular parameters, it is necessary to substitute $\Phi'(\bar{s}^2)^{3/2}/M^2$, see Equation (45), for the intrinsic viscosity in Equation (55) which results in

$$A_2 = [\Phi'(\bar{s}^2)^{3/2}/M^2] \left\{1.65 \log_{10} [1 + 4.50 (\alpha^2 - 1)]\right\} . \tag{119}$$

Thus, the second virial coefficient specifically depends on the volume occupied by the polymer molecule through $(\bar{s}^2)^{3/2}$. This dependence is modified by a logarithmic term which depends on the polymer-solvent interaction. The interaction may be regarded as a "noninterpenetration factor" for molecular domains (42).

The solvent quality has two effects on the second virial coefficient. First, the better the solvent, the larger will be the volume term, $(\bar{s}^2)^{3/2}$. Secondly, the better the solvent, the greater will be the molecular expansion factor, α, and thereby the interpenetration of the molecular domains will be decreased. The logarithmic term is considerably less sensitive to solvent quality than is the size of the molecule (42). For good solvents, the noninterpenetration term is of secondary importance and the size of the molecular domain is predominant in determining the value of A_2.

Experimental values of the second virial coefficient obtained from light-scattering data are listed in Table XI along with a summary of other molecular parameters.

It is of interest to examine the left-hand side of Equation (55). This quantity, $A_2 M_w/[\eta]$, takes on values of about 0.2 to 0.4 for cellulose derivatives

TABLE XI

MOLECULAR PARAMETERS FOR FRACTIONATED GUARAN TRIACETATE IN ACETONITRILE

Fraction	$[\eta]$, dl./g.	$\underline{M}_w \times 10^{-6}$	$(\underline{s}^2_z)^{1/2}$, A.	$\underline{A}_2$, moles ml. $g.^{-2} \times 10^4$	$\underline{M}_z:\underline{M}_w:\underline{M}_n$	α	$\underline{A}_2\underline{M}_w/[\eta]$
2A	9.45	5.34	1300	0.38	1.9:1.7:1.0	1.04	0.21
2B	9.12	4.84	1250	0.38	1.9:1.7:1.0	1.04	0.20
3	7.03	3.30	1160	0.81	2.1:1.6:1.0	1.07	0.38
4	6.78	2.68	1050	1.42	2.1:1.6:1.0	1.12	0.56
2C	5.60	2.06	980	1.40	1.9:1.7:1.0	1.11	0.51
5	3.87	0.85	680	2.90	2.1:1.6:1.0	1.15	0.64
6	1.79	0.33	470	2.48	2.1:1.6:1.0	1.09	0.46
7	1.16	0.23	440	3.91	2.1:1.6:1.0	1.20	0.78
8	0.44	0.074	250	4.70	2.1:1.6:1.0	1.20	0.79

(65). For guaran triacetate this range is exceeded, and $A_2 M_w/[\eta]$ approaches a limiting value that is greater than 0.8 as evidenced in Table XI.

MOLECULAR EXPANSION FACTOR

The molecular expansion factor, α, accounts for the influence of the volume of the molecular segments within the effective hydrodynamic volume and for the interaction of the chain segments with the solvent (24). It is useful in ascertaining the unperturbed molecular dimensions as shown in Equations (48) and (49). Values of α calculated from the Flory-Krigbaum-Orofino relationship recommended by Stockmayer (43), Equation (55), are listed in Table XI.

Values of α were also calculated in three other ways. First, it was calculated from the Orofino-Flory relationship (42), Equation (54). For the other methods, the value of the intrinsic viscosity in acetonitrile at the theta point, $[\eta]_\theta$, was estimated from Equation (53). Then, α was evaluated by means of Equation (52) proposed by Flory (24) for Gaussian chains, and from the relationship

$$[\eta]/[\eta]_\theta = \alpha^{2.43}, \qquad (120)$$

which was proposed by Kurata, Stockmayer, and Roig (95) to account for the non-Gaussian character of chains with excluded volume. The difference in α was 2 to 5% for Fractions 2A through 6 and about 15% for Fractions 7 and 8 when calculated by these three methods and compared with the results from the Flory-Krigbaum-Orofino relationship (43).

The results in Table XI indicate that α increases with decreasing molecular weight. The magnitude of these values are consistent with the findings of other investigators of naturally occurring polysaccharides. For cellulose trinitrate in ethyl acetate and in acetone (92, 96), α was about 1.03 to 1.09; for cellulose

tricaproate in 1-chloronaphthalene and in (100:7) dioxane-water (97), α was 1.05; for hydroxyethyl cellulose in water (98), α was about 1.02 to 1.04; and for cellulose in Cadoxen (99), α varied from 1.04 to 1.23. The low values of the molecular expansion factor in the β-1,4-linked polysaccharides indicates that the molecules are well extended.

HINDERED CHAIN ROTATION

Burchard and Husemann (100) list two expressions that describe the mean-square unperturbed radius of gyration of a linear polymer, as cellulose, in terms of chain dimensions and bond and bond-plane angles. The first of these relationships is

$$(\bar{s}^2)_o = (N/6)\left\{\left[\frac{a^2(1+\cos\theta)(1+\overline{\cos\phi})}{(1-\cos\theta)(1-\overline{\cos\phi})}\right] + \left[\frac{b^2(1+\overline{\cos\phi})}{(1-\overline{\cos\phi})}\right]\right\}. \qquad (121)$$

In this expression N is the degree of polymerization and θ is the supplement to the oxygen valence angle of 110°. Since guaran and cellulose have the same molecular conformation and fiber repeat distance, the monomer dimensions shown in Fig. 3 may be used for a and b. The angle ϕ is the angle between the planes through a given monomeric unit and its predecessor and successor, respectively (101).

When the unperturbed radius of gyration is known, it is possible to evaluate $\overline{\cos\phi}$, which is a measure of the average steric hindrance to rotation in the polymer chain. When there is free rotation about the carbon-oxygen bonds linking the pyranose rings, $\overline{\cos\phi} = 0$. If there is a complete absence of rotational freedom about these bonds, $\overline{\cos\phi} = 1$ and the molecule has its maximum extension.

In β-1,4-linked polysaccharides, each chain member is twisted through 180° with respect to its nearest neighbor. For this reason two rotational potential minima should exist, one at 0° and one at 180°. Thus, the monomeric units can

exist with equal probability in two positions. The mean-square radius of gyration is given in Equation (121) for a single potential minimum and by the following expression for two potential minima (100),

$$(\bar{s}^2)_o = (N/6)(1/2)\left\{\frac{a^2(1+\cos\theta)}{(1-\cos\theta)} + b^2\right\}\left\{\frac{(1+\overline{\cos\phi})}{(1-\overline{\cos\phi})} + \frac{(1-\overline{\cos\phi})}{(1+\overline{\cos\phi})}\right\}. \quad (122)$$

In Equations (121) and (122) a random coil model has been introduced by making the assumption that $(\bar{r}^2)_o = 6(\bar{s}^2)_o$. Keeping this in mind, values of $\overline{\cos\phi}$ were calculated and are shown in Table XII. It should be remembered that previously it has been shown that guaran triacetate molecules approximate a random coil only at very high molecular weights. The z-average degrees of polymerization, N_z, were used in these calculations.

TABLE XII

VALUES OF $\overline{\cos\phi}$, A MEASURE OF STERIC HINDRANCE TO ROTATION, AND RELATED PARAMETERS FOR GUARAN TRIACETATE IN ACETONITRILE AT 25°C.

Fraction	N_z	$(\bar{s}_z^2)_o = (\bar{s}_z^2)/\alpha^2$	$\overline{\cos\phi}$ Equation (121)	$\overline{\cos\phi}$ Equation (122)
2A	13,810	1.57×10^6	0.84	0.92
2B	12,520	1.45×10^6	0.84	0.92
3	10,000	1.16×10^6	0.84	0.92
4	8,150	8.80×10^5	0.83	0.91
2C	5,330	7.73×10^5	0.87	0.94
5	2,590	3.49×10^5	0.86	0.93
6	1,000	1.86×10^5	0.90	0.95
7	690	1.35×10^5	0.90	0.95
8	225	4.45×10^4	0.90	0.95

Over-all, the values of $\overline{\cos\phi}$ vary by about 7% between the minimum and maximum values when evaluated from Equation (121) and about 3% when evaluated from Equation (122). Since guaran triacetate is coil-like only at high molecular weights, the essentially constant values of $\overline{\cos\phi} = 0.84$ and $\overline{\cos\phi} = 0.92$ for the four largest fractions will be taken to be the measure of average steric hindrance. Large values of $\overline{\cos\phi}$ have been observed for cellulose and its derivatives; for cellulose tricarbanilate (100), $\overline{\cos\phi} = 0.798$ from Equation (121), and $\overline{\cos\phi} = 0.893$ from Equation (122); for hydroxyethyl cellulose (98), $\overline{\cos\phi} = 0.89$; and for cellulose in Cadoxen (99), $\overline{\cos\phi} = 0.78$ [the latter two values were calculated from Equation (121)].

The steric hindrance can be accounted for by allowing a limited rotation through an average angle $\pm\bar{\phi}$ about the carbon-oxygen bonds (85). The approximation of Debye (102),

$$\bar{\phi} = \sin\bar{\phi}/\overline{\cos\phi}, \qquad (123)$$

may be used to evaluate $\bar{\phi}$. Equation (123) was solved by a trial and error method with the result that $\bar{\phi} = 40.6°$ for $\overline{\cos\phi} = 0.92$ and $\bar{\phi} = 57.8°$ for $\overline{\cos\phi} = 0.84$. This would indicate a permitted angle of rotation of $\sim 81°$ in the first case and $\sim 116°$ in the second case.

The large values of $\overline{\cos\phi}$ indicate that the molecule is sterically hindered in such a manner as to produce a highly extended molecule. It is appropriate to note that recently Swenson and Thompson (103) examined Fischer-Hirschfelder models of the pyranose ring and point out that the primary alcohol of carbon-6 projects beyond the ether bond and prevents rotation of the adjacent anhydrosugar unit around the carbon-oxygen linkage. When carbon-6 is removed, as in a xylan chain, the pyranose rings rotate freely with respect to one another on the model and the

molecule appears to be more flexible which is in agreement with their experimental findings. Thus, it would seem that the presence of carbon-6 on the main chain mannan units is the primary cause of the stiffness of the polymer chain.

POROD-KRATKY CHAIN MODEL

A measure of relative chain stiffness may be obtained from the persistence length as defined in the Porod-Kratky chain model (104). For this model, the polymer chain direction varies continuously instead of at specified bond junctions. The stiffness of the chain is characterized by a factor termed the persistence length, q, which may be defined as the mean length of projection of an infinitely long chain on the direction of its first link (101). When q is large, the chain is very stiff and rodlike, and when q is small, the chain is more flexible and coil-like.

Benoit and Doty (69) used this model when deriving the following expression relating the unperturbed mean-square radius of gyration, $(\bar{s}^2)_o$, to the persistence length

$$(\bar{s}^2)_o = q^2 \left\{(x/3) - 1 + (2/x) - 2\,[1 - \exp(-x)]/x^2\right\} . \qquad (124)$$

In this relation, x is the number of Porod units per molecule and is defined as

$$x = r_{max}/q, \qquad (125)$$

where r_{max} is the length of the fully extended chain ($r_{max} = bN = 5.15N$ for guaran triacetate). When $x > 6$, Equation (124) reduces to the following,

$$(\bar{s}^2)_o = q^2 \left\{(x/3) - 1 + (2/x)\,[1 - (1/x)]\right\} . \qquad (126)$$

To correct for molecular heterogeneity, Hunt, et al. (92) show that Equation (126)

should be written

$$(\overline{s}_z^2)_o = q^2 \left\{(x_z/3) - 1 + (2/x_w)\,[1 - (1/x_n)]\right\}, \qquad (127)$$

where the subscripts z, w, and n indicate that the z-average, weight average, and number average values of N were used to determine the appropriate value of x. When x is large, Equation (126) may be approximated by

$$(\overline{s}_z^2)_o = (r_{max})_z(q/3). \qquad (128)$$

Table XIII summarizes the pertinent values involved in the Porod-Kratky chain model for guaran triacetate. From this table, it can be seen that q decreases with increasing molecular weight. For the four highest molecular weight fractions, it reaches a limiting value of approximately 67 A. which may be taken as the characteristic persistence length for these molecules. Cowie (105) found q = 47 ± 1.0 A. for amylose triacetate, Brown (98) found the mean value of q = 83 A. for hydroxyethyl cellulose, and Hunt, et al. (92) found q = 117 A. for cellulose trinitrate. For purposes of comparison, polystyrene, polyisobutylene, polymethylmethacrylate, and polyvinyl acetate, which are said to have flexible chains, have values for q in the range of 8 to 10 A. (92). Other persistence length values for synthetic polymers are given by Krigbaum, Kurz, and Smith (106).

The ratio $(\overline{s}_z^2)_o/M_z$ for the fractions of guaran triacetate are given in Table XIII and plotted as a function of M_z in Fig. 48. The dashed line in this figure is the theoretical curve calculated from Equations (124) and (126) using a value for q of 67 A., and the solid line approximately follows the experimental data. The ratio of $(\overline{s}_z^2)_o/M_z$ decreases with increasing molecular weight and approaches a limiting value of about 0.26. Thus, the Porod-Kratky model requirements are not met since the theoretical curve predicts a decrease in this ratio with decreasing

molecular weight as the polymer molecule deviates from a Gaussian configuration. Similar deviations from the theoretical curve have been shown by a number of other investigators who worked with naturally occurring polysaccharides (98, 99, 105, 107). Krigbaum and Sperling (107), who worked with cellulose tricaproate, explained this deviation from theory by assuming a shift in the population of bonds among the various rotational states. At low molecular weight one rotational conformation is favored, but as the molecular weight is increased the bond population in the available rotational sites becomes more randomly distributed. It should be noted that the data of Hunt, et al. (92) and Holtzer, Benoit, and Doty (90) for cellulose trinitrate show the theoretical decrease in $(\bar{s}_z^2)_o/M_z$ with decreasing molecular weight in accordance with the Porod-Kratky model.

TABLE XIII

PARAMETERS INVOLVED IN THE POROD-KRATKY CHAIN MODEL FOR GUARAN TRIACETATE

Fraction	$M_z \times 10^{-6}$	$(\bar{s}_z^2)_o^{1/2}$, A.	q, A.	$(\bar{s}_z^2)_o/M_z$, $A.^2$ mole/g.
2A	5.96	1250	66	0.26
2B	5.40	1200	67	0.27
3	4.33	1080	67	0.27
4	3.52	940	63	0.25
2C	2.30	880	84	0.34
5	1.12	590	79	0.31
6	0.43	430	109	0.43
7	0.30	370	113	0.45
8	0.097	210	115	0.46

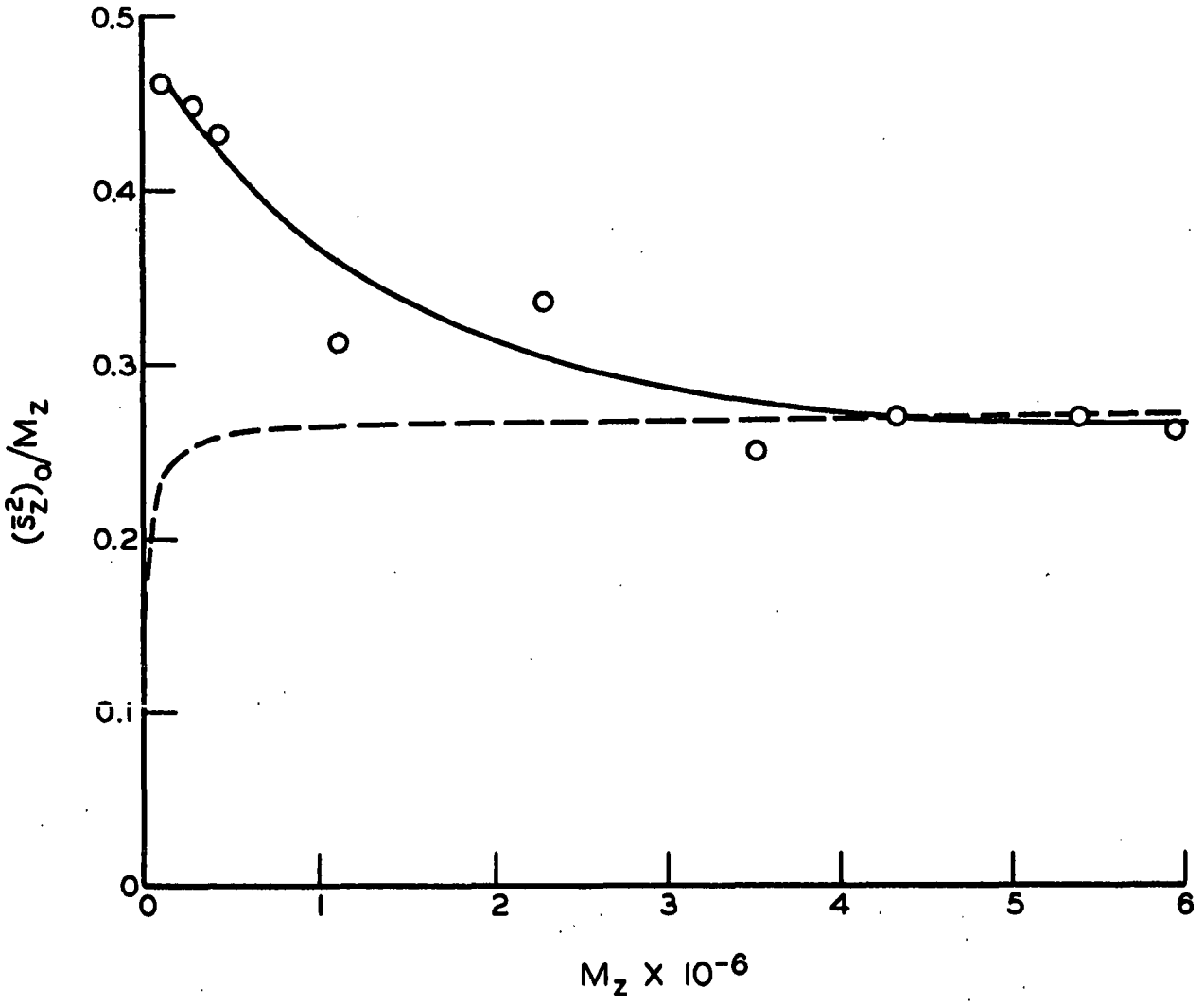

Figure 48. Dependence of $(\bar{s}_z^2)_o/M_z$ on M_z. Circles and Solid Line Are Experimental Values, Dashed Line Is the Theoretical Curve Calculated from q = 67 A. Guaran Triacetate in Acetonitrile

RADIUS OF GYRATION AND MOLECULAR WEIGHT

The mean-square radius of gyration can be correlated with the molecular weight according to the relationship (101)

$$(\bar{s}^2) = K_2 M^{(1 + \epsilon)}, \qquad (129)$$

where K_2 is a constant and ϵ is a measure of the solvent quality. Figure 49 is a plot of $(\bar{s}^2_z)$ as a function of M_z. By using the method of least squares to fit the data, the expression

$$(\bar{s}^2_z) = (9.06) M_z^{0.78} \qquad (130)$$

was obtained, which indicates that $\epsilon = -0.22$. The standard error of the regression coefficient for this expression was $\pm$ 0.02.

Theory predicts that ϵ should be zero in a theta solvent and positive in other solvents (108). The negative value of ϵ obtained with guaran triacetate in acetonitrile is similar to those obtained for certain derivatives of cellulose. Uda and Meyerhoff (109) determined a value of $\epsilon = + 0.07$ for methyl cellulose, but list negative values of ϵ obtained with ethylhydroxyethyl cellulose and ethyl cellulose. These and other results are summarized in Table XIV.

Negative values of ϵ may be explained on the basis of the shift in bond population with molecular weight (107). At the low molecular weights the measured RMS radius of gyration is greater than would be expected from a random coil because of this shift in bond population. This results in a lower slope than expected in the $\log(\bar{s}^2_z)$ versus $\log M_z$ plot and hence in negative values of ϵ.

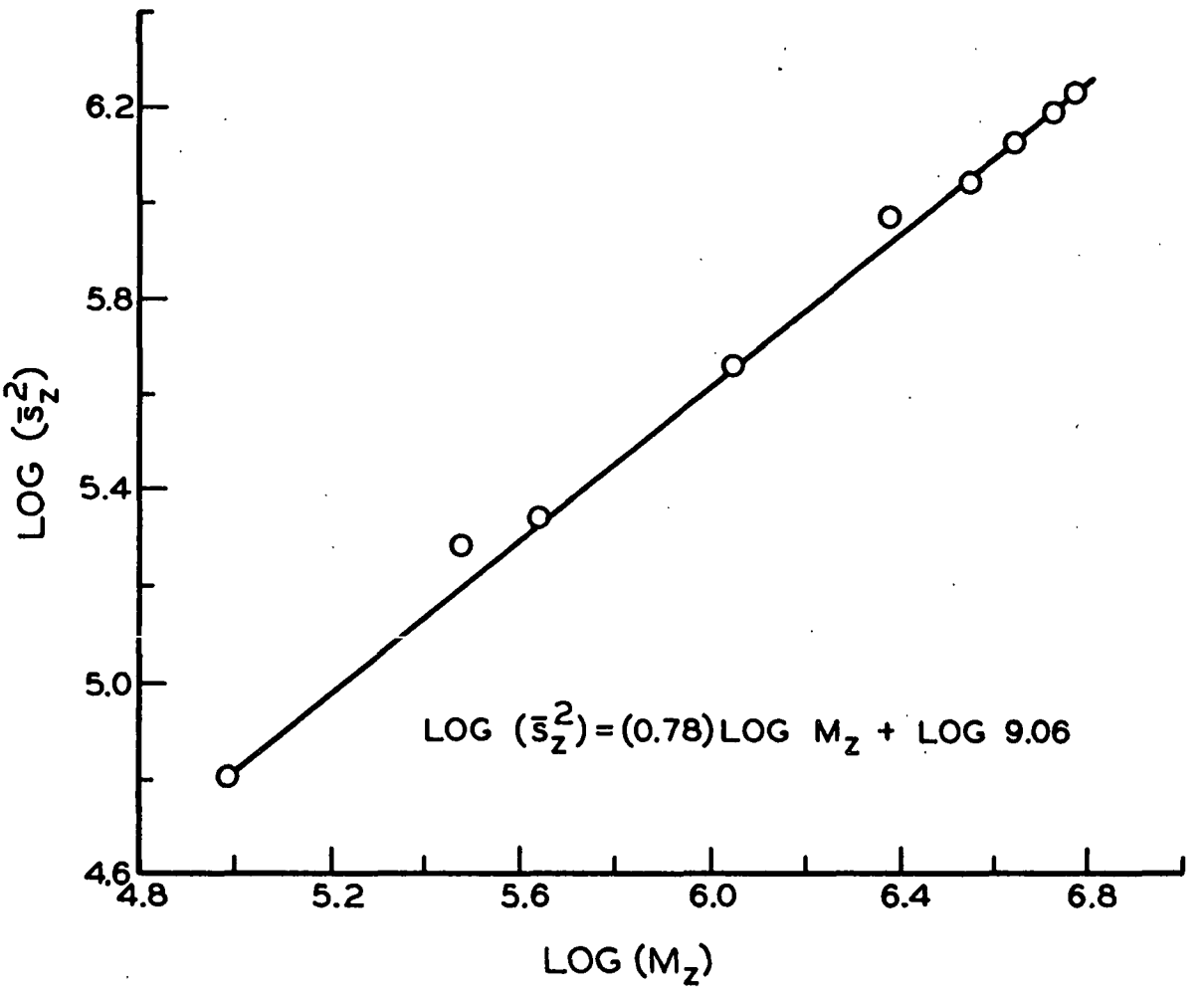

Figure 49. Log-Log Plot of the Square of Radius of Gyration Versus Molecular Weight. Guaran Triacetate in Acetonitrile, 22.5°C.

TABLE XIV

VALUES OF ϵ FOR DERIVATIVES OF SOME NATURALLY OCCURRING POLYMERS

Polymer	Solvent	ϵ	Reference
Guaran triacetate	acetonitrile	-0.22	--
Ethylhydroxyethyl cellulose	water	-0.10	(109)
Ethyl cellulose	methanol	-0.70	(109)
Hydroxyethyl cellulose	--	-0.30	(109)
Hydroxyethyl cellulose	water	-0.04	(98)
Cellulose	Cadoxen	0	(99)
Methyl cellulose	water	+0.07	(109)
Cellulose nitrate	acetone	+0.33	(109)
Cellulose tricarbanilate	pyridine	+0.26	(100)
Amylose tricarbanilate	pyridine	+0.32	(100)

COMPARISON OF THE RADIUS OF GYRATION WITH THAT OF OTHER POLYMERS

The radius of gyration of guaran triacetate will be compared with that of certain cellulose derivatives and polystyrene by means of a form of the extension ratio (38). Rather than using the ratio of end-to-end distance to contour length, $(\bar{r}^2)^{1/2}/r_{max}$, which defines the extension ratio, the ratio of unperturbed radius of gyration to contour length, $(\bar{s}^2)_o^{1/2}/r_{max}$, was used since the radius of gyration is the experimental quantity usually measured. This ratio will then be examined as a function of contour length so that the various polymers may be compared at the same extended length.

Values for this ratio are shown in Fig. 50 as a function of chain contour length. The dashed line in this figure is the theoretical curve for the Porod-Kratky chain model (104) of guaran triacetate using a persistence length of 67 A.

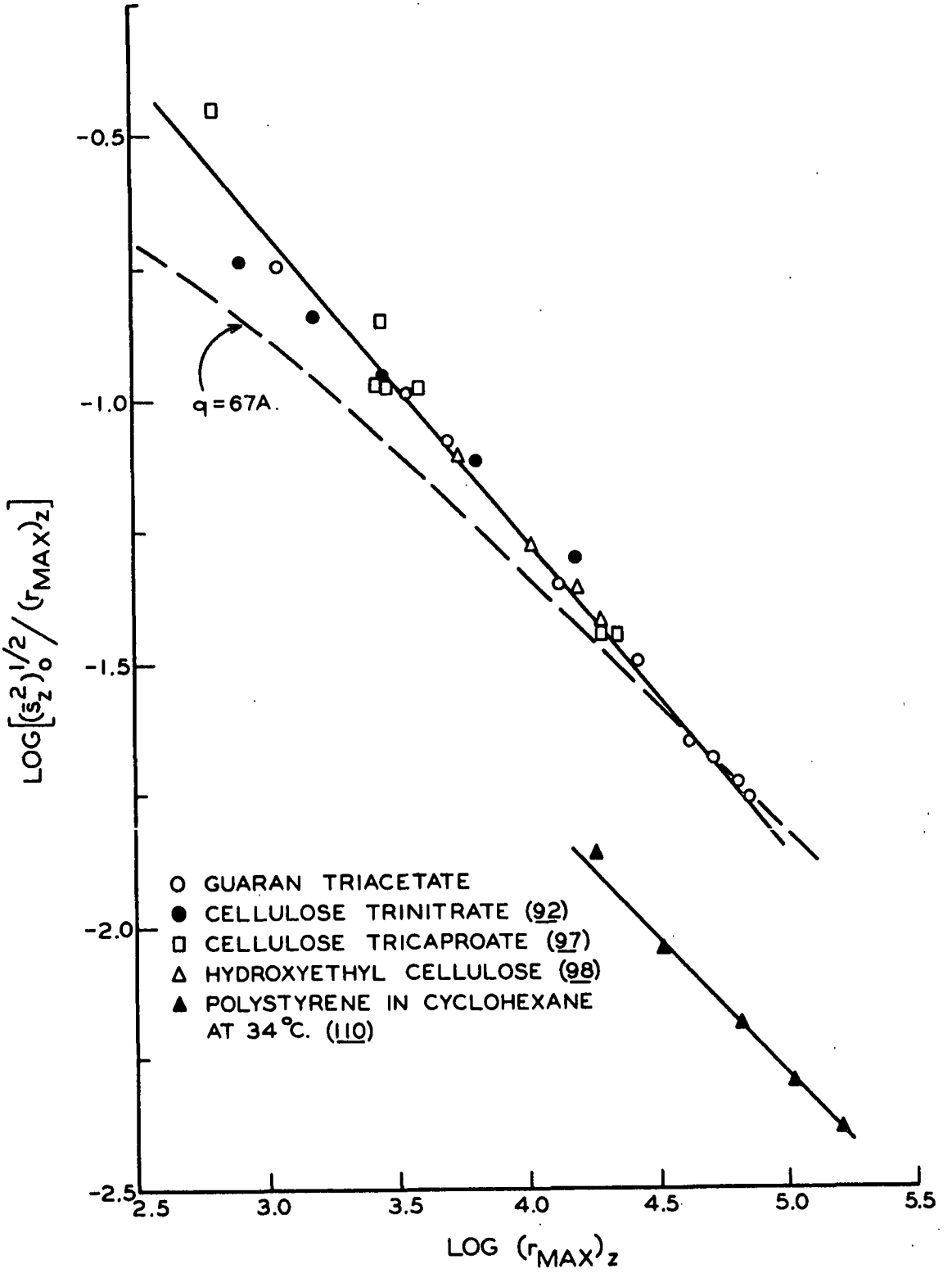

Figure 50. Dependence of the Ratio Log $[(\bar{s}_z^2)_o^{1/2}/r_{max})_z]$ on Log$(r_{max})_z$ for Various Polymers

As was expected, the theoretical Porod-Kratky data fit the experimental guaran triacetate data only at the four highest molecular weights where the persistence length of the molecules is constant and equal to ~67 A. (see Table XIII). The most interesting factor in Fig. 50 is that the data for the β-1,4-linked polymers all follow the same straight line. That is, the chains of cellulose nitrate in ethyl acetate (92), of cellulose tricaproate in 1-chloronaphthalene, dimethylformamide, and 100 to 7 dioxane–water (97), of hydroxyethyl cellulose in water (98) and of guaran triacetate in acetonitrile are sterically hindered to about the same degree at a given chain length. In contrast to these relatively stiff molecules, the flexible polystyrene chains in cyclohexane at 34°C. (110), which is a theta solvent at essentially the theta temperature, show a marked difference as would be expected.

Newman, et al. (38) working with flexible polymer molecules found that when the extension ratio was less than 0.1, which would be equivalent to about 0.04 for the ratio of $(\bar{s}^2)_o/r_{max}$ if one assumes the polymer molecule is a random coil, the spatial arrangement of the polymer chains approximated spherical symmetry and the molecules behaved as random coils. From what is known about the guaran triacetate molecules, it would seem that for these more inflexible molecules the ratio investigated would have to be less than about 0.02 before the coiling in the molecule is such that a random coil is approximated.

HYDRODYNAMIC PARAMETERS

INTRODUCTION

Previously, a number of hydrodynamic theories that describe the polymer molecule in solution were presented. These theories now will be used to describe guaran triacetate in solution. It will be shown that the excluded volume effect

is negligible, and with this factor described, the effective bond length of the molecules in solution will be determined. Then, the end-to-end chain distance of the polymer molecules will be calculated from the various hydrodynamic theories and compared to the values obtained from light scattering. Finally, values of Flory's Constant, Φ, will be evaluated and corrected for molecular heterogeneity to further describe guaran triacetate molecules in solution.

EXCLUDED VOLUME AND EFFECTIVE BOND LENGTH

Burchard (111) utilizes the theory of Kurata and Yamakawa (29) to obtain the following expression,

$$[\eta]/M^{1/2} = \pi^{3/2} N_A (b_e^2/6M_o)^{3/2} XF_o(X) [1 + p(X)(q_v)M^{1/2}], \qquad (131)$$

in which b_e is the effective bond length and q_v is a term that is proportional to the excluded volume. The other terms in this expression have been described previously. Equation (131) has the property of approaching a limiting slope at large values of the molecular weight. In addition, for large values of M, the value of the draining parameter, X, is large and the limiting values of $XF_o(X) = 1.259$ and $p(X) = 1.55$ are applicable. Therefore, in the limit, Equation (131) may be used to evaluate b_e and q_v from a knowledge of the intrinsic viscosity and molecular weight by plotting $[\eta]/M^{1/2}$ against $M^{1/2}$.

Figure 51 is a plot of $[\eta]/M_w^{1/2}$ against $M_w^{1/2}$ for guaran triacetate in acetonitrile. The least square line describing the limiting values of $[\eta]/M_w^{1/2}$ as a function of $M_w^{1/2}$ is given by

$$[\eta]/M_w^{1/2} = (4.06 \times 10^{-3}) - (1.76 \times 10^{-8}) M_w^{1/2}. \qquad (132)$$

From the slope of this plot, q_v is essentially zero indicating that the excluded volume effect is unimportant for guaran triacetate molecules in acetonitrile.

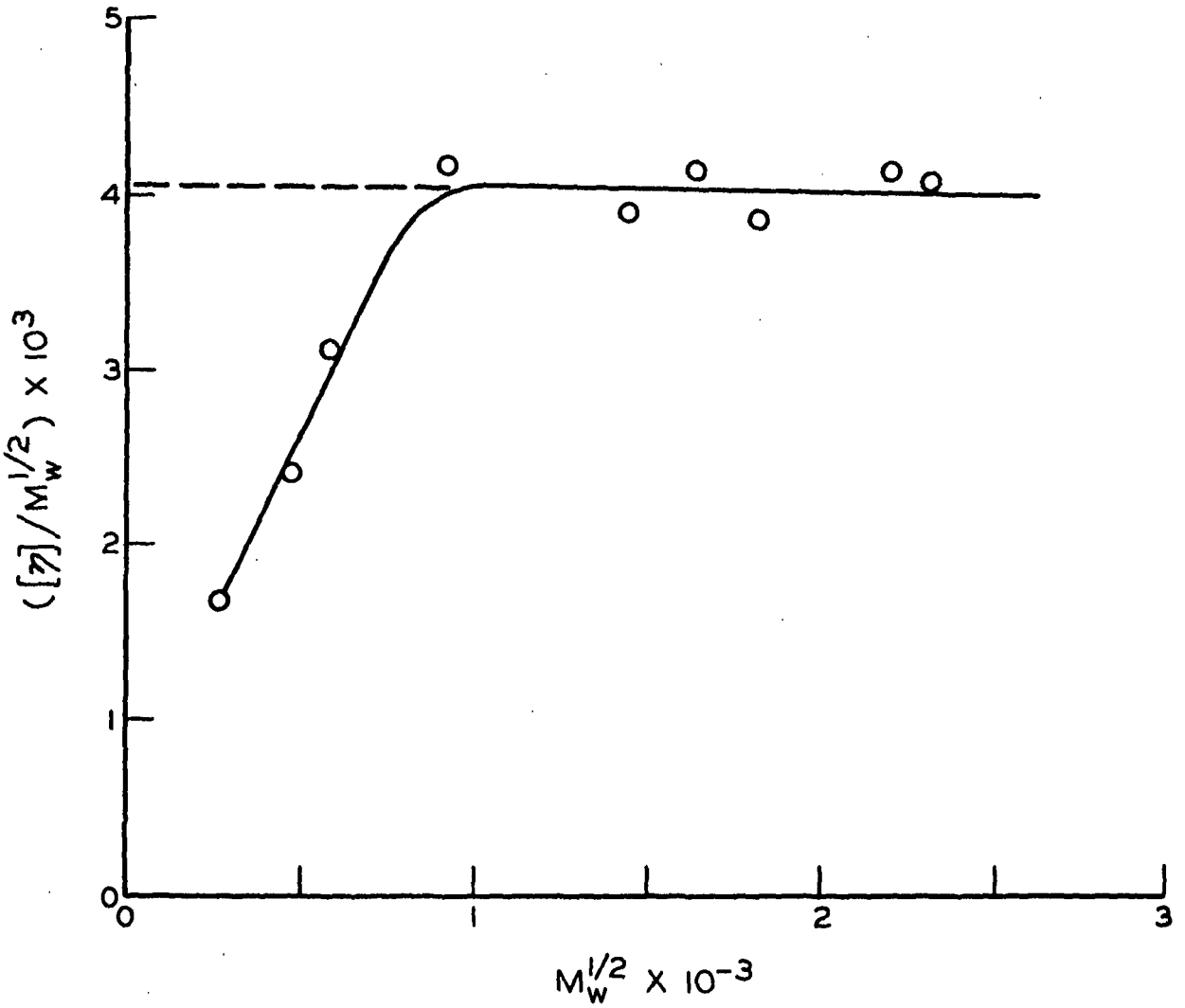

Figure 51. $[\eta]/\underline{M}_w$ as a Function of $\underline{M}_w^{1/2}$ for Guaran Triacetate in Acetonitrile

When the intercept is used to evaluate the equivalent bond length, b_e, a value of 23.5 A. is obtained.

It also is possible to evaluate the effective bond length from the Kirkwood-Riseman hydrodynamic theory (28), which does not account for excluded volume effects, by means of Equation (24). The values of b_e from this theory are summarized later in this thesis in Table XV, but the arithmetic average value of b_e for the higher values of molecular weight is 23.5 A. Since this value is identical to the one obtained by the method of Burchard (111) as described by Equation (131), it is further proof that excluded volume effects are negligible.

Burchard (111) also utilizes the Kurata-Yamakawa theory (29) to obtain the following equation,

$$(\overline{s^2})/M = (b_e^2/6M_o)(1 + 1.278\ q_v M^{1/2}), \qquad (133)$$

which may be used to evaluate b_e from light-scattering data. Figure 52 is a plot of $(\overline{s^2}_w)/M_w$ as a function of $M_w^{1/2}$ for guaran triacetate in acetonitrile. [To obtain the values of $(\overline{s^2}_w)$, it was assumed that $(\overline{s^2}_z)/(\overline{s^2}_w) = M_z/M_w$ (97).] At the highest molecular weights, the values of $(\overline{s^2}_w)/M_w$ are approaching an asymptotic limit. When b_e is evaluated from the limiting values of this parameter, it has a value of about 27 A. Since the slope is approaching zero, one can conclude that the excluded volume as expressed by q_v is again negligible.

The value of b_e obtained from light-scattering data is about 15% higher than the values obtained from intrinsic viscosity data. It is possible that a portion of this error came about when $(\overline{s^2}_z)$, the measured value of the radius of gyration, was converted to $(\overline{s^2}_w)$ by means of the molecular weight distributions found through ultracentrifugation. However, equally significant is the fact that the errors in

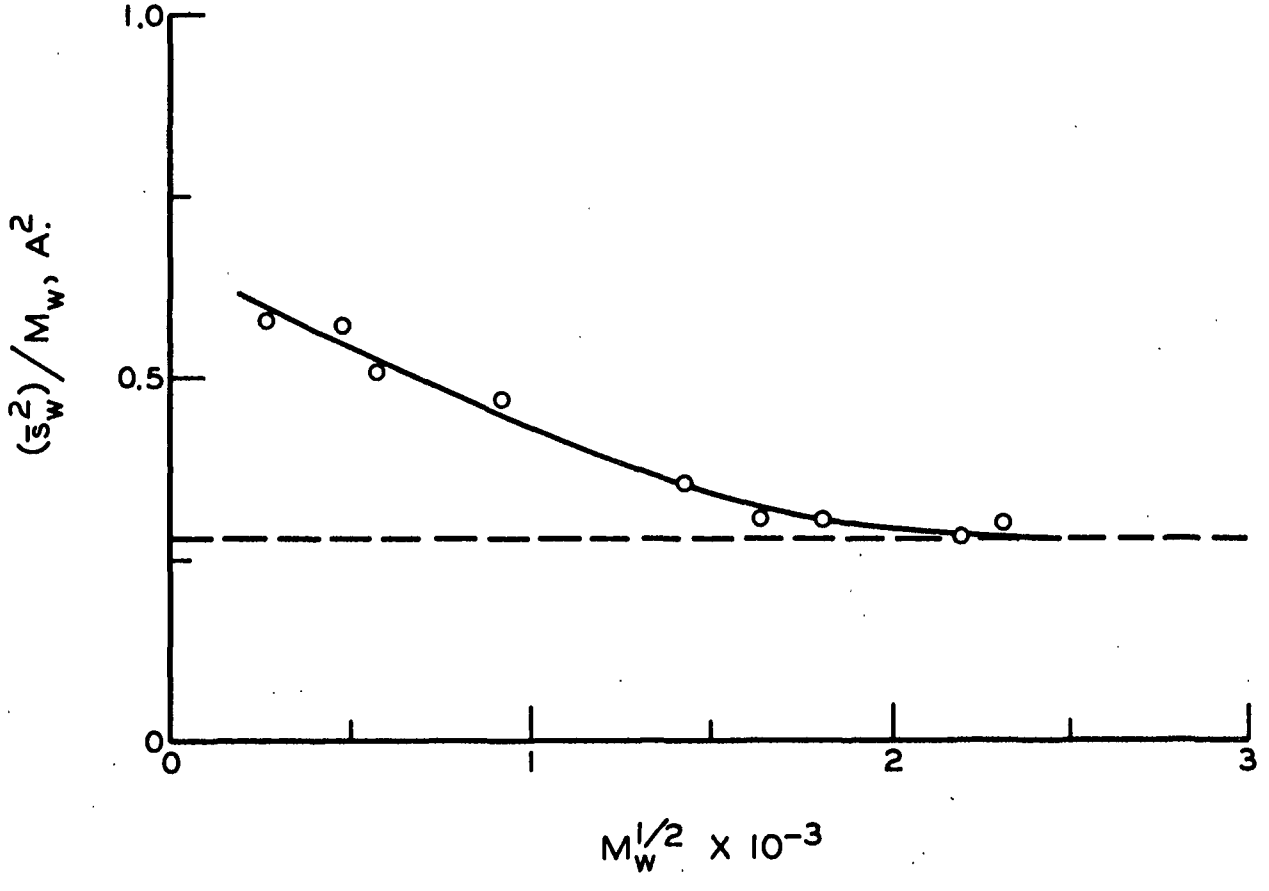

Figure 52. $(\underline{\bar{s}^2_w})/\underline{M}_w$ Against $\underline{M}_w^{1/2}$ for Guaran Triacetate in Acetonitrile

$(\overline{s_z^2})$ obtained from light scattering are greater than the errors involved in determining the intrinsic viscosity. Burchard (111) also found that values of b_e for polymethylmethacrylate and for polystyrene were higher when evaluated from light-scattering data and compared to values obtained from the intrinsic viscosity.

MOLECULAR DIMENSIONS FROM HYDRODYNAMIC THEORIES

The previously discussed hydrodynamic theories require the polymer molecules to be homogeneous with respect to composition and molecular weight. In addition, the molecules must have a particular configuration which usually is required to be a random coil. Guaran triacetate has a constant chemical composition; but in spite of the fact that the polymer was carefully fractionated from a dilute solution, there is considerable molecular heterogeneity. The $1/P(\theta)$ versus $\sin(\theta/2)$ curves indicated that the molecules did not have the configuration of a random coil. However, it is of interest to calculate the RMS end-to-end separation, $(\overline{r^2})^{1/2}$, from these theories to ascertain whether or not any of the models will approximate the configuration of guaran triacetate. In addition, it should be possible to draw certain conclusions about the configuration and hydrodynamic properties of these polymer molecules from deviations from theory.

Table XV contains values for $(\overline{r^2})^{1/2}$ as calculated from the hydrodynamic theories for random coils. The value of this configurational parameter obtained by multiplying the radius of gyration obtained from light scattering by $(6)^{1/2}$, i.e., assuming the polymer chain to be a random coil, is also listed for purposes of comparison. In this table, two values of $(\overline{r^2})^{1/2}$ are listed for Fraction 5. These values are different for the Debye-Bueche theory and for the Kirkwood-Riseman theory. The $[\eta]$ and M_w for Fraction 5 fit both expressions for the $[\eta]$-M_w relationships. Thus, it is possible to use two different values of $\Phi(\sigma)$ and $XF_o(X)$ when evaluating $(\overline{r^2})^{1/2}$ for this fraction. The first listed value is obtained using

TABLE XV

ROOT-MEAN-SQUARE END-TO-END SEPARATION VALUES IN A. FOR GUARAN TRIACETATE IN ACETONITRILE

Fraction	$\underline{M}_w \times 10^{-6}$	Light Scattering $(\underline{r}_z^2)^{1/2} = \sqrt{6}(\underline{s}_z^2)^{1/2}$	Peterlin $(\underline{r}^2)^{1/2}$	Kirkwood-Riseman $(\underline{r}^2)^{1/2}$	b, A.	Debye-Bueche $(\underline{r}^2)^{1/2}$	Flory, $\Phi = 2.1 \times 10^{21}$ $(\underline{r}^2)^{1/2}$
2A	5.34	3200	2720	2630	23.6	1810	2880
2B	4.48	3070	2680	2510	23.7	1730	2760
3	3.30	2830	2120	2030	23.2	1391	2230
4	2.68	2570	1920	1860	23.6	1283	2050
2C	2.06	2390	1680	1600	23.2	1103	1770
5[a]	0.85	1670	1080	1060	23.8	725	1160
5[a]	0.85	1670	1080	1750	39.4	1230	1160
6	0.329	1150	670	990	35.8	695	660
7	0.228	1080	560	760	32.8	534	500
8	0.074	620	320	380	28.8	264	250

[a]See text for reason Fraction 5 was repeated in this table.

the $[\eta]$-$\underline{M}_{\underline{w}}$ relation exponent equal to 0.52, and the second value is for this exponent equal to 0.87.

To determine the value of $(\overline{\underline{r}^2})^{1/2}$, Equation (12) was used for the Debye-Bueche theory, Equation (40) for the Peterlin theory, and Equation (42) with Φ equal to 2.1×10^{21} for the Flory-Fox theory. For the Kirkwood-Riseman theory, Equation (24) with the revised $\underline{XF}_o(\underline{X})$ values of Kurata and Yamakawa (29) was used to evaluate $\underline{b}_{\underline{e}}$, and $(\overline{\underline{r}^2})^{1/2}$ was evaluated from

$$(\overline{r^2})^{1/2} = b_e N^{1/2}. \qquad (134)$$

Figure 53 is a plot of $\underline{M}_{\underline{w}}/[\eta]$ against $\underline{M}_{\underline{w}}^{1/2}$ which was used to evaluate tan γ for use in Peterlin's theory (36).

None of the theoretical values listed in Table XV have been corrected for molecular heterogeneity. Since the weight average value of molecular weight was used along with the intrinsic viscosity, the values of $(\overline{\underline{r}^2})^{1/2}$ are probably nearer to their weight average value than to the $\underline{z}$-average value obtained from light scattering. Thus, it should be kept in mind that the values of $(\overline{\underline{r}^2})^{1/2}$ would be higher if $\underline{z}$-average values of molecular weight were used or if corrections were made for heterogeneity in some other fashion.

In general, none of the hydrodynamic theories predict a value of $(\overline{\underline{r}^2})^{1/2}$ that is large enough throughout the molecular weight range investigated. These results are similar to those found by Cowie (85) for amylose in dimethyl sulfoxide. It should be noted that for the two highest molecular weights the Kirkwood-Riseman, Peterlin, and Flory-Fox theories yield values that are near those obtained by light scattering. In addition, if a correction were made for heterogeneity, the values would be increased and probably would be quite near the light-scattering values. The values of $(\overline{\underline{r}^2})^{1/2}$ from the Debye-Bueche theory differ from the

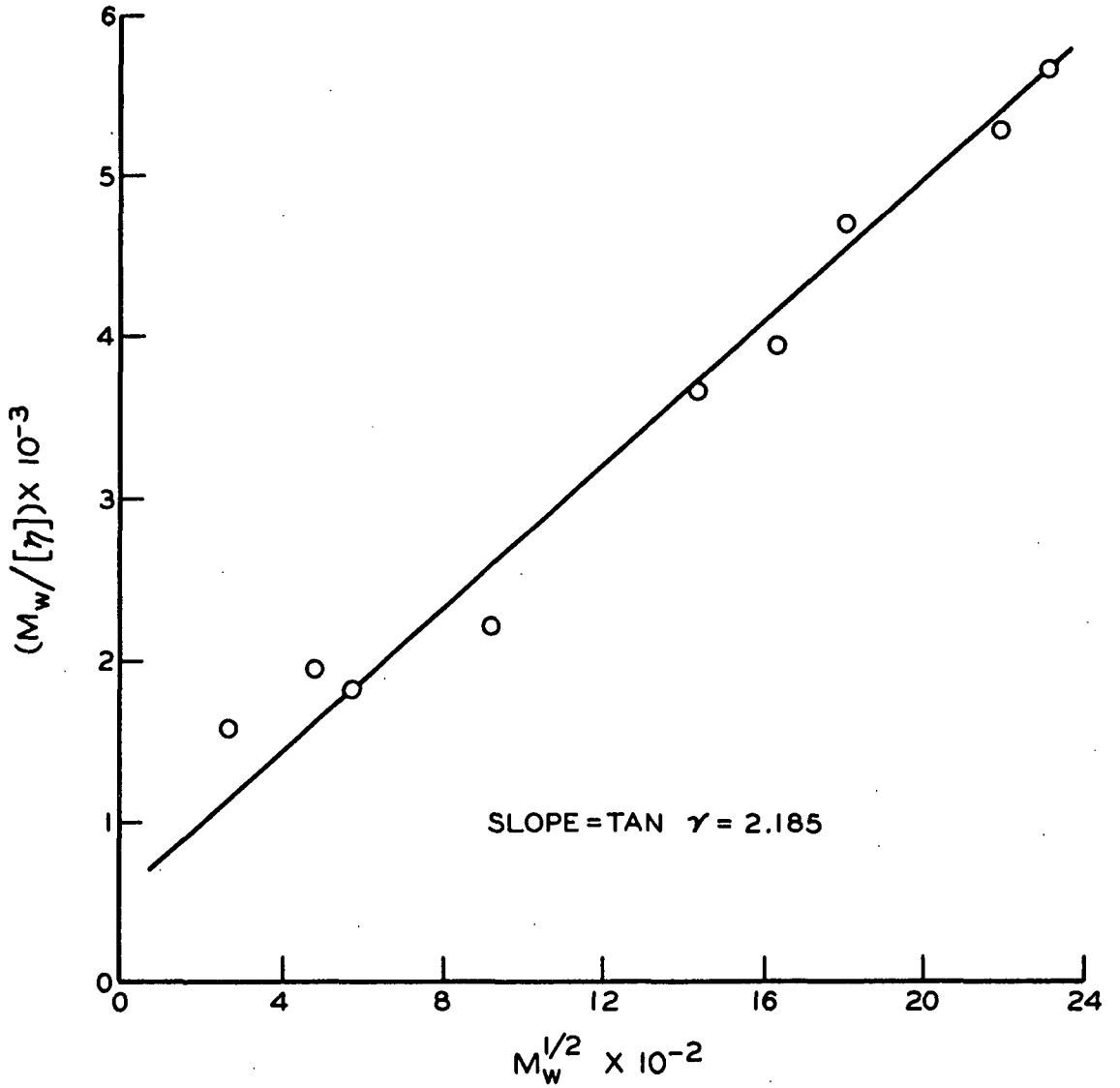

Figure 53. $\underline{M}_w/[\eta]$ as a Function of $\underline{M}_w^{1/2}$, $[\eta]$ Expressed as ml./g. Slope of this Curve is tan γ where γ is the Term Described in Peterlin's Theory (36)

experimental values by about 100% throughout the entire molecular weight range. Differences such as this cannot be accounted for by polydispersity. The same is true for Fractions 3 through 8, although the errors are not of this magnitude except at the lowest molecular weights.

Thus, it would seem that the hydrodynamic theories do not hold for guaran triacetate except at the highest molecular weights. The discrepancy between the experimental and theoretical results would be increased if the results of the $1/\underline{P}(\theta)$ against $\sin(\theta/2)$ plots are considered. These plots indicate that guaran triacetate molecules approximate a coil model at high molecular weights and a rigid rodlike model at the low molecular weights. Thus, except for the highest molecular weights, the multiplier of $(6)^{1/2}$ used to convert $(\overline{\underline{s}}^2)^{1/2}$ to $(\overline{\underline{r}}^2)^{1/2}$ is too small and the experimental light-scattering values of $(\overline{\underline{r}}^2)^{1/2}$ are actually larger than indicated in Table XV.

FLORY CONSTANT

The Flory Constant, Φ, see Equation (42), has been found to be a variable (32) that has a theoretical value of 2.86×10^{21}. Polymolecularity can cause a variation in the measured value of Φ; however, it is possible to correct for polymolecularity through an expression such as that given by Equation (46), if one has a knowledge of the molecular weight distribution. In addition, Φ will be a decreasing function of temperature in the vicinity of the Flory theta temperature, and Φ will depend on solvent nature in that it will decrease with increasing expansion of the polymer coil or with increasing solvent power (112). Kurata and Yamakawa (29) predict that, in general, two types of phenomena can cause the deviation of Φ from constancy. One of these is related to the excluded volume effect. The other one is related to the draining effect and is often found for relatively short

chain molecules or rigid molecules such as the cellulose derivatives. Another general reason that can be given for the variation in Φ can be related to the shift in the population of bonds among the various rotational states with molecular weight that has been previously discussed.

Values of Φ'/q_o were calculated from Equation (45) by utilizing light-scattering and viscosity data. To correct for polymolecularity, q_o was evaluated from the molecular distribution data through Equations (46) and (47). The theoretical value of Φ' is equal to $4.20 \times 10^{22} = (6)^{3/2}(2.86 \times 10^{21}) = (6)^{3/2}\Phi$. The values of Φ' and related parameters are summarized in Table XVI.

The importance of correcting for polymolecularity can be seen by examining the values of q_o shown in Table XVI. The calculated values of Φ are actually about 75% low for this reason. When the q_o factor is applied, the highest molecular weight fractions have a value for Φ' or Φ that is almost at the theoretical limit. It is in this region that the guaran triacetate molecules most closely fit a random coil model. As the molecular weight decreases, Φ' rapidly decreases as shown in Fig. 54. Since excluded volume effects were shown to be negligible, the shift in bond population and variation in drainage characteristics are the principal factors causing the variation in Φ.

It is possible to rewrite Equation (45) as

$$(\Phi'/q_o) = [M_w/(\bar{s}^2_z)] \quad [\eta]/(\bar{s}^2_z)^{1/2} \quad . \qquad (135)$$

Values for $\underline{M}_w/(\underline{\bar{s}^2_z})$ and $[\eta]/(\underline{\bar{s}^2_z})^{1/2}$ are given in Table XVI. Both of these factors decrease with decreasing molecular weight, and the decrease in Φ' is due in a complicated fashion to changes in bond population and in drainage characteristics.

TABLE XVI

VALUES OF FLORY'S CONSTANT AND RELATED PARAMETERS UTILIZING CORRECTION FACTORS FOR A ZIMM-SCHULZ DISTRIBUTION

Fraction	$\underline{M}_w \times 10^{-6}$	g_o	$\Phi'/g_o \times 10^{-22}$ Equation (45)	$\Phi' \times 10^{-22}$	$\Phi \times 10^{-21}$	$[\eta]/(\overline{s^2}_z)^{1/2} \times 10^{+3}$	$\underline{M}_w/(\overline{s^2}_z)$
2A	5.34	1.77	2.28	4.04	2.75	7.25	3.14
2B	4.84	1.77	2.25	3.98	2.71	7.28	3.08
3	3.30	1.69	1.51	2.55	1.73	6.09	2.47
4	2.68	1.69	1.57	2.65	1.80	6.46	2.44
2C	2.06	1.77	1.24	2.20	1.49	5.74	2.17
5	0.85	1.69	1.05	1.77	1.20	5.69	1.84
6	0.33	1.69	0.57	0.96	0.65	3.81	1.50
7	0.23	1.69	0.31	0.53	0.36	2.64	1.19
8	0.074	1.69	0.20	0.34	0.23	1.74	1.16

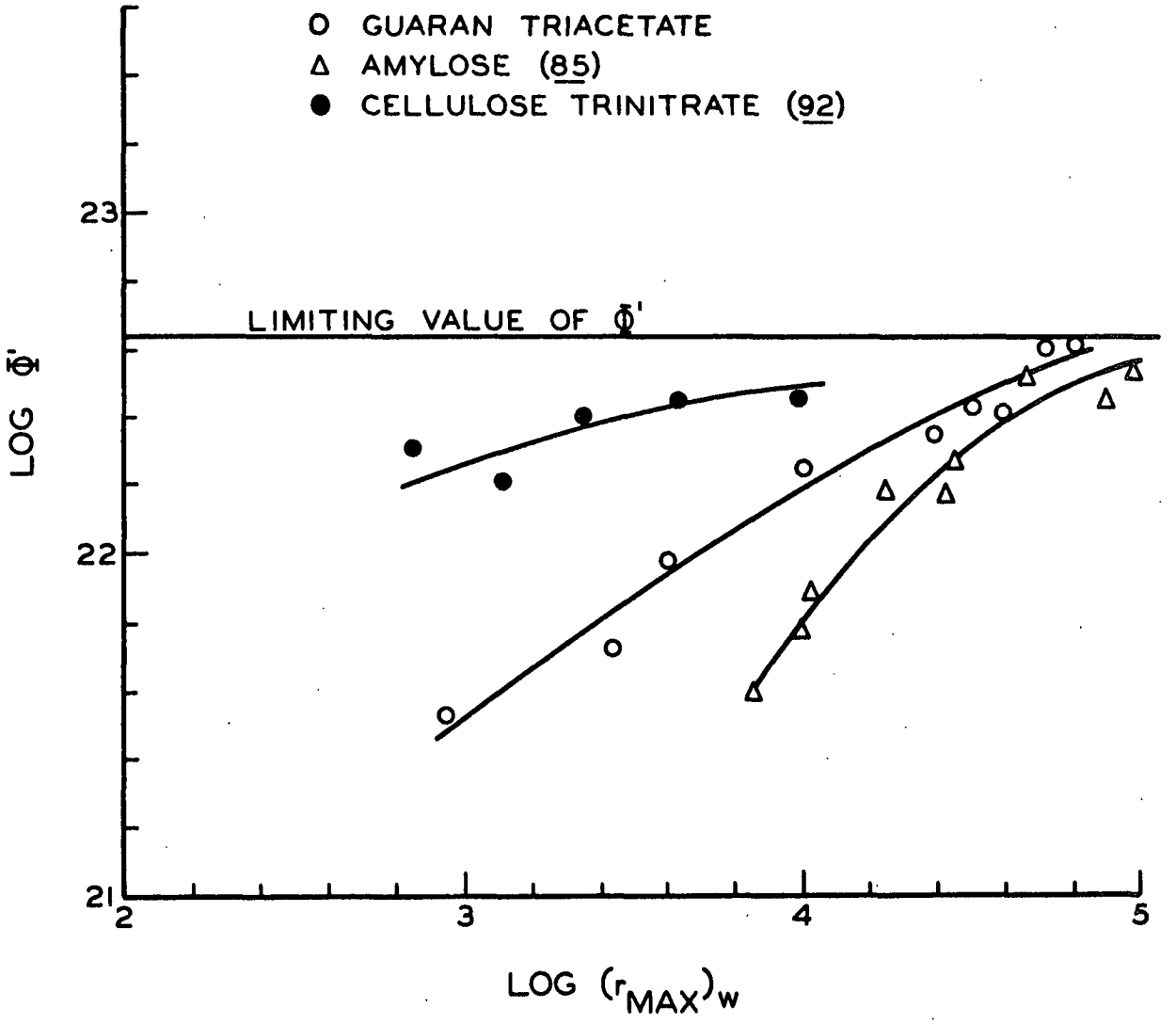

Figure 54. The Logarithmic Dependence of Φ' on the Fully Extended Chain Length

The factor $\underline{M}_w/(\overline{\underline{s}^2}_z)$ is essentially the reciprocal of the term discussed in the Porod-Kratky theory (104), and its decrease with molecular weight can be attributed to the shift in bond population (107). The molecule becomes effectively stiffer, and thus relatively more extended, as the molecular weight decreases due to a particular rotational conformation being favored which results in a decrease in Φ'.

The decrease in $[\eta]/(\overline{\underline{s}^2}_z)^{1/2}$ is similar to that found for amylose triacetate (105) and for cellulose trinitrate (96). For these latter polymers, the decrease in this factor was attributed to an increase in the free draining characteristics of the molecules with decreasing molecular weight. However, it should be noted that in the present case the variation in bond population also will affect this term by causing $(\overline{\underline{s}^2}_z)^{1/2}$ to be larger than that of a comparable random coil as the molecular weight decreases.

In addition, the intrinsic viscosity of guaran triacetate exhibits a transition from an essentially nondraining molecule to a partially free draining molecule as the molecular weight decreases. This causes a relative decrease in the intrinsic viscosity which serves to accentuate the decrease in the $[\eta]/(\overline{\underline{s}^2}_z)^{1/2}$ term.

Above molecular weights of about 1×10^6 the intrinsic viscosity is proportional to $\underline{M}_w^{0.52}$. According to the Kirkwood-Riseman (28) and Kurata-Yamakawa (29) theories, the draining parameter, $\underline{X}$, is very large for these molecules and is approaching indefinitely large values at the highest molecular weight. This is characteristic of a nondraining molecule. Below molecular weights of about 1×10^6 there is a break in the log $[\eta]$-log $\underline{M}_w$ curve (see Fig. 46 and 47), and the intrinsic viscosity is proportional to $\underline{M}_w^{0.87}$. For this relationship $\underline{X}$ is approximately 0.5

which is indicative of a partially free draining molecule. As stated previously, this transition in draining character also contributes to a rapid decrease in Φ as the molecular weight decreases.

A similar decrease in Φ' with molecular weight has been shown for cellulose nitrate (92, 96), for ethyl cellulose (113), for ethyl hydroxyethyl cellulose (114), for amylose triacetate (105), and for amylose (85) although Φ does not approach its theoretical value as closely in these cases. The complicated dependence of Φ' on chain length is shown in Fig. 54 when values are compared for several polymers. Newman and Flory (115) note that Equations (43) and (45) can be expected to hold, with Φ as a constant, for cellulose derivatives only at molecular weights that lie a decade higher than those of more flexible polymers and that Φ does vary strongly with molecular weight for these polymers.

ACKNOWLEDGMENTS

I gratefully acknowledge the guidance and encouragement of my thesis advisory committee, Dr. S. F. Kurath, Dr. W. P. Riemen, and Mr. H. A. Swenson, and of Dr. L. E. Wise who took an active interest in the progress of this thesis. In particular, it should be noted that the initial idea for this study was suggested by Dr. Kurath, whose patience and understanding materially contributed to comprehending the system studied.

It would be difficult to mention each staff or faculty member who aided in the completion of this work; however, I would like to express thanks in particular to Miss O. Smith for the electron microscopy studies, to Mr. J. A. Carlson for operation of the ultracentrifuge, to Dr. D. G. Williams for his help with the x-ray studies, and to Mr. L. O. Sell for the infrared studies.

I gratefully acknowledge the financial assistance, in the form of a four-year scholarship, from The Institute of Paper Chemistry and the generosity of the numerous organizations and individuals who contributed to the Scholarship Fund.

And last but certainly not least, my continuing gratitude to my wife, Mary Anne, for help in correcting, typing, and proofreading this thesis.

GLOSSARY OF SYMBOLS

a	dimension in a unit cell
	dimension of a monomeric unit
	exponent of the intrinsic viscosity-molecular weight relationship
	working standard constant in light scattering
A_o	area under a schlieren peak at a given time
A_2	second virial coefficient from light scattering
A'_2	second virial coefficient from osmotic pressure
b	dimension in a unit cell
	dimension of a monomeric unit
$\vec{b}$	bond vector
b_e	effective bond length
b_o	length of a bond vector
c	dimension in a unit cell
	concentration in weight per volume
C_o	concentration in optical units in a sector cell
C_s	actual concentration in a sector cell at a particular distance from the center of rotation in weight per volume
C_u	Cabannes factor
d	diameter of a sphere
dc/dx	concentration gradient
dn/dc	specific refractive index gradient
D	diffusion coefficient
E	energy of vaporization
$\vec{f}_i$	force on a particular bead, i
$f(M)$	distribution function pertaining to molecular weights

$\underline{F}$	filter factor
	free energy
$\underline{F}_o(\underline{X})$	a hydrodynamic function of the draining parameter
$\underline{\vec{F}}$	total force on a molecule
$\underline{g}$	gravitational constant
$\underline{g}^*(\underline{S})$	apparent distribution function pertaining to sedimentation coefficients
$\underline{g}(\underline{S})$	distribution function pertaining to sedimentation coefficients corrected for diffusion effects
$\underline{g}(\underline{S}^o)$	distribution function pertaining to sedimentation coefficients corrected for diffusion and concentration effects
$\underline{G}_\theta, \underline{G}_o$	galvanometer reading at angle θ and at angle 0°.
$\underline{h}$	diaphragm width on light-scattering apparatus
	mean hydrostatic head in viscometry
$\underline{H}$	constant in light-scattering equations
	heat of mixing
$\underline{k}$	Boltzman constant
	constant that relates optical concentration units to actual concentration units in sedimentation calculations
	constant used to suitably spread concentration data on Zimm plot
$\underline{k}_s$, $\underline{k}'_s$	constants in the expression for the concentration dependence of the sedimentation coefficient
$\underline{k}'$	proportionality constant in the sedimentation coefficient-molecular weight relationship
$\underline{K}_2$	proportionality constant in the mean-square radius of gyration-molecular weight relationship
$\underline{K}'$	proportionality constant in the intrinsic viscosity-molecular weight relationship
$\underline{K}''$	proportionality constant in the frictional coefficient-degree of polymerization relationship
$\underline{L}$	shielding length in the Debye-Bueche theory

$\underline{L}$	length of a rigid rod molecule
	optical path length in specific refractive index gradient measurements
	length of the capillary tube in a viscometer
$\underline{m}$	mass of a polymer molecule
$\underline{m}_e$	end correction in viscometry
$\underline{m}'$	mass of a single chain element in a polymer molecule
$\underline{M}$	molecular weight, subscript of $\underline{n}$, $\underline{w}$, or $\underline{z}$ indicates the number, weight, or $\underline{z}$-average molecular weight, respectively
$\underline{M}_o$	molecular weight of a monomeric unit
$\underline{n}_o$, $\underline{n}$	refractive index of solvent and of solution
$\underline{N}$	number of polymer chain elements (beads, monomeric units), subscript of $\underline{n}$, $\underline{w}$, or $\underline{z}$ indicates the number, weight, or $\underline{z}$-average of the quantity
$\underline{N}_A$	Avogadro's number
$\underline{p}$	slope of reduced viscosity as a function of concentration plot
$\underline{p}(\underline{X})$	a hydrodynamic function of the draining parameter
$\underline{P}(\theta)$	particle scattering factor
$\underline{q}$	persistence length
	slope of the natural logarithm of the relative viscosity divided by concentration as a function of concentration plot
$\underline{q}_o$	a correction term for polymolecularity
$\underline{q}_v$	a term related to the excluded volume
$\underline{q}(\underline{X})$	a hydrodynamic function of the draining parameter
$\underline{r}/\underline{r}'$	calibration factor for the narrow slit system of the light-scattering apparatus and the circular cell
$(\underline{\bar{r}}^2)$	mean-square end-to-end distance. The subscript $\underline{n}$, $\underline{w}$, or $\underline{z}$ appearing inside the brackets refers to the number, weight, or $\underline{z}$-average quantity, respectively
$(\underline{\bar{r}}^2)^{1/2}$	root-mean-square end-to-end distance
$(\underline{\bar{r}}^2)_o^{1/2}$	unperturbed root-mean-square end-to-end distance

$\underline{r}_{\underline{b}}$ radius of a bead in the pearl string model

diameter of the spherical Kurata-Yamakawa element

$\underline{r}_{max}$ length of the fully extended polymer chain. If enclosed in brackets and then subscripted with n, w, or z the number, weight, or z-average of the quantity is indicated, respectively

$\underline{R}$ radius of capillary tube in a viscometer

gas constant

$\underline{R}_{\underline{h}}$ hydrodynamic radius in Peterlin's theory

$\underline{R}_{\underline{s}}$ radius of equivalent sphere in Debye-Bueche theory

$\underline{R}_{\underline{w}}/\underline{R}_{\underline{c}}$ correction factor for incomplete compensation of refraction effects

$\underline{R}_{90}$ Rayleigh ratio at 90° scattering angle

$\underline{\vec{s}}$ a point whose location is measured from the center of mass of a molecule

$(\underline{\bar{s}^2})$ mean-square radius of gyration. The subscript n, w, or z appearing inside the brackets refers to the number, weight, or z-average quantity, respectively

$(\underline{\bar{s}^2})^{1/2}$ root-mean-square radius of gyration

$(\underline{\bar{s}^2})_o^{1/2}$ unperturbed root-mean-square radius of gyration

$\underline{S}$ sedimentation coefficient

entropy

$\underline{S}^o$ sedimentation coefficient extrapolated to zero concentration

$\underline{\bar{S}}^o$ mean sedimentation coefficient extrapolated to zero concentration

$\underline{t}$ elapsed time in a centrifuge run

efflux time for a solution

$\underline{t}_{\underline{e}}$ equivalent time at desired operating speed of centrifuge during acceleration

$\underline{t}_o$ efflux time for a solvent

$\underline{T}$ absolute temperature

$\underline{\underline{TD}}$ experimentally determined product of the diffuse transmittance of an opal glass reference standard and a diffuser correction factor

$\underline{u}$	excluded volume
$\underline{u}_o$	an energy parameter in the Kurata-Yamakawa theory
$\underline{\vec{U}}$	velocity of a monomeric unit in a moving fluid
$\underline{\bar{v}}$	partial specific volume
$\underline{V}$	volume of a viscometer bulb
$\underline{\vec{V}}$	relative velocity of a polymer molecule with respect to the liquid
$\underline{\vec{V}'}$	perturbation in flow caused by presence of the polymer molecule
$\underline{\vec{V}}_j$	fluid velocity at point of location of monomer unit $\underline{j}$
$\underline{V}_m$	total volume of a mixture
$\underline{\vec{V}}_r$	relative velocity of the liquid with respect to some particular bead
$\underline{V}_1$, $\underline{V}_2$	volume of Component 1 and Component 2 of a mixture
$\underline{x}$	number of Porod units in the polymer chain
	distance from center of rotation in the ultracentrifuge to a particular point on the schlieren curve's distance axis
$\underline{x}_o$	original boundary location between solvent and solution from the center of rotation of the ultracentrifuge
$\underline{X}$	draining parameter
$\underline{X}\underline{F}_o(\underline{X})$, $\underline{X}\underline{G}_o(\underline{X})$	hydrodynamic functions of the draining parameter
$\underline{Y}$	a molecular weight distribution width parameter
$\underline{z}$	a parameter in the Kurata-Yamakawa theory related to the excluded volume
$\underline{Z}$	dissymmetry
$[\underline{Z}]$	intrinsic dissymmetry
α	molecular expansion factor
	a designation of mode of linkage between anhydrosugar units
β	a designation of mode of linkage between anhydrosugar units
$\Gamma(\ )$	a gamma function
γ	argument of the tangent in Peterlin's theory

δ	solubility parameter
$\dot{\epsilon}$	rate of shear stress
ϵ	a parameter in the exponent of the mean-square radius of gyration-molecular weight relationship
ζ	frictional coefficient of a bead in the pearl necklace model
η_o	viscosity of the solvent
$[\eta]$	intrinsic viscosity
$[\eta]_\theta$	intrinsic viscosity at the Flory temperature
η_{rel}	relative viscosity
η_{sp}	specific viscosity
η'_{sp}	specific viscosity uncorrected for kinetic energy effects
$\eta_{sp}/\underline{c}$	reduced viscosity
θ	Flory temperature
	scattering angle
	supplement of the fixed bond angle
λ	wavelength of light
λ'	wavelength of light in a given medium
ν	bead density of pearl string model
Ξ	frictional coefficient for entire polymer molecule
π	3.1416 or osmotic pressure when so indicated
ρ	density
ρ_o	solvent density
$\rho_{\underline{u}}$	depolarization ratio at zero concentration
$(\rho_{\underline{u}})_{\underline{c}}$	depolarization ratio at a given concentration
σ	shielding ratio
τ	absolute turbidity
$\tau_{\underline{R}}$	shear stress

τ_{90} absolute turbidity at 90° scattering angle

ϕ angle between successive bond planes

schlieren blade angle

$\phi(\sigma)$ a hydrodynamic parameter in the Debye-Bueche theory

ϕ_1, ϕ_2 volume fraction of Component 1 and Component 2 in a mixture

Φ Flory constant based on end-to-end distance

Φ' Flory constant based on radius of gyration

$\psi(\sigma)$ a hydrodynamic parameter in the Debye-Bueche theory

ω angular velocity in radians per second

ω_f operating speed of centrifuge in radians per second

Ω_s volume of equivalent sphere, Debye-Bueche theory

η^*_{sp}/c apparent reduced viscosity at a particular shear stress

LITERATURE CITED

1. Greenwood, C. T. The size and shape of some polysaccharide molecules. In Advances in carbohydrate chemistry. p. 289-332. New York, Academic Press, 1952.

2. Aspinall, G. O. Structural chemistry of the hemicelluloses. In Advances in carbohydrate chemistry. p. 429-68. New York, Academic Press, 1959.

3. Heyne, E., and Whistler, R. L., J. Am. Chem. Soc. 70:2249-52(1948).

4. Moe, O. A., Miller, S. E., and Iwen, M. H., J. Am. Chem. Soc. 69:2621-5(1947).

5. Whistler, R. L., Li, T. K., and Dvonch, W., J. Am. Chem. Soc. 70:3144-5(1948).

6. Swanson, J. W., J. Am. Chem. Soc. 71:1510(1949).

7. Ahmed, Z. F., and Whistler, R. L., J. Am. Chem. Soc. 72:2524-5(1950).

8. Palmer, K. J., and Ballantyne, M., J. Am. Chem. Soc. 72:736-41(1950).

9. Smart, C. L., and Whistler, R. L., J. Polymer Sci. 4:87-90(1949).

10. Whistler, R. L., and Durso, D. F., J. Am. Chem. Soc. 73:4189-90(1951).

11. Whistler, R. L., and Durso, D. F., J. Am. Chem. Soc. 74:5140-1(1952).

12. Whistler, R. L., and Smith, C. G., J. Am. Chem. Soc. 74:3795-6(1952).

13. Ott, E., and Spurlin, H. M. Cellulose and cellulose derivatives. 2d ed. New York, Interscience Publishers, Inc., 1955. 1601 p.

14. Zimm, B. H., and Stockmayer, W. H., J. Chem. Phys. 17:1301-14(1949).

15. Boggs, A. D. The molecular weight-viscosity relation of amylose, amylopectin, and guaran. Master's Thesis. Lafayette, Indiana, Purdue University, 1949.

16. Reeves, R. E., J. Am. Chem. Soc. 71:215-17(1949).

17. Greenwood, C. T., and Rossotti, H., J. Polymer Sci. 27:481-8(1958).

18. Reeves, R. E., J. Am. Chem. Soc. 72:1499-1506(1950).

19. Bently, Ronald, J. Am. Chem. Soc. 81:1952-6(1959).

20. Palmer, K. J., and Hartzog, M. B., J. Am. Chem. Soc. 67:1865-6(1945).

21. Benoit, H., J. Polymer Sci. 3:376-88(1948).

22. Eliezner, S., and Hayman, H. J. G., J. Polymer Sci. 23:387-402(1957).

23. Burchard, W., Makromol. Chem. 42:151-64(1960).

24. Flory, P. J. Principles of polymer chemistry. Ithaca, New York, Cornell University, 1953. 672 p.

25. Debye, P., J. Chem. Phys. 14:636-9(1946).

26. Debye, P., and Bueche, A. M., J. Chem. Phys. 16:573-9(1948).

27. Einstein, A., Ann. Phys. 34:591-2(1911); Furth, R., and Cowper, A. D. Investigations on the theory of the Brownian movement by Albert Einstein, Dover Publications, Inc., 1956. 119 p.

28. Kirkwood, J. G., and Riseman, J., J. Chem. Phys. 16:565-73(1948).

29. Kurata, M., and Yamakawa, H., J. Chem. Phys. 29:311-25(1958).

30. Kirkwood, J. G., and Riseman, J., J. Chem. Phys. 22:1626-7(1954).

31. Kirkwood, J. G., Zwanzig, R. W., and Plock, R. J., J. Chem. Phys. 23:213-14 (1955).

32. Ptitsyn, O. B., and Eizner, Y. E., Soviet Phys.: Tech. Phys. 4:1020-36(1959).

33. Auer, Peter L., and Gardner, C. S., J. Chem. Phys. 23:1545-6(1955).

34. Auer, P. L., and Gardner, C. S., J. Chem. Phys. 23:1546-7(1955).

35. Kurata, M., Yamakawa, H., and Teramoto, E., J. Chem. Phys. 28:785-91(1958).

36. Peterlin, A., J. Polymer Sci. 5:473-82(1950).

37. Flory, P. J., and Fox, T. G., Jr., J. Am. Chem. Soc. 73:1904-8(1951).

38. Newman, S., Krigbaum, W. R., Laugier, C., and Flory, P. J., J. Polymer Sci. 14:451-62(1954).

39. Zimm, B. H., J. Chem. Phys. 16:1093-9(1948).

40. Beattie, W. H., and Booth, C., J. Polymer Sci. 44:81-91(1960).

41. Krigbaum, W. R., J. Polymer Sci. 18:315-20(1955).

42. Orofino, T. A., and Flory, P. J., J. Chem. Phys. 26:1067-76(1957).

43. Stockmayer, W. H., Makromol. Chem. 35:54-74(1960).

44. Haug, A. J., Tappi 36:47-53(1953).

45. Saeman, J. F., Moore, W. E., Mitchell, R. L., and Millett, M. A., Tappi 37:336-43(1954).

46. White, L. M., and Secor, G. E., Arch. Biochem. Biophys. 43:60-6(1953).

47. Pridham, J. B., Anal. Chem. 28:1967-8(1956).

48. Carson, J. F., and Maclay, W. D., J. Am. Chem. Soc. 70:293-5(1948).

49. McKee, S. C. An investigation of the hydrolysis of a reduced 4-O-methylglucuronoxylan. Doctor's Dissertation. Appleton, Wis., The Institute of Paper Chemistry, 1961. 53 p.

50. Genung, L. B., and Mallatt, R. C., Ind. Eng. Chem., Anal. Chem. 13, no. 5:369-74(1941).

51. Karnik, M. G., Morak, A. J., and Ward, Kyle, Jr., Tappi 46, no. 2:130-4(1963).

52. Yundt, A. P., Tappi 34:89-91(1951).

53. Marchessault, R. H., J. Polymer Sci. 51:S66-8(1961).

54. Manley, R. St. J., J. Polymer Sci. 47:509-12(1960).

55. Hildebrand, J., and Scott, R. The solubility of nonelectrolytes. 3d ed. New York, Reinhold Publishing Corp., 1949. 488 p.

56. Small, P. A., J. Appl. Chem. (London) 3:71-80(1953).

57. Burrell, H., Interchem. Rev. 14, no. 1:3-16(1955).

58. Burrell, H., Interchem. Rev. 14, no. 2:31-46(1955).

59. Debye, P., and Cashin, W. M., J. Chem. Phys. 19:510(1951).

60. Vermillion, F. J. Anodic reactions of simple phenolic compounds. Doctor's Dissertation. Appleton, Wis., The Institute of Paper Chemistry, 1963. 127 p.

61. Scott, R. L., Ind. Eng. Chem. 45:2532-7(1953).

62. McCormick, H. W., J. Polymer Sci. 34:341-9(1959).

63. Taylor, D. L. An evaluation of column thermal diffusion as a means of polymer characterization. Doctor's Dissertation. Appleton, Wis., The Institute of Paper Chemistry, 1962. 123 p.

64. Baldwin, R. L., J. Phys. Chem. 63:1570-3(1959).

65. Yamakawa, H., J. Chem. Phys. 36:2995-3001(1962).

66. Debye, P., J. Phys. Colloid Chem. 51:18-32(1947).

67. Zimm, B. H., J. Chem. Phys. 16:1099-1116(1948).

68. Doty, P., and Steiner, R. F., J. Chem. Phys. 18:1211-20(1950).

69. Benoit, H., and Doty, P., J. Phys. Chem. 57:958-63(1953).

70. Peterlin, A., J. Polymer Sci. 47:403-15(1960).

71. Stacey, K. A. Light scattering in physical chemistry. New York, Academic Press, Inc., 1956. 230 p.

72. Debye, P., J. Appl. Phys. 15:338-42(1944).

73. Beattie, W. H., and Booth, C., J. Phys. Chem. 64:696-7(1960).

74. Phoenix Precision Instrument Co. The new Brice Phoenix light-scattering photometer. Operation manual OM-1000. Philadelphia, Pa., The Co., 1955. 52 p.

75. Maron, S. H., and Lou, R. L. H., J. Polymer Sci. 14:29-36(1954).

76. Kratohvil, J. P., Dezelic, G., Kerker, M., and Matijevic, E., J. Polymer Sci. 57:59-78(1962).

77. International Critical Tables. Vol. III. p. 28. New York, McGraw-Hill Book Co., 1928.

78. International Critical Tables. Vol. VII. p. 34. New York, McGraw-Hill Book Co., 1930.

79. Swenson, H. A., Morak, A. J., and Kurath, Sheldon, J. Polymer Sci. 51:231-45 (1961).

80. Tanford, C. Physical chemistry of macromolecules. New York, John Wiley and Sons, Inc., 1961. 710 p.

81. Cabannes, J., and Rocard, Y. La diffusion moleculaire de la lumiere. Les Presses Universitaires de Paris, 1929.

82. Everett, W. W., and Foster, J. F., J. Am. Chem. Soc. 81:3464-9(1959).

83. Gueidushek, E. P., and Doty, P., Biochem. et Biophys. Acta 9:609(1952); Stacey, K. A. Light scattering in physical chemistry. New York, Academic Press Inc., 1956. 230 p.

84. Timell, T. E., Svensk Papperstidn. 57:777-88(1954).

85. Cowie, J. M. G., Makromol. Chem. 42:230-47(1961).

86. Schurz, J., and Immergut, E. H., J. Polymer Sci. 9:279-81(1952).

87. Moore, W. J. Physical chemistry. 2d ed. New Jersey, Prentice Hall, Inc., 1955. 431 p.

88. Goldberg, P., and Fuoss, R. M., J. Phys. Chem. 58:648-53(1954).

89. Badgley, W. J., and Mark, H., J. Phys. Colloid Chem. 51:58-70(1947).

90. Holtzer, A. M., Benoit, H., and Doty, P., J. Phys. Chem. 58:624-34(1954).

91. Munster, A., J. Polymer Sci. 8:633-49(1952).

92. Hunt, M. L., Newman, S., Scheraga, H. A., and Flory, P. J., J. Phys. Chem. 60:1278-90(1956).

93. Davies, O. L. Statistical methods in research and production. 3d ed. p. 160. New York, Hafner Publishing Co., 1958.

94. Marx-Figini, M., and Schulz, G. V., Makromol. Chem. 54:102-18(1962).

95. Kurata, M., Stockmayer, W. H., and Roig, A., J. Chem. Phys. 33:151-5(1960).

96. Huque, M. M., Goring, D. A. I., and Mason, S. G., Can. J. Chem. 36:952-69(1958).

97. Sperling, L. H. Molecular conformation of cellulose tricaproate in solution. Doctor's Dissertation. Durham, N. C., Duke Univ., 1958. 96 p.

98. Brown, W., Arkiv Kemi 18:227-84(1961).

99. Henley, D., Arkiv Kemi 18:327-92(1961).

100. Burchard, W., and Husemann, E., Makromol. Chem. 44-46:358-87(1961).

101. Peterlin, A., Ann. N. Y. Acad. Sci. 89:578-607(1961).

102. Debye, P. Collected papers. p. 507. New York, Interscience Publishers, Inc., 1954.

103. Swenson, H. A., and Thompson, N., Submitted to J. Polymer Sci.

104. Kratky, O., and Porod, G., Rec. Trav. Chim. 68:1106(1949); Hunt, M. L., Newman, S., Scheraga, H. A., and Flory, P. J., J. Phys. Chem. 60:1278-90(1956).

105. Cowie, J. M. G., J. Polymer Sci. 49:455-71(1961).

106. Krigbaum, W. R., Kurz, J. E., and Smith, P., J. Phys. Chem. 65:1984-91(1961).

107. Krigbaum, W. R., and Sperling, L. H., J. Phys. Chem. 64:99-108(1960).

108. Meyerhoff, G., J. Polymer Sci. 43:269-72(1960).

109. Uda, K., and Meyerhoff, G., Makromol. Chem. 47:168-84(1961).

110. Notley, N. T., and Debye, P. J. W., J. Polymer Sci. 17:99-106(1955).

111. Burchard, W., Makromol. Chem. 50:20-36(1961).

112. Kurata, M., Yamakawa, H., and Utiyama, H., Makromol. Chem. 34:139-51(1959).

113. Scherer, P. C., Tanenbaum, A., and Levi, D. W., J. Polymer Sci. 43:531-5(1960).

114. Manley, R. St. J., Arkiv Kemi 9:519(1956); Kurata, M., and Yamakawa, H., J. Chem. Phys. 29:311-25(1958).

115. Newman, S., and Flory, P. J., J. Polymer Sci. 10:121-3(1953).

APPENDIX I

SOLUBILITY PARAMETERS (55-58)

The solubility parameter, δ, is a calculable parameter that may be obtained from readily available data such as structural formula, density, and boiling point.

The free energy equation when applied to dissolving a polymer in a solvent states that the free energy change on mixing, ΔF, is equal to the heat of mixing, ΔH, minus the product of temperature, T, and entropy change, ΔS, that is,

$$\Delta F = \Delta H - T\Delta S. \tag{136}$$

If ΔF is negative, solution will take place. It is readily seen that increasing the temperature favors solution since increasing T tends to make ΔF more negative. The entropy increase should be large and will be positive when a polymer dissolves since the disorder increases to a great extent on solution. Therefore, the magnitude of the heat term, ΔH, is the deciding factor in determining the sign of the free energy change, and it is a study of this term which gives the clue to solubility. The value of ΔH can be expressed as (57)

$$\Delta H = V_m \left[(\Delta E_1/V_1)^{0.5} - (\Delta E_2/V_2)^{0.5}\right]^2 \phi_1 \phi_2, \tag{137}$$

where ΔH is the over-all heat of mixing in calories, V_m is the total volume of the mixture in milliliters, ΔE is the energy of vaporization of Component 1 or 2 in calories, and ϕ is the volume fraction of Component 1 or 2 in the mixture.

The term $\Delta E/V$ is the energy of vaporization per milliliter, and it has been described as the "internal pressure" or the "cohesive energy density." Equation (137) may be rewritten as

$$(\Delta H/V_m \phi_1 \phi_2) = \left[(\Delta E_1/V_1)^{0.5} - (\Delta E_2/V_2)^{0.5}\right]^2 \tag{138}$$

or the heat of mixing per unit volume at a given concentration is equal to the square of the difference between the square roots of the cohesive energy density of the components. The solubility parameter, δ, by definition, is given by the square root of the cohesive energy density

$$\delta = (\Delta E/V)^{0.5}. \tag{139}$$

Thus, the heat of mixing depends on $(\delta_1 - \delta_2)^2$, and to keep ΔH small enough as to not prevent mixing, $(\delta_1 - \delta_2)^2$ must be kept small. In fact, if $(\delta_1 - \delta_2)^2 = 0$, solution will be assured by the entropy factor. That is, if the δ values of two substances are equal, the substances will be miscible. Methods for calculation of δ for solvents and polymers are given in the above-cited references.

APPENDIX II

SECONDARY STANDARD POLYSTYRENE SOLUTION

Since it is difficult to obtain Cornell Standard polystyrene, excess turbidity data were taken on B-6 polystyrene (62) so that a more available material could be used to periodically check the light-scattering instrument. It should be noted that this material is very polydisperse. Table XVII shows the values of excess turbidity along with the light-scattering function (Hc/τ).

TABLE XVII

EXCESS TURBIDITY DATA FOR B-6 POLYSTYRENE AT 436 mμ, 22.5°C., $H = 42.8 \times 10^{-7}$, $dn/dc = 0.112$, $n = 1.4978$

Concentration, g./ml. x 10^3	Excess Turbidity, τ, $cm.^{-1} \times 10^4$	Hc/τ, x 10^6
5.86	31.1	8.07
4.88	30.2	6.91
4.50	29.0	6.65
3.66	26.9	5.82
3.22	25.2	5.46
2.77	23.4	5.06

The physical properties of B-6 polystyrene calculated from the excess turbidity data are as follows:

$C_u = 0.99$,

$1/P(\theta) = 1.105$*,

Apparent $M_w = 388{,}000$,

*Determined by assuming that polystyrene in toluene at 22.5°C. is a polydisperse coil.

Corrected $\underline{M}_{\underline{w}}$ = (apparent $\underline{M}_{\underline{w}}$)($\underline{C}_{\underline{u}}$)[1/$\underline{P}(\theta)$] = 424,000,

$[\underline{Z}]$ = 1.139,

$(\overline{\underline{r}^2}_{\underline{w}})^{1/2}$ = 360 A.

The molecular weight of 424,000 for B-6 polystyrene compares reasonably well with the values obtained by McCormick (62) and by Taylor (63) who used sedimentation experiments to study this polymer. This determination is a further check on the performance of the light-scattering photometer used in this work.

TABLE XVIII

RECIPROCAL PARTICLE SCATTERING FACTORS, $1/P(\theta)$,
FOR GUARAN TRIACETATE FRACTIONS IN ACETONITRILE AT 4358 A.

		Reciprocal Particle Scattering Factors								
		Unfractionated	Fraction							
θ, °	Sin(θ/2)	Polymer	2A	2B	3	4	2C	5	6	7
45	0.383	2.27	2.38	2.24	2.00	1.89	1.75	1.38	1.08	1.24
48	0.407	--	--	2.42	--	--	1.86	--	--	--
50	0.423	--	2.78	2.56	2.29	2.18	1.96	--	--	--
52	0.438	--	--	2.72	2.44	--	2.06	--	--	--
55	0.462	--	3.08	2.91	2.66	2.39	2.18	--	--	--
58	0.485	--	--	3.10	2.71	--	2.27	--	--	--
60	0.500	3.36	3.40	3.20	2.89	2.66	2.35	1.65	1.16	1.39
62	0.515	--	--	3.34	2.96	--	2.45	--	--	--
65	0.537	--	3.80	3.52	3.17	2.85	2.56	--	--	--
68	0.559	--	--	3.73	--	--	--	--	--	--
70	0.574	--	4.16	3.86	3.39	3.09	2.76	--	--	--
75	0.609	4.35	4.48	4.18	3.64	3.31	2.94	1.93	1.27	1.47
80	0.643	--	4.82	4.48	3.90	3.58	3.12	--	--	--
85	0.676	--	5.15	4.76	4.11	3.72	3.30	--	--	--
90	0.707	5.10	5.33	5.06	4.32	3.84	3.44	2.15	1.33	1.54
95	0.737	--	5.61	5.30	4.50	4.02	3.58	--	--	--
100	0.766	--	5.84	5.52	4.66	4.15	3.66	--	--	--
105	0.793	5.68	6.11	5.70	4.83	4.36	3.78	2.34	1.38	1.57
110	0.819	--	6.31	5.93	4.96	4.45	3.89	--	--	--
115	0.843	--	6.55	6.05	5.08	4.56	3.98	--	--	--
120	0.866	6.05	6.67	6.15	5.17	4.63	4.08	2.51	1.45	1.64
125	0.887	--	6.70	6.25	5.24	4.75	4.12	--	--	--
130	0.906	--	6.75	6.25	5.25	4.82	4.13	--	--	--
135	0.924	6.36	6.52	6.15	5.17	4.89	4.13	2.62	1.50	1.69

APPENDIX IV

VARIABLE SHEAR VISCOMETER AND SOLVENT EFFLUX TIMES

The viscometer used in this work was a variable shear viscometer of a modified Ubbelohde design (Cannon 47-A1) which is described by Schurz and Immergut (86) and is shown in Fig. 55. Table XIX lists the pertinent measurements on this viscometer.

TABLE XIX

MEASUREMENTS OF THE VARIABLE SHEAR VISCOMETER, CANNON 47-A1

L, length of capillary	15.0 cm.
R, radius of capillary	0.02 cm.
V, volume of each bulb	1.00 cc.
m_1, height of top mark from ground level	16.315 cm.
m_2, height of second mark from ground level	14.313 cm.
m_3, height of third mark from ground level	12.240 cm.
m_4, height of fourth mark from ground level	10.040 cm.
m_5, height of fifth mark from ground level	7.735 cm.
h_1, mean hydrostatic head for top bulb	15.28 cm.
h_2, mean hydrostatic head for second bulb	13.27 cm.
h_3, mean hydrostatic head for third bulb	11.11 cm.
h_4, mean hydrostatic head for bottom bulb	8.84 cm.

The dilution bulb of this viscometer has a capacity of 30 milliliters. A minimum of six milliliters should be used when beginning a run, although five milliliters could be used if only very small amounts of solution are available.

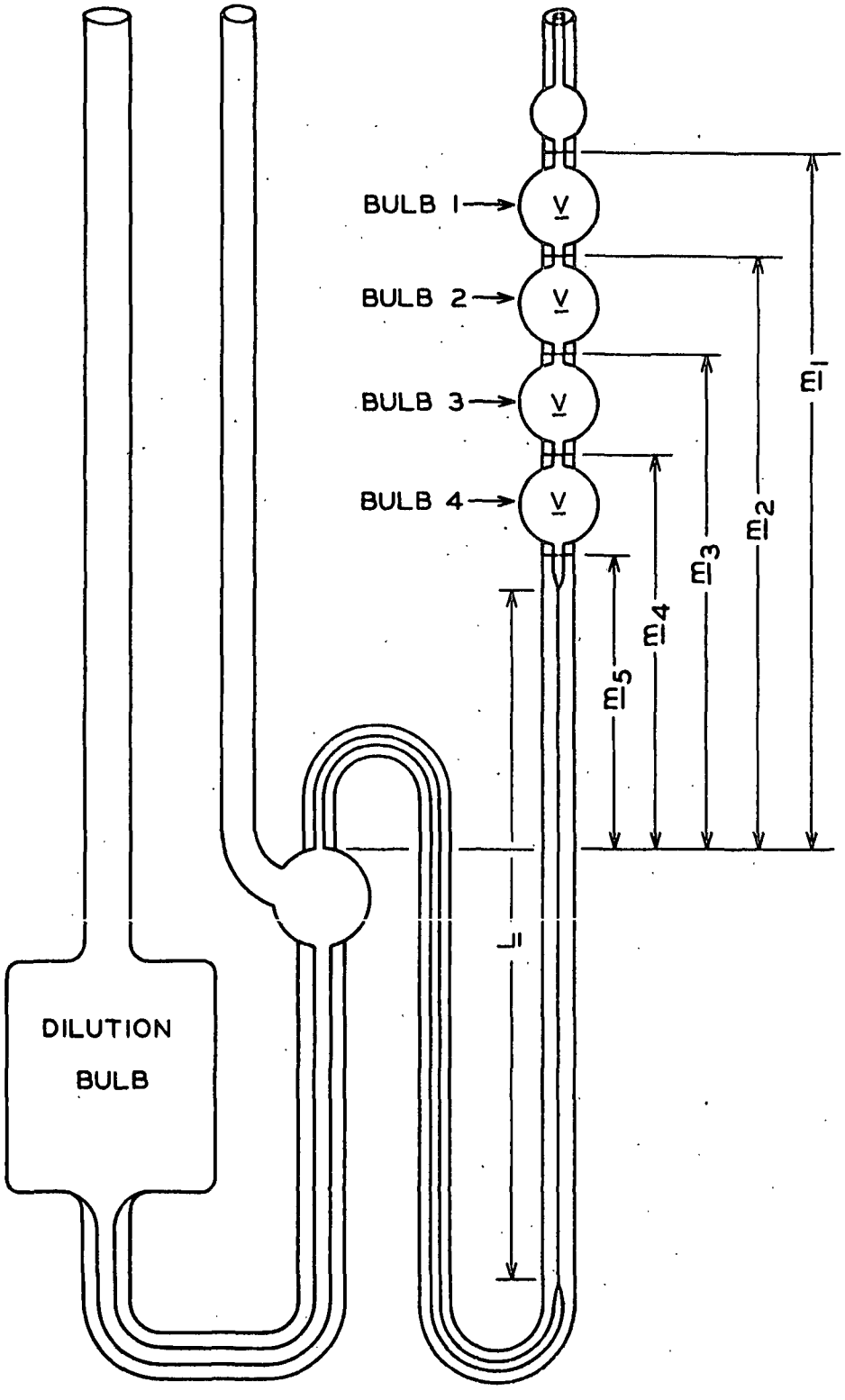

Figure 55. Variable Shear Viscometer

Equation (106) becomes the following when the appropriate constants are evaluated for each bulb,

Bulb 1: $\tau_{\underline{R}} = 9.982\ \rho$

Bulb 2: $\tau_{\underline{R}} = 8.669\ \rho$

Bulb 3: $\tau_{\underline{R}} = 7.258\ \rho$

Bulb 4: $\tau_{\underline{R}} = 5.775\ \rho$

The efflux times for various solvents from the various bulbs of this viscometer are shown in Table XX.

TABLE XX

EFFLUX TIMES FOR SOLVENTS AT 25.0°C.
FROM CANNON 47-A1 VISCOMETER

Solvent	Bulb 1, sec.	Bulb 2, sec.	Bulb 3, sec.	Bulb 4, sec.
Water	143.5	165.2	201.1	254.2
Acetonitrile	70.6	81.3	99.1	125.3
1,2,3-Trichloropropane	258.0	297.6	362.4	458.5
1,1,2-Trichloroethane	124.0	142.8	174.4	220.2

The absolute viscosity of acetonitrile at 25.0°C. was 5.65×10^{-3} poise when calculated from the efflux times shown in Table XX and Equation (110).